UNIVERSITA' DEGLI STUDI DI VERONA

DEPARTMENT OF

Neurosciences, Biomedicine and Movement Sciences

PhD SCHOOL

Life and Health Sciences

DOCTORAL PROGRAM IN

Molecular Biomedicine

The project leading to this application has received funding from the European Union's Horizon 2020 research and innovation programme under the Marie Skłodowska-Curie grant agreement No 754345, under Region of Veneto Decree nr. 193 of 13/09/2016 and under Università degli Studi di Verona

XXXIV Cycle / 2018-2021

PANCREATIC CANCER STEM CELLS EXHIBIT ADAPTATION OF MITOCHONDRIAL PHYSIOLOGY BASED ON THEIR ENERGETIC REQUIREMENTS

S.S.D. BIO/10

Coordinator: Prof. Massimo Donadelli

Signature

Tutor: Prof. Ilaria Dando

Signature

Doctoral Student: Cristian Andres Carmona Carmona

Signature

Pancreatic cancer stem cells exhibit adaptation of mitochondrial physiology based on their energetic requirements

Cristian Andres Carmona Carmona
PhD thesis
Verona, 10 March 2022

1. TABLE OF CONTENT

2. ABSTRACT

Pancreatic ductal adenocarcinoma (PDAC) is the most common type of pancreatic cancer with an overall 5-year survival rate of less than 9%. Over the past decades, few advances in PDAC treatment have been made. Furthermore, approximately 80% of PDAC patients are diagnosed at an advanced stage and mostly have no effective treatment options. The high aggressiveness of PDAC is associated with increased resistance to conventional therapies, early progression to metastatic disease, and a significant recurrence rate. All these aggressive traits are linked to the presence of a subpopulation of cancer cells with a greater tumorigenic capacity, generically called cancer stem cells (CSCs). CSCs are typically in a quiescent state that, under certain stimuli, can proliferate and give rise to a new progeny of tumor cells. Given that a single CSC could regenerate the whole tumor, the study of CSCs hallmarks is crucial for the design of new therapeutic strategies to prevent cancer progression and relapse. Some studies show that CSCs exhibit increased glycolytic rate and decreased mitochondrial function, whereas other studies report a dependence of these cells on mitochondrial oxidative phosphorylation, suggesting that CSCs likely present a heterogeneous metabolic profile. Metabolic plasticity would not be possible without mitochondrial remodelling to maintain cellular homeostasis. Although mitochondrial functions are deeply studied in cancer, the role of this organelle in the development and maintenance of CSCs has not yet been clarified. To determine the role of mitochondria in CSCs over longer periods, which may reflect more accurately their quiescent state, we studied the mitochondrial physiology in CSCs at three de-differentiation stages (at 2, 4, and 8 weeks of culture) using a PDAC cellular model previously described by our group. We found that CSCs show a significant increase in mitochondrial mass, more mitochondrial fusion, and higher mRNA expression of genes involved in mitochondrial biogenesis than parental cells. These changes are accompanied by increased ROS generation, regulation of the activities of electron transport chain complexes and supercomplexes assembly. Furthermore, the proteins OPA1 and IF1, which are involved in mitochondrial dynamics and inhibition of ATPase synthase, respectively, are overexpressed in CSCs and modulate the tumorsphere formation. Finally, we identified that lomerizine, a calcium channel blocker and an inhibitor of mitochondrial respiration, exhibits potent anticancer activity, particularly against pancreatic CSCs. Our findings indicate that CSCs undergo mitochondrial remodelling during the stemness acquisition process, which could be exploited to find vulnerabilities in mitochondrial function as a promising therapeutic target against pancreatic CSCs.

3. ABBREVIATIONS

ABCG2	ATP binding cassette subfamily G member 2
AKT	Protein kinase B
ALDH1	Aldehyde dehydrogenase 1
ATP	Adenosine triphosphate
B2M	Beta-2 microglobulin
BNGE	Blue-native gel electrophoresis
BRCA	Breast cancer type 1 susceptibility protein
CAFs	Cancer-associated fibroblasts
CAT	Catalase
CDH1	Epithelial cadherin
CDK4	Cyclin Dependent Kinase 4
CI	Complex I
CII	Complex II
CII	Complex III
CIV	Complex IV
CSCs	Cancer stem cells
CuZnSOD	copper-zinc superoxide dismutase
CV	Complex V
CXCR	C-X-C Motif chemokine receptor 4
DAPI	4 ',6-diamidino-2-fenilindol
DCFH-DA	2,7-Dichlorodihydroflurescein diacetate
DCPIP	2,6-Dichlorophenolindophenol
DDR	DNA damage response
DM	Differentiated-cell medium
DMEM	Dulbecco's modified eagle medium
DMSO	Dimethyl Sulfoxide
DNA	Deoxyribonucleic acid
DRP1	Dynamin-related protein 1
EDTA	Ethylenediaminetetraacetic acid
EGF	Epidermal growth factor
EMT	Epithelial to mesenchymal transition
ER	Endoplasmic reticulum
ERK	Extracellular signal-regulated kinases
ERRα	Estrogen related receptor α
ESCs	Embryonic stem cells
ETC	Electron transport chain
FACS	Fluorescence-activated single-cell sorting
FAD	Flavin adenine dinucleotide
FBS	Fetal bovine serum
FDA	Food and Drug Administration
FGF	Fibroblast growth factor
FIS1	Mitochondrial Fission 1 protein

FMN	Flavin mononucleotide
GPX	Glutathione peroxidase
GTP	Guanosine triphosphate
HER2	Human epidermal growth factor receptor 2
HIF-1α	Hypoxia-inducible factor 1-alpha
HSP60	Heat shock protein 60
IDH1	Isocitrate dehydrogenase 1
IF1	ATPase Inhibitory Factor 1
IMM	Inner mitochondrial membrane
IS	Intermembrane space
KPC	K-ras$^{LSL.G12D/+}$; Trp53$^{R172H/+}$; Pdx-1-Cre
KRAS	Kirsten rat sarcoma
LC3	Protein 1A/1B-light chain 3
MAPK	Mitogen-activated protein kinases
MDR1	Membrane-associated protein
MEFs	Mouse embryonic fibroblasts
MET	Mesenchymal–epithelial transition
MFF	Mitochondrial fission factor
MFN	Mitofusin
MiD49	Mitochondrial dynamics protein of 49 kDa
MnSOD	Manganese superoxide dismutase
MOPS	3-(N-morpholino) propanesulfonic acid
mtDNA	Mitochondrial DNA
mTOR	Mammalian target of rapamycin
MTS	Mitochondrial-targeting sequence
NAD	Nicotinamide adenine dinucleotide
ND1*	NADH:Ubiquinone Oxidoreductase Core Subunit 1
NDUFAF1	NADH dehydrogenase 1 alpha complex assembly factor 1
NF-KB	Nuclear factor kappa-light-chain-enhancer of activated B cells
NIH	National Institutes of Health
NRF2	Nuclear respiratory factor 2
OCR	Oxygen consumption rate
OCT3/4	Octamer-binding transcription factor 4
OMA1	Metalloendopeptidase OMA1
OMM	Outer mitochondrial membrane
OPA1	Optic Atrophy 1
OXPHOS	Oxidative phosphorylation
PBS	Phosphate-buffered saline
PCG-1α	Peroxisome proliferator-activated receptor gamma coactivator 1-alpha
PCNA	Proliferating cell nuclear antigen
PDAC	Pancreatic ductal adenocarcinoma
PI3K	Phosphoinositide 3-kinase

PKA	Protein kinase A
PMSF	Phenylmethylsulfonyl fluoride
POX	Peroxidase
qPCR	Quantitative polymerase chain reaction
RIPA	Radioimmunoprecipitation assay buffer
RNA	Ribonucleic acid
ROS	Reactive Oxygen Species
RPMI	Roswell Park Memorial Institute
SCs	Supercomplexes
SDHA	Succinate Dehydrogenase Complex Flavoprotein Subunit A
SDS	Sodium dodecyl sulphate
SEM	Standard error of the mean
SOX2	Sex determining region Y-box 2
SsM	Stem-specific medium
TBST	Tris-buffered saline with 0.1% Tween
TCA	The tricarboxylic acid cycle
TFAM	Mitochondrial transcription factor A
TGF-β	Transforming growth factor beta
TP53	Tumor protein P53
VEGFA	Endothelial growth factor A

4. INTRODUCTION

4.1. Pancreatic ductal adenocarcinoma

Pancreatic ductal adenocarcinoma (PDAC) is the most common type of pancreatic cancer and it is the seventh leading cause of cancer-related death in the world [1]. The 5-year overall survival rate at the time of diagnosis is less than 9%, as about 80% of patients present metastatic disease [2]. The advances in PDAC treatment have been few over the past decades, with surgical resection and neoadjuvant/adjuvant chemotherapy regimens, such as FOLFIRINOX and nab-paclitaxel plus gemcitabine, the only therapeutic options. However, these combinations provide only modest improvements in survival rate with considerable toxicity [3]. Furthermore, because of rapid progression, the absence of specific symptoms, and the lack of diagnostic markers, most patients with PDAC are diagnosed when the tumor is unresectable [3]. Therefore, new strategies to detect pancreatic tumors at earlier stages and the identification of specific therapeutic targets are desperately needed. To achieve the latter, it is necessary to understand the alterations and factors that contribute to the development and progression of this type of tumor. The main features of PDAC are discussed below, highlighting the importance to understand the pancreatic tumor as a heterogeneous population of cancer cells with different tumorigenic capacities, metabolic requirements, and chemoresistance profiles.

4.1.1. Cellular and molecular alterations of pancreatic ductal adenocarcinoma

Pancreatic tissue is composed primarily of acinar and ductal cells that produce digestive enzymes and deliver enzymes into the first section of the small intestine. Altogether, these cells execute the exocrine function of the pancreas and represent the starting point from which precursor intraepithelial neoplasias arise. These precursor lesions progress in a stepwise manner and culminate in the development of pancreatic ductal adenocarcinoma [4]. PDAC is characterized by the formation of a dense stroma called desmoplasia. The components of the stroma, including collagen, are produced mainly by myofibroblasts known as pancreatic stellate cells, which are also responsible for the poor vascularization of the tumor. Other cells present in the stroma are endothelial cells, adipocytes, immune and inflammatory cells that constitute a dynamic microenvironment involved in the process of tumor formation, invasion, and metastasis (Figure 1) [5].

Genetic alterations mediate the progression from the precursor intraepithelial lesions to more severe dysplasia and ultimately to metastatic carcinoma. These alterations include (Figure 1 A):

The inactivation of tumor-suppressor genes CDKN2A and TP53. *CDKN2A* encodes the protein P16, an inhibitor of the cyclin-dependent kinase 4 (CDK4), which prevents progression from the G1 to the S phase of the cell cycle. Thus, the inactivation of CDKN2 results in a loss of P16 protein and a subsequent increase in cell proliferation [6]. On the other hand, *TP53* encodes the well-recognized tumor suppressor P53. This protein is considered "the guardian of the genome" due to its role in preventing genome mutations. The primary result of *TP53* mutations is the loss of wild-type P53 functions, which contributes to genomic instability and represents a relevant advantage during tumor development by depriving the cells of DNA damage checkpoints and apoptosis signals [5]. Recently, some authors have described additional roles of this mutated protein in the tumor microenvironment, adaptation to proteotoxic stress, and reprogramming of cell metabolism. In fact, mutp53 may promote metabolic plasticity in cancer cells, facilitating their adaptation to nutrient requirements and increasing their metastatic capacity [7].

Deletion of SMAD4. SMAD4 is a protein that serves as the main signal transducer for TGF-β cell-surface receptors. The activation of TGF-β induces SMAD accumulation in the nucleus and regulates the expression of diverse genes, including collagen, integrin, E-cadherin, and others. The TGF-β/SMAD4 pathway functions as a tumor suppressor in benign pancreatic epithelial cells by promoting their cell cycle arrest. However, persistent activation of TGF-β and the loss of SMAD4 lead to induction of the RAS-ERK pathway in PDAC, which has been demonstrated to be involved in many different stages of tumor progression [8].

Activation of the KRAS oncogene. RAS proteins are small GTPases that couple cell membrane growth factor receptors to intracellular signaling pathways, such as mitogen-activated protein kinase (MAPK) and phosphatidylinositol 3-kinase (P13K) that regulate cell growth and survival. More than 90% of the precursor intraepithelial lesions of PDAC are characterized by point mutations in the *KRAS* isoform, particularly in codon 12 [5]. These mutations produce a RAS protein that is constitutively active, resulting in the activation of proliferative and antiapoptotic signaling pathways in the absence of stimulation. In the past decade, numerous studies have shown that KRAS plays an important role during the adaptation of cancer cell metabolism, supporting the biosynthetic requirements of the tumor cells and maintaining redox homeostasis [9]. Therefore, it is not surprising that the inhibition of the effector metabolic pathways activated by KRAS can be exploited for therapeutic purposes.

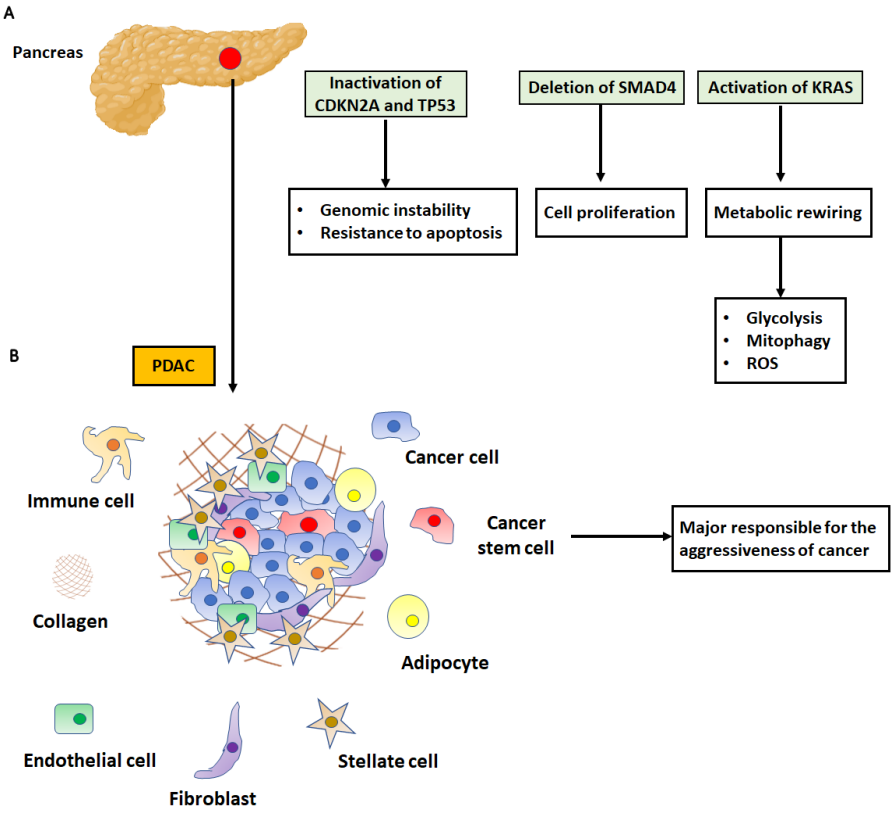

Figure 1. Genetic alterations and components of pancreatic ductal adenocarcinoma (PDAC). **(A)** Main genetic alterations associated with the origin and progression of PDAC. **(B)** PDAC tumors are composed of different types of cells that constitute a dynamic microenvironment involved in the process of tumor formation, invasion, and metastasis. Of note, a small group of cells known as cancer stem cells (CSCs) are considered key players during metastasis and tumor relapse.

4.1.2. Metabolism of pancreatic ductal adenocarcinoma

One of the most important metabolic hallmarks of cancer cells is the upregulation of glycolysis even in the presence of oxygen, known as the Warburg effect [10,11]. The "aerobic glycolysis" provides several intermediates necessary for the synthesis of macromolecules required for rapid proliferation. It also contributes to maintaining the redox balance and enhances the invasion of cancer cells [12]. Initially, the upregulation of glycolysis was assumed to be a consequence of mitochondrial impairment. However, this view has been re-evaluated based on further studies demonstrating that tumor mitochondria do respiration and ATP production [13–15]. The idea that cancer cells switch from oxidative phosphorylation to glycolysis has also been challenged by the evidence that cancer cells display distinct metabolic requirements, which are determined by genetic background and tumor microenvironment [16].

In the case of pancreatic adenocarcinoma, even in the same patient, the primary tumor and metastatic lesions may exhibit different gene expression and metabolic alterations [17,18]. In

pancreatic cancer cells, various genetic alterations are considered responsible for metabolic rewiring, especially in the modulation of mitochondrial function to support carcinogenesis. Among the most relevant of these alterations are the oncogenic mutations of *KRAS* [9]. These mutations render KRAS constitutively active, promoting tumor growth and evasion of immune destruction. Cells carrying *KRAS* mutations are characterized by increased glucose uptake and flux through glycolysis due to KRAS-dependent regulation of glycolytic enzyme expression. This glycolytic phenotype correlates with a worse prognosis in patients with PDAC [9].

Furthermore, KRAS-driven cancer cells modulate total mitochondrial content by inducing mitophagy. In this process, cells recycle tricarboxylic acid (TCA) cycle metabolites required for biosynthesis and bioenergetics pathways [19]. Activation of KRAS leads to a decrease in oxygen consumption and an increase in the generation of reactive oxygen species (ROS), possibly due to a decrease in the expression of NDUFAF1 (NADH dehydrogenase 1 alpha complex assembly factor 1) [20]. Mitochondrial ROS are essential for tumor progression in mouse models, but in turn, mitophagy prevents excessive levels of ROS and removes damaged mitochondria. This apparent mitochondrial dysfunction associated with KRAS mutations might be compensated by the upregulation of other proteins such as OPA3, which promotes and maintains cellular metabolism [21].

So far, it is clear that all these metabolic alterations modulate aggressiveness and response to therapy in PDAC tumors [22]. In fact, Krasinski and colleagues recently reported that a classification of pancreatic cancer according to metabolic subgroups (quiescent, oxidative, glycolytic, and mixed) could predict the prognosis of the disease. For example, a glycolytic subtype is associated with poor survival in patients with PDAC [23]. Thus, targeting metabolic pathways of PDAC provides promising therapeutic opportunities for personalized medicine.

4.1.3. The aggressiveness of pancreatic ductal adenocarcinoma

As mentioned at the beginning, PDAC is one of the most aggressive solid malignancies. The high aggressiveness of PDAC is associated with an early progression to metastatic disease, increased resistance to conventional therapies, and a significant recurrence rate. Metastatic dissemination occurs commonly to adjacent organs, such as the gallbladder and the liver [24]. One of the requirements to initiate metastasis is the transition of epithelial cells to motile mesenchymal cells, a process known as epithelial-mesenchymal transition (EMT). In PDAC cells, this process is mainly induced by TGF-β through the activation of target genes, e.g. *SLUG*, *SNAIL1*, and *TWIST* [24]. On the other hand, resistance to chemotherapy in PDAC cells

is mediated by diverse mechanisms, including the reduction of drug transporters and inactivation of enzymes that participate in the metabolism of drugs, among the others deoxycytidine kinase, which is indispensable for intracellular activation of gemcitabine (a drug used as standard first-line treatment for PDAC patients) [25]. Finally, recurrence in pancreatic cancer after successful treatment of the primary tumor is primarily attributable to a phenomenon called dormancy. Tumor dormancy is a stage in which cancer cells exist in a quiescent state for long time until the microenvironment, an active immune response, or limitations in blood supply trigger their proliferation to form a new tumor, which is generally more aggressive than the previous one [26].

Most interesting, recent studies demonstrate that all these aggressive traits are linked to the presence within the tumor of a subpopulation of cancer cells with a greater tumorigenic capacity, generically named cancer stem cells (CSCs) or tumor-initiating cells [27,28]. The next section describes the main features of these cells and their role in the development and progression of PDAC.

4.2. Pancreatic cancer stem cells

Over the last two decades, compelling evidence has shown that solid tumors are composed of heterogeneous populations of cells with different proliferative and differentiation capabilities [28]. Within these subpopulations, cancer stem cells (CSCs) represent a group of cells in a quiescent state that can self-renew by asymmetric division, differentiate into the different lineages of cancer cells, and give rise to a new tumor when they are transplanted [27,28]. CSCs can also colonize distant sites from the primary tumor, contributing to metastasis, the leading cause of cancer mortality [28]. Furthermore, these cells are particularly resistant to conventional therapies, such as radiotherapy, chemotherapy, and even immunotherapy, possibly due to their slow cycle, overexpression of multiple drugs transporters, greater DNA repair capacity, and more resistance to mitochondria-mediated cell death than other cells [29,30]. Given that a single CSC could regenerate the whole tumor, the study of CSCs characteristics is crucial for the design of new therapeutic strategies to prevent cancer progression and relapse.

4.2.1. Detection and isolation of pancreatic cancer stem cells

Pancreatic cancer stem cells represent only a small percentage of the total number of cells in the tumor mass, making their detection, isolation, and study really challenging [30]. Currently, CSCs can be detected using antibodies against some cell surface markers (e.g., CD44, CD24,

ESA, CD133, CXCR4) by cell sorting (Figure 2) [31]. In addition to these markers, other internal properties have been used to detect and isolate CSCs, including high levels of aldehyde dehydrogenase 1 (ALDH1) activity, low activity of the 26S proteasome, and autofluorescence by flow cytometry [30,32]. However, none of these markers seems to identify uniquely CSCs, likely due to the high level of heterogeneity of these cells that originates from their genotypic and phenotypic plasticity [33]. After sorting CSCs based on markers expression, these cells in culture quickly re-establish their pre-sorting heterogeneity within 3 days in culture [34]. As a result, numerous groups have tried to develop methods that could facilitate a long-term CSCs enriched culture [33–35]. For instance, our group recently reported that growing pancreatic cancer cells for 8 weeks in a stem-specific medium progressively increased the expression of the stem, EMT, and quiescence markers [35]. This type of cell model represents an interesting platform to characterize CSCs features that could lead to the identification of new therapeutical targets against CSCs.

4.2.2. Chemoresistance mechanisms of pancreatic cancer stem cells

Currently, it is well accepted that CSCs are resistant to conventional treatments and are responsible for cancer metastasis and tumor relapse after clinical remission in different types of cancer [30]. In the case of PDAC, some authors have reported that pancreatic cancer cell lines show typical properties of EMT when they are grown in a culture medium containing gemcitabine. In addition, these gemcitabine-resistant cells expressed an increased level of cell surface markers associated with stemness, including CD24, CD44, CD133, and ESA [36]. Similar results were reported in human primary pancreatic cancer xenografts treated with ionizing radiation [37]. These studies demonstrate that chemotherapy and radiotherapy can eliminate most of the bulk cancer cells, whereas the CSC-enriched population survives and develops chemoresistance during the treatment. There are different cellular mechanisms proposed to explain this drug resistance phenotype, some of which will be briefly discussed below (Figure 2).

Activation of pathways related to stemness. Growing evidence suggests that some signaling pathways such as Wnt/β-catenin, Hedgehog, Notch, and TGF-β, which are upregulated in CSCs, may contribute to chemoresistance [30]. For example, Wnt signaling can promote DNA damage response, while β-catenin can activate the expression of survivin that is known to protect the pancreatic cancer cell lines in response to apoptotic agents [38].

Overexpression of ABC transporters. These transporters are widely known as mediators of chemoresistance in different types of tumors. In pancreatic CSCs, overexpression of ABCG2 and multidrug-resistant protein 1 (MDR1) allows an efficient efflux and elimination of the chemotherapeutic agents [30]. Most interestingly, ABCG2 also facilitates the accumulation of toxic agents within the cytoplasmic vesicles in CSCs of primary tumors [32].

Cell quiescence. One of the characteristics of CSCs is their quiescent state, where cells are maintained in the G0/G1 phase, this means that CSCs divide in response to physiological stimuli or do not divide at all [39]. Because most chemotherapeutic agents target proliferating cells, these drugs have a minimal effect on CSCs [29].

Resistance to DNA damage. Currently, radiotherapy and some drugs such as cisplatin, eliminate cancer cells by promoting DNA damage. It has been reported that CSCs have an elevated DNA damage response (DDR) compared to bulk cancer cells [40]. Indeed, CSCs spheroids from HPAC and Panc1 show a significantly higher expression of DNA repair genes, such as *BRCA1* and *RAD51,* compared to parental cells [41].

Cellular plasticity. This feature is defined as the ability of CSCs to undergo phenotypic and molecular changes including differentiation, de-differentiation, and trans-differentiation within a hierarchical order [42]. These changes occur in response to microenvironmental signals, genetic alterations, or stress-induced by therapeutic agents, contributing to increase cell heterogeneity and chemoresistance [42]. In PDAC, the presence of CSCs at different stages has been extensively documented in the solid tumor [43], but also as circulating cells [44]. All of these CSC subpopulations display a certain degree of cell plasticity and could regenerate the tumor and participate in cell migration/invasion [30]. The heterogeneity of CSCs represents a big challenge for the identification of drugs that may be effective for their elimination, so it is necessary to develop new models that reflect their different stages during the process of stemness acquisition.

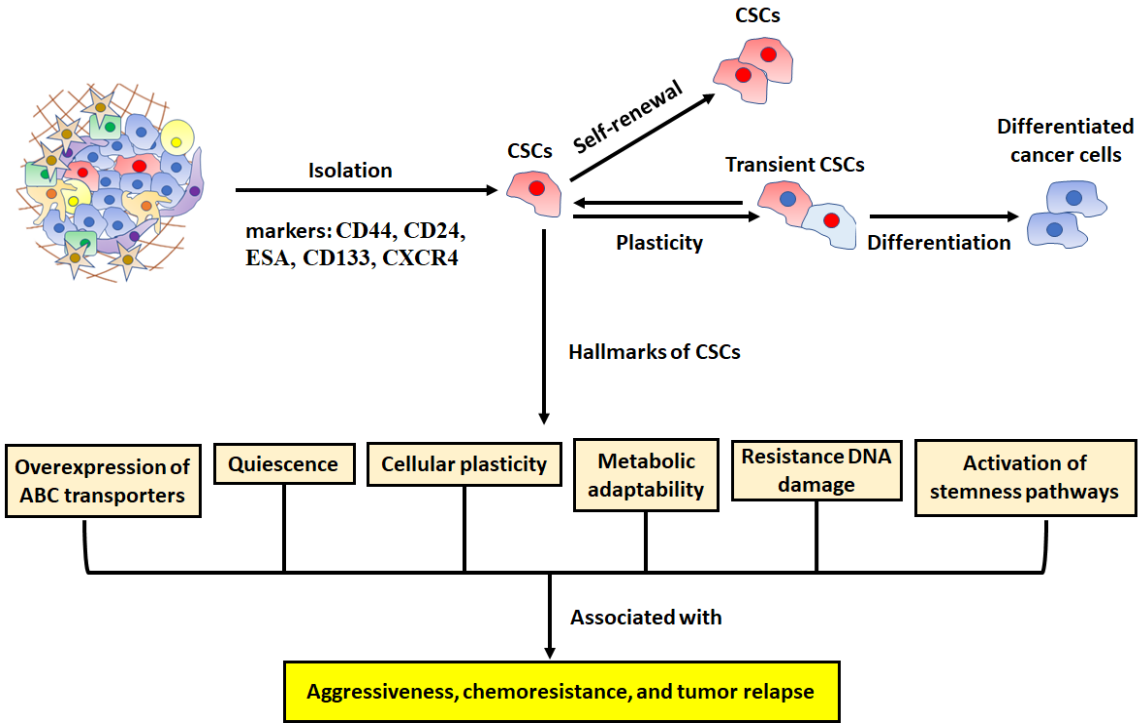

Figure 2. Pancreatic cancer stem cells and their chemoresistance mechanisms. Pancreatic CSCs can be detected using antibodies against some cell surface markers by cell sorting. CSCs can self-renew by symmetrical division resulting in two CSCs or differentiate into cancer cells by asymmetrical division. During the process of differentiation, CSCs give rise to "transient-hybrid CSCs" with less tumorigenic potential but with the capacity of reprogramming into CSCs. Pancreatic CSCs have specific characteristics that give them numerous advantages to resist conventional therapies.

4.2.3. Metabolism of pancreatic cancer stem cells

In the last few years, it has been claimed that the metabolic adaptability of CSCs is fundamental to maintain continuous self-renewal capability and to avoid chemotherapeutic elimination [42]. However, the metabolism of CSCs remains controversial, possibly because it could depend on the type of tumor and on the intrinsic heterogeneity of the CSC subpopulation [42,45]. In fact, some authors have reported that CSCs from glioblastoma [46], nasopharyngeal carcinoma [47], and breast cancer [48] preferentially rely on a glycolytic metabolism with an increased expression of enzymes involved in this pathway. Glycolytic metabolism reduces ROS production and provides intermediate substrates that can be used for CSCs proliferation [49]. In contrast, other authors have reported that CSCs from pancreatic [50], lung [51], and ovarian cancer [52] rely on oxidative phosphorylation (OXPHOS) metabolism with an increase in mitochondrial mass and function. Additionally, recent publications evidence that CSCs from the same cancer type show different metabolism, revealing that the surrounding microenvironments could be critical to define the nutrient requirement and metabolic profile

of CSCs [45]. For instance, stromal cells can secrete metabolic intermediates that are used by CSCs in metabolic pathways, for example the TCA cycle [53]. Interestingly, in breast tumors, cancer-associated fibroblasts (CAFs) can transfer mitochondrial DNA (mtDNA) to CSCs, leading to the activation of mitochondrial function [54]. Taken together, these reports clearly evidence the metabolic heterogeneity of CSCs, which could be crucial for their survival, particularly under stress conditions, including chemotherapy.

In the case of PDAC, most of the reports point out that pancreatic CSCs are highly dependent on OXPHOS metabolism [30]. Already in 2014, it was identified that a subpopulation of dormant cancer cells responsible for tumor relapse exhibited a high expression of genes involved in mitochondrial function, as well as an increase in OXPHOS metabolism [55]. Later, Sancho et al. observed that pancreatic cancer stem cells rely on mitochondrial function for energy production. This metabolic dependence has been shown to be regulated by the expression of PCG-1α, which plays a key role in mitochondrial biogenesis [50]. On the other hand, the same research group also identified the presence of a subset of pancreatic CSCs with reduced mitochondrial mass and resistance to mitochondrial inhibitors, demonstrating the metabolic heterogeneity in CSCs from pancreatic tumors [43,56]. In addition, Nimmakayala et al. demonstrated that pancreatic CSCs adapt specific metabolic profiles according to the organ that colonize during metastasis [57]. For example, liver metastasis showed CSCs with aerobic glycolysis metabolism, whereas lung metastasis displayed CSCs with oxidative metabolism [57]. Recently, our group also revealed this metabolic plasticity in an *in vitro* model of gradually de-differentiated CSCs derived from PDAC cell lines [35]. Basically, these cells shift their metabolism from a glycolytic to an oxidative one and lastly gain a quiescent state. These quiescent cells can re-start to proliferate and re-activate the metabolic machinery accumulating lactate, a typical sign of high aggressiveness [35]. This metabolic plasticity of CSCs may represent a big obstacle to the use of specific metabolic inhibitors.

CSC metabolic rewiring would not be possible without mitochondrial remodelling to maintain cellular homeostasis. Indeed, the virtual dependence of pancreatic CSCs on OXPHOS metabolism renders the mitochondrion a possible target to develop new therapeutic strategies against PDAC [30,49]. In the next section, the role of mitochondria in pancreatic cancer will be explained, emphasizing the interplay between bioenergetics and mitochondrial dynamics during the tumor progression.

4.3. Mitochondria

Mitochondria are key organelles involved in several functions within the cell. These functions include the regulation of programmed cell death, calcium homeostasis, fatty acid oxidation, and cell signaling. However, the most important role of mitochondria is the production of ATP, which maintains the energetic metabolism [58]. This organelle has an outer mitochondrial membrane (OMM) in contact with the cytosol that is permeable to ions and molecules under 6 kDa of size. Inside of the outer membrane, and separated by the intermembrane space, lies the inner mitochondrial membrane (IMM), which contains a central space named matrix. IMM presents membrane invaginations named mitochondrial cristae that harbor respiratory chain complexes (structures necessary for oxidative phosphorylation) (Figure 3 A) [59]. The lipid bilayer of IMM contains a high proportion of cardiolipin, a phospholipid that does not exist in other membranes that helps to make the membrane impermeable to ions [58]. The matrix is the site where protein biosynthesis, mtDNA replication, and the Krebs cycle take place. MtDNA encodes for 13 subunits of the electron transport chain complexes (ETC), 2 ribosomal RNAs, and 22 transfer RNAs [59].

The numerous functions of mitochondria make them pivotal organelles during adaptation of tumor cells under adverse conditions, such as hypoxia, nutrient depletion, and chemotherapy, making mitochondria function an interesting therapeutical target [60,61]. Indeed, the old view about a possible mitochondrial impairment as a cause of cancer has been re-bated by different authors, who explain the importance of oxidative phosphorylation and eventually of an active mitochondrion, as a central energy source for some types of tumors, including PDAC [30,62]. The study of OXPHOS mechanisms that contribute to tumor progression represents an attractive field of research. Some of these mechanisms and how mitochondria participate in energy production are discussed below.

4.3.1. Electron transport chain and oxidative phosphorylation

In biological oxidations, the hydrogens obtained from the substrates are gradually transferred through different acceptors, such as NAD and FAD, which undergo reversible changes in their redox state (Figure 3 B). These acceptors are organized according to the potential gradient and are closely associated with a series of transmembrane protein complexes in the mitochondrial inner membrane that catalyze the transfer reactions [58]. While the electrons pass through the electron transport chain complexes, protons are pumped from the mitochondrial lumen into the intermembrane space, forming a proton gradient across the IMM. The protons go back from the intermembrane space into the mitochondrial matrix through ATP synthase, also called

complex V, favoring ATP synthesis. The terminal electron acceptor is oxygen [58,63]. Except for cytochrome C (located on the outer face of the IMM) and ubiquinone (located in the membrane lipid bilayer), the rest of the components of the ETC are organized into five complexes (Figure 3 B) [58]:

Complex I (CI) corresponds to NADH-ubiquinone reductase. The complex is composed of seven Fe-S centers and the coenzyme flavin mononucleotide (FMN). The coenzyme FMN of the complex receives reduction equivalents and then the electrons are transferred to coenzyme Q (ubiquinone).

Complex II (CII) is also known as a succinate-ubiquinone reductase. It is composed of three Fe-S centers. Its function is to transfer electrons from succinate to coenzyme Q.

Complex III (CIII) or ubiquinone-cytochrome c reductase. This complex is composed of cytochrome c_1, b_{562}, b_{566}, and a Fe-S center. Its function is to transfer electrons from ubiquinone to cytochrome c.

Complex IV (CIV) is also known as cytochrome oxidase. This complex is composed of two Cu atoms and cytochromes a and a_3. CIV catalyzes the reduction of O_2 to H_2O.

ATP synthase or Complex V (CV). This complex contains 9 polypeptides, where the catalytic subunit (F_1 portion) is bound to the membrane by the protonic channel (F_0 portion) that is embedded in the lipid bilayer. The return of protons from the intermembrane space into the mitochondrial matrix can only occur through ATP synthase. This complex binds P_i to ADP to form ATP, thanks to the energy released by the flow of protons [58].

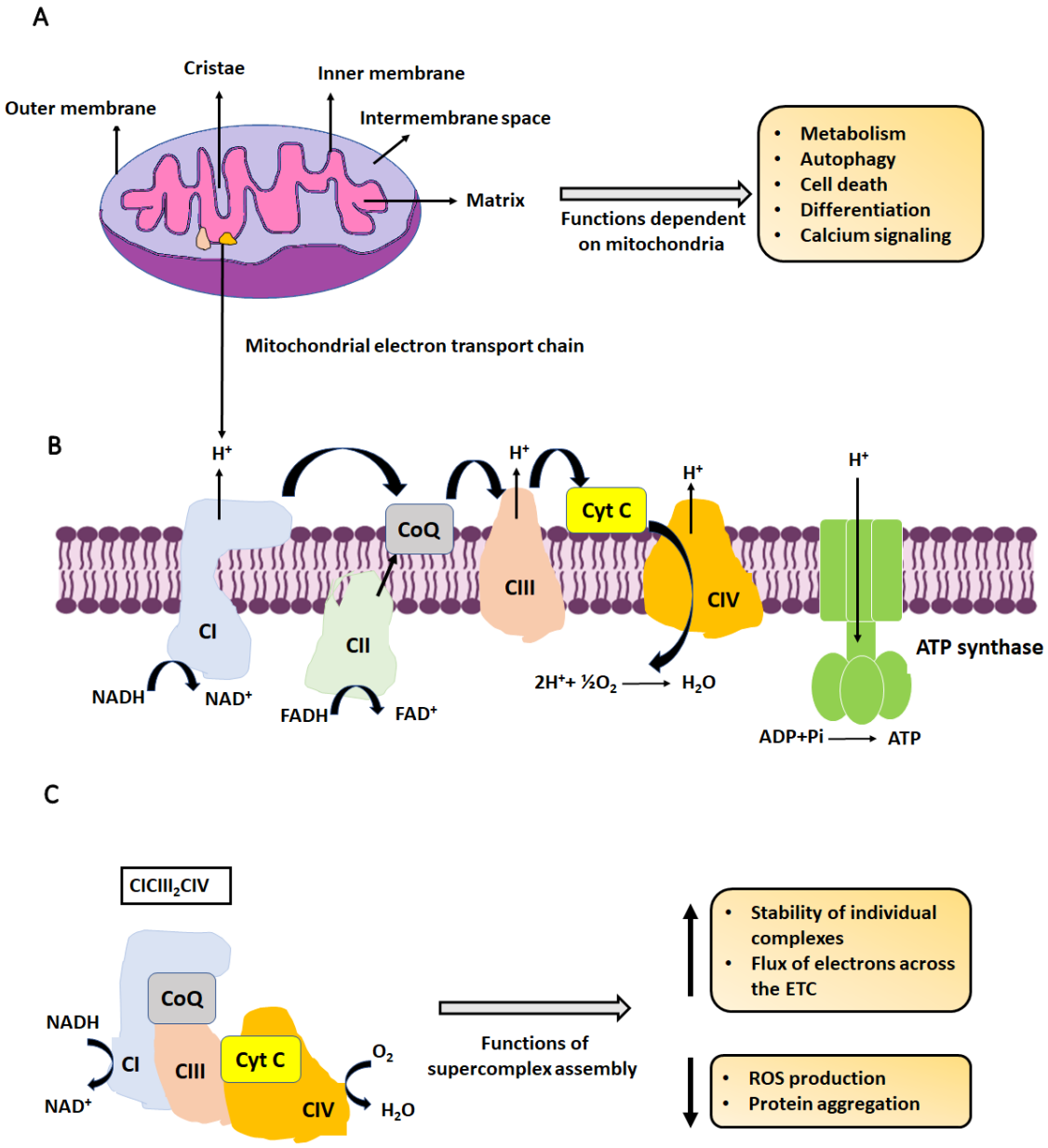

Figure 3. Mitochondrial electron transport chain (ETC). A. Mitochondria structure and key functions dependent on mitochondria are listed. **B.** ETC is composed of a series of transmembrane proteins in the IMM, known as complex I (CI), complex II (CII), complex III (CIII), complex IV (CIV), complex V (CV or ATP synthase), coenzyme Q10 (CoQ), and cytochrome c (Cyt C). The ETC utilizes the energy in form of the reducing equivalents (NADH and FADH) coming from the tricarboxylic acid cycle, generating a proton gradient across the inner mitochondrial membrane (IMM). The protons go back from the intermembrane space into the mitochondrial matrix through ATP synthase, also called complex V, driving the synthesis of ATP. The terminal electron acceptor is oxygen. **C.** Example of one of the existing supercomplex composed of CI, $CIII_2$ (complex III dimers), and complex IV. The electron carriers (CoQ and Cyt C) are also indicated.

4.3.2. Respiratory chain supercomplexes: function and assembly

The organization of the respiratory chain complexes in the mitochondrial inner membrane has attracted the attention of different scientists during the last decades. Initially, a "fluid model"

has been proposed in which the complexes diffuse freely in the membrane, and both cytochrome C and coenzyme Q move without any restriction [64]. In contrast, another "solid model" predicts that respiratory enzymes that catalyze individual reactions associate with each other to form single units now known as respiratory supercomplexes (SCs) (Figure 3 C) [64,65]. The formation of these SCs was demonstrated three decades ago using blue native gel electrophoresis (BNGE) [66]. The assembly of stable SCs has been reported in plants, yeast, bacteria, and mammalian cells [64]. In fact, in mitochondria can be identified SCs with varying stoichiometry including CI-CIII-CIV, CI-CIII, and CIII-CIV. Interestingly, about 90% of CI is found in supercomplexes, whereas CII and CV do not participate in mitochondrial supercomplex formation [64].

The function of SCs in cell physiology is beginning to emerge, especially since some genetic diseases related to alterations in complex subunits and SCs assembly factors always lead to drastic phenotypes, especially neurodegenerative disorders [65]. The main role of SCs may be to maximize the flux of electrons across the ETC, probably through a mechanism of substrate channelling. For example, in yeast and bovine mitochondria, CI and CIII form a single unit where electron transfer occurs through a channel between the two complexes avoiding coenzyme Q mobilization in the membrane [67]. These structures may also reduce electron leakage and, consequently, decrease the production of ROS. Moreover, SCs help to stabilize the assembly of individual complexes and prevent protein aggregation in the IMM (Figure 3 C) [68]. Despite the advances in recognizing the structure of these multi-enzyme assemblies, it is worth mentioning that the function of SCs in normal cells is still incipient and represents almost an unexplored field in cancer.

4.3.3. Electron transport chain complexes and pancreatic cancer

The ratio of supercomplexes to free complexes can have an impact on cellular metabolism. In fact, cancer cells can adapt their metabolism to different microenvironmental conditions by changing the organization of ETC complexes. The inhibition of SCs assembly promotes glycolytic metabolism in different types of cancer [69]. The most well-known alterations in SCs organization are associated with mutations in subunits of the complex I, considering that this complex is found mainly in SCs. For example, mutations in the subunit ND2 favor glycolysis and confer tumorigenic potential to cancer cells [70], while downregulation of NADH:Ubiquinone Oxidoreductase Core Subunit S1 (NDUFS1) in drug therapy increases chemoresistance and aggressiveness [71]. In contrast, SCs assembly could also be enhanced by oncogenes such as *HER2* in breast cancer, and *KRAS* in pancreatic cancer cells [69]. This

mechanism could be an intrinsic defence to limit electron leakage and ROS overload.PDAC is characterized by poor vascularization and a dense stroma, resulting in a significant hypoxic microenvironment. Despite these harsh conditions, pancreatic cancer cells maintain active mitochondria and the oxidative metabolism necessary for the biosynthesis of metabolites for tumor proliferation [30]. Hollinshead et al. demonstrated that PDAC cell lines maintain OXPHOS during hypoxia by increasing mitochondrial supercomplexes assembly. Indeed, inhibition of SCs assembly abolishes the PDAC cell lines growth and tumor formation *in vivo* [18]. Similar results were obtained in a model of breast and endometrial cancer [72]. Another study found that phenformin, a complex I inhibitor, overcomes the gemcitabine chemoresistance in high OXPHOS pancreatic cancer cell lines [73]. These studies suggest that disrupting SCs assembly and targeting mitochondrial bioenergetics may have therapeutic applications for PDAC.

4.3.4. Reactive oxygen species (ROS) and pancreatic cancer

Another process closely related to ETC and mitochondria oxygen consumption is the generation of ROS. Basically, the last stage of ETC is the reduction of an oxygen molecule by the transfer of 4 electrons $(O^{-2})_2$. However, partial reduction of oxygen generates superoxide anion (O_2^-) or hydrogen peroxide (H_2O_2) [58]. The superoxide anion is produced mainly in the CI and CIII. ROS generated by CI are released in the mitochondrial matrix, while those produced by CIII are mostly released into the intermembrane space [74]. The interaction between O_2^- and H_2O_2 forms the hydroxyl radicals, which have toxic effects on different components of the cells, such as DNA, protein, and lipids. The cell counts with different enzymes as defense mechanisms against ROS excess. For example, superoxide dismutase eliminates the superoxide anion, catalase contributes to eliminating hydrogen peroxide, and glutathione peroxidase is involved in the reduction of organic hydroperoxides and hydrogen peroxide [58,74].

Under physiological conditions, low levels of ROS have relevant functions on cell proliferation, differentiation, and cell death. Moreover, ROS can function as secondary messengers at specific concentrations and locations, regulating global processes within cells such as cell cycle, migration, and angiogenesis [75]. These biological processes are pivotal in cancer, where a balance between ROS production and ROS response provides a survival advantage. About pancreatic cancer, oncogenic *KRAS* participates in ROS production by regulating hypoxia-inducible factor 1 (HIF-1α) and transferrin receptor, the last one has been found overexpressed in PDAC [76]. The importance of ROS in PDAC has been demonstrated

in vivo models of mice, where the depletion of ROS using antioxidants leads to a significant decrease in the formation and progression of pancreatic lesions [77]. Interestingly, to compensate for the excess of ROS, the same oncogenic *KRAS* can induce the expression of nuclear respiration factor (NRF2), a transcription factor that regulates different antioxidant genes. NFR2 activity in PDAC can also be enhanced by somatic mutations that affect the interaction with its inhibitor (keap1) [76,77].

In the case of cancer stem cells and similarly to embryonic stem cells (ESCs), low ROS levels could be a strategy to maintain stem-like profiles and avoid DNA damage [75]. In breast CSCs, low levels of ROS are associated with increased activity of free radicals scavenging systems. In fact, the inhibitors of these scavengers significantly increased sensibility to radiotherapy in breast CSCs [78]. However, some studies have found that ROS are fundamental during EMT due to their crosstalk with different cell signaling pathways. For example, ROS act as key players in TGF-β induced EMT by activation of MAPK and subsequently activation of SMAD pathway [79]. Furthermore, it has been reported that in spheroids from lung and colon cancer, loss of anchorage in culture (a hallmark of cancer stem cells) enhances the generation of ROS accompanied by changes in glucose and glutamine metabolism [80]. Interestingly, the acquisition of stem properties in pancreatic cancer by gemcitabine treatment is mediated by ROS and activation of NF-KB [81]. Jagust et al recently found that primary pancreatic CSCs show increased glutathione content, which correlates with stem-like phenotype and chemoresistance in these cells [82]. To summarize, these studies demonstrate that a delicate balance between ROS production and antioxidant response is crucial for the survival of CSCs within the tumor.

4.4. Mitochondria dynamics

Mitochondria are not rigid structures, instead, they have a high degree of shape modifications and their subcellular distribution is always changing according to the requirements of the cell. Under certain circumstances, mitochondria can combine to form networks (fusion), whereas in other conditions mitochondria can divide into small fragments (fission). In terms of energy demand, fragmented mitochondria are associated with a nutrient-rich environment, whereas elongated mitochondria are related to starvation (Figure 4) [83]. In fact, mitochondrial elongation leads to an increase in energetic efficiency, in order to maintain ATP production when the availability of nutrients is limited [84]. In addition to content mixing, mitochondrial dynamics allows the selective removal of dysfunctional mitochondria, ensuring a healthy population of mitochondria in the cell, mainly through mitophagy. The balance between fusion

and fission is involved in cell death, calcium homeostasis, cell respiration, and autophagy. Alterations in mitochondrial dynamics have been associated mainly with neuropathies and neurodegenerative diseases, such as Parkinson's and Alzheimer's disease [85]; however, the studies of mitochondrial dynamics in metabolic diseases and cancer have increased considerably during the last decade, attributing a potential role in the origin and progression of these pathologies [62]. A deeper investigation of the molecular mechanisms underlying the alterations in the balance of fission/fusion might contribute to the identification of potential therapeutic targets for the development of new treatments in cancer. The main players in this process are discussed below, emphasizing how fusion/fission can impinge on the progression of pancreatic cancer.

4.4.1. Mitochondrial fusion

Mitochondrial fusion is the binding of two mitochondria into one larger. This merge implies that both outer membrane and inner membrane fuse, while the matrix components mix to form a new mitochondrion. This process mainly requires three GTP-hydrolysing enzymes of the dynamin family: the mitofusins, MFN1 and MFN2 are required for OMM fusion, whereas Optic Atrophy 1 (OPA1) is involved in the IMM fusion (Figure 4). The function of both mitofusins is essential for embryonic development because mice deficient either MFN1 or MFN2 die in midgestation [86]. Nevertheless, the overexpression of MFN1 or MFN2 in fibroblasts deficient of MFN2 or MFN1, respectively, can restore the mitochondrial network, proving that these proteins have redundant functions to promote mitochondrial fusion [86]. The expression of mitofusins is regulated by transcription factors involved in mitochondrial biogenesis and oxidative phosphorylation. For instance, PGC1β induces the expression of MFN2 at the transcriptional level by coactivating the nuclear receptor Estrogen Related Receptor α (ERRα) [87]. In addition to its role as a mitochondrial fusion protein, the importance of MFN2 in oxygen consumption and the activity of ETC complexes has been widely documented in muscle and liver cells [88–90]. However, it has been reported that, in the long-term, MFN2 knockout cells can develop adaptive mechanisms that allow maintaining the function of OXPHOS, showing that MFN1 might compensate for the loss of MFN2 to maintain energy metabolism [91]. In addition, MFN1 (but not MFN2) is required to promote OPA1-driven mitochondrial fusion in mouse embryonic fibroblasts (MEFs) [92].

On the other hand, OPA1 has eight variants in humans, resulting from differential splicing of exons 4, 4b, and 5b [93]. The protein structure that includes S1 and S2 proteolysis sites is encoded by exon 5 and 5b, respectively. In addition, OPA1 has a mitochondrial-targeting

sequence (MTS) that determines its location in the inner membrane. Removal of MTS during import into the mitochondrial matrix produces the long (L) isoforms, which are anchored to the inner membrane, with most of the protein facing the intermembrane space (IS). These L-isoforms are processed by OMA1 and YME1L in the S1 and S2, respectively, to generate short isoforms. These short isoforms do not have an anchor domain and could be soluble in the IS, but they are bound to long-isoforms to modulate mitochondrial fusion [94,95]. The study of the individual OPA1 isoforms shows that, in general, long isoforms are more related to the maintenance of mitochondrial fusion, whereas short isoforms are more essential for energy efficiency [96]. Interestingly, for a complete restoration of mitochondrial network morphology, the balance of both long and short isoforms is necessary [97,98].

4.4.2. Mitochondrial fission

Mitochondrial fission or mitochondrial division is primarily mediated by DRP1, which is another large dynamin-related GTPase protein (Figure 4). This protein moves from the cytosol to the outer mitochondrial membrane where it binds to its receptors (FIS1, MiD49, MiD51, and MFF) to initiate the mitochondrial constriction and, as a result, the division of a mitochondrion into two smaller ones. It has been widely reported that mitochondria should establish contact with endoplasmic reticulum (ER) tubules before DRP1 recruitment [99]; in fact, the ER plays an active role in defining the mitochondrial fission sites, which together with the actin cytoskeleton allows membrane constriction [59]. The function of DRP1 is tightly regulated by post-translational modifications, where the phosphorylation mechanism is the most studied. Indeed, it has been demonstrated that phosphorylation at Ser616 by ERK2 stimulates mitochondrial fission [100], whereas the phosphorylation at Ser637 by PKA decreases DRP1 GTPase activity and leads to mitochondrial elongation [101]. In contrast, the role of DRP1 outer membrane receptors in the mitochondrial division is less clear. A conditional knockout model of FIS1 in colon carcinoma cells showed that FIS1 is dispensable for mitochondrial fission [102], although it can act in sequence with MFF at ER-mitochondrial sites, favoring some types of mitophagy [103]. Either MiD49 or MiD51 can mediate DRP1 recruitment in the absence of MFF or FIS1 [104], but their overexpression has been shown that increase mitochondrial elongation due to sequestration and inactivation of DRP1 on the mitochondrial outer membrane, blocking mitochondrial fission [105]. Altogether, these studies demonstrate that multiple proteins can bind and recruit DRP1, thus displaying an effect on mediating mitochondrial division.

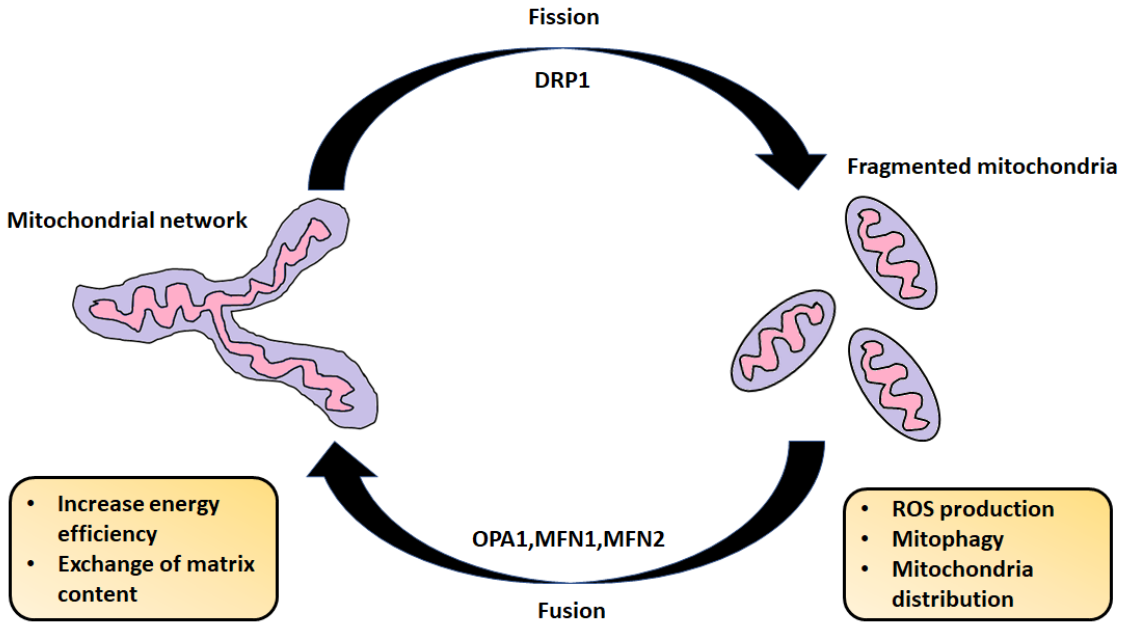

Figure 4. Mitochondrial dynamics. The mitochondrial shape is always changing according to cell requirements. For example, fused organelles favor the exchange of matrix content and an increase in ATP production. By contrast, fragmented mitochondria are associated with mitophagy and ROS production. Mitochondrial dynamics are regulated by different proteins e.g., the cytoplasmic protein DRP1 is the main regulator of mitochondrial fission, whereas mitochondrial proteins OPA1 and mitofusins regulate the fusion process.

4.4.3. Mitochondrial fusion in pancreatic cancer

Although PDAC cells generally exhibit abnormally fragmented mitochondria due in part to the expression of the *KRAS* oncogene, as described above, the role of mitochondrial fusion in this type of tumor remains controversial. Indeed, since mitochondrial fusion is more commonly observed in normal tissue in comparison to tumoral ones, some authors have hypothesized that the induction of this process could balance the mitochondrial dynamics and reduce oncogenicity [106,107]. In this regard, Yu et al. showed that the overexpression of MFN2 in both *in vitro* and *in vivo* models of PDAC promoted autophagy and a reduction in mitochondrial mass, Oxygen Consumption Rate (OCR), and ATP production. This reduction in oxidative phosphorylation by MFN2 overexpression correlated with decreased cell proliferation, increased G1 arrest, and reduced metastatic lung colonization after tail vein injection. Pharmacological induction of mitochondrial fusion by leflunomide, the FDA-approved anti-arthritis drug, showed similar effects to those of MFN2 overexpression, improving survival in different mouse models of pancreatic cancer [107]. In addition to this observation, other authors demonstrated that the expression of MFN2 was significantly decreased in tumor tissues, while MFN2 overexpression affects the levels of proliferating cell nuclear antigen (PCNA) and

endothelial growth factor A (VEGFA) in HUVEC cells, thus inhibiting cell growth and angiogenesis [108]. Furthermore, MFN2 overexpression suppresses cell proliferation and induces cell autophagy in PDAC cells by inhibiting the PI3K/AKT/mTOR signaling pathway [109]. Altogether, these observations support the notion of exploiting mitochondrial fusion as an effective strategy in PDAC therapy. However, this approach could be a double-edged sword. Indeed, it is necessary to understand, for instance, the molecular mechanisms through which the induction of MFN2 reduces the OXPHOS metabolism in PDAC, since numerous authors have reported that mitochondrial fusion favors an increase in the energy efficiency of both tumor and normal cells [88,110–112].

In contrast, although the inhibition of mitochondrial fusion in PDAC cells has not been studied in-depth, some other studies have shown that some proteins involved in mitochondrial fusion are emerging as key molecules for cancer progression and chemoresistance. Among these, OPA1 has been identified as a prognosis-related gene in several types of cancer and its expression at high levels has been found to correlate with a worse prognosis in PDAC patients [113,114]. In addition, the inhibition of the interaction between Hsp90 and OPA1 in PDAC tumors studied in KPC mice led to a reduction in mitochondrial cristae amount and energy production [115]. Although this evidence suggests a pro-tumorigenic role of mitochondrial fusion, other studies should be carried out to determine if the pharmacological inhibition of OPA1 in PDAC cells curtails tumor growth by targeting angiogenesis, as has already been reported in *in vivo* models of melanoma and breast adenocarcinoma [113,116], or directly affects tumor cells.

In summary, the study of mitochondrial fusion in pancreatic cancer is still at an early stage from a molecular and therapeutic point of view. One of the main challenges is to explain the apparent contradictions found between *in vitro* and *in vivo* models. For example, increased mitochondrial fission found in different PDAC cell lines is correlated with the promotion of glycolic flux [117,118], while in mice, the higher metastatic capacity of PDAC cells was associated with OXPHOS increased, likely due to the expression of proteins involved in mitochondrial fusion [119]. Another necessary evaluation is to understand whether the inhibition of fusion proteins, such as OPA1 and MFN2, has any consequence in the progression and chemoresistance of PDAC, and to determine whether it could be a realistic therapeutic approach considering their important role also in normal tissues, such as the heart and muscle.

4.4.4. Mitochondrial fission in pancreatic cancer

Mitochondrial fission has a pro-tumorigenic role in several cancer types, including lung, colon, breast cancer, melanoma, and hepatocellular carcinoma [62]. Regarding pancreatic cancer, low-moderate levels of DRP1 phosphorylation in Ser616 have been observed in 11 over 12 pancreatic tumor specimens analyzed. In addition, a high level of Ser616-phosphorylated DRP1 and a fragmented mitochondria phenotype have been found in PDAC cell lines and patient-derived cells [100]. In cellular models with RAS activation ($HRas^{G12V}$ expressing), it has been demonstrated that RAS promotes phosphorylation of DRP1 at Ser616 by direct activation of the MAPK pathway, in particular ERK2, and mitochondrial fragmentation. On the other side, DRP1 knockdown has been shown to inhibit the fragmented mitochondria phenotype and tumor cell growth in a mouse model of KRAS-driven pancreatic cancer [118,120]. A study performed on a cohort of 137 patients showed that DRP1 is significantly more expressed in pancreatic tumor tissue than adjacent non-tumor tissues [120]. Furthermore, in addition to the function of DRP1 in mitochondrial dynamics, this protein also affects the regulation of cell proliferation. Indeed, despite the divergent studies about the link between DRP1 and apoptosis, it has been shown that its knockdown reduces cell growth by inhibiting G1-S cell cycle transition and inducing apoptosis in pancreatic cancer cell lines. Moreover, DRP1 knockdown inhibits pancreatic cancer cell migration and invasion by suppressing matrix metallopeptidase 2; conversely, DRP1 overexpression promotes cell growth, migration, and invasion in PDAC cell lines [120]. The role of DRP1 in pancreatic cancer glycolytic metabolism has also been identified by different authors, who reported different facets of the role of this protein in metabolic regulation. Indeed, Nagdas et al. showed that DRP1 knockdown determines a decrease in Hexokinase II expression and, consequently, in glycolytic flux in both RAS-transformed mouse embryonic fibroblasts and PDAC cells. In addition, they showed that the loss of DRP1 reduces efficient fatty acid oxidation and electron transport chain functionality [118]. Liang et al. showed that DRP1 supports aerobic glycolysis, demonstrating that its knockdown dramatically decreased glucose consumption and lactate production, while its overexpression significantly increased these phenomena in a pancreatic cancer cell line [120].

The discrepancies found in the effect of mitochondrial fission on tumor cell growth could be attributed to the non-direct effect of DRP1 or to the extent of mitochondrial fragmentation and, certainly, the role of mitochondrial fission as a pro-oncogene needs further investigation.

4.4.5. Mitochondria dynamics in pancreatic cancer stem cells

A peculiar feature of CSCs is their link to the epithelial-to-mesenchymal transition (EMT) that strictly associates them with metastasis formation. During EMT induction, cells can intravasate, migrate throughout the bloodstream, and colonize a secondary organ. The establishment of a tumor in a new place implies that cells must undergo the opposite mechanism, which is the mesenchymal-to-epithelial transition (MET) [121]. EMT activation in cancer cells is also necessary for their entrance into the CSC state. Recently, we have shown that during progressive de-differentiation, CSCs also undergo, among the modifications cited above, a metabolic shift from a more glycolytic to a more oxidative metabolism [35]. This remodeling may be linked to mitochondrial dynamics and could be important in determining the cell state. Indeed, given the striking changes in mitochondrial architecture that occur when stem cells differentiate, it is reasonable to ask what role mitochondrial dynamics might play [122]. Notably, mitochondrial dynamics are essential for successful asymmetric division in normal stem cells [123] and have been linked to the proliferation and survival of stem cells in normal tissues and some types of cancer [82,122]. Considering that pancreatic CSCs are particularly dependent on the activity of their mitochondria, it might be important to focus on mitochondrial dynamics as a critical process in the homeostasis of these organelles.

Firstly, it is important to highlight that the metabolic plasticity of tumor cells is fundamental during tumor development and metastasis [35]. As recently described, pancreatic CSCs mainly rely on mitochondrial metabolism to maintain their stemness, therefore representing a putative target for their elimination [124]. In this regard, Sancho et al. found that pancreatic CSCs are particularly sensitive to mitochondrial targeting, due to their dependence on OXPHOS [50]. In agreement with this, disrupting mitochondrial function in CSCs by inhibiting the electron transport chain or altering the redox state significantly makes them more sensitive to chemotherapy [56,82]. Thus, these results identified mitochondrial activity as a key vulnerability for pancreatic CSCs. Nevertheless, the relationship between mitochondrial dynamics and stemness in PDAC has not yet been well understood. Indeed, Courtois et al. highlighted that pancreatic CSCs are characterized by the accumulation of small mitochondria and by an increased DRP1/MFN2 ratio in comparison to the differentiated counterpart, indicating that these cells rely on mitochondrial fission. They also demonstrated that DRP1 is overexpressed in PDAC tissues, and this signature is related to lower survival in patients with pancreatic cancer. Moreover, the pharmacological inhibition of mitochondrial fission results in the accumulation of dysfunctional mitochondria that leads to two different aspects: on the one hand, an energy crisis with the consequent cell death by apoptosis; on the other hand, the

inhibition of stemness-related tumorigenicity and invasiveness. These data suggest that the inhibition of mitochondrial fission may represent a promising strategy for designing specific therapies against pancreatic cancer. However, there are still profound inconsistencies, because elevated fission activity results in fragmented mitochondria and less oxidative phosphorylation, which is in contradiction with the general assumption that pancreatic cancer stem cells primarily rely on OXPHOS metabolism. This discrepancy highlights the strong need for further studies on this complex but also important topic.

5. AIM

The high aggressiveness of PDAC is associated with increased resistance to conventional therapies, early progression to metastatic disease, and a significant recurrence rate. Recent studies demonstrate that all these aggressive traits are linked to the presence of a subpopulation of cells within tumors called cancer stem cells (CSCs). Given that a single CSC could regenerate the whole tumor, the study of CSCs hallmarks is crucial for the design of new therapeutic strategies to prevent cancer progression and relapse. CSCs display a heterogenous metabolic profile, which could be fundamental for their adaptability to different environmental stresses and, eventually, to evade chemotherapy. This metabolic plasticity would not be possible without mitochondrial remodeling to maintain cellular homeostasis. However, the role of mitochondria in pancreatic CSCs is not clear yet and, in some cases, even contradictory. Additionally, previous studies of mitochondria arrangement in CSCs have been mainly performed on short-term culture, whereas the mitochondrial function in CSCs over longer periods of culture, which may more accurately reflect their quiescent state *in vivo*, is practically unexplored.

In order to understand the role of mitochondria in long-term CSCs-enriched culture, the general aim of this thesis is to characterize the mitochondrial physiology in progressively dedifferentiated CSCs at three stages of culture (2, 4, and 8 weeks) using a PDAC cellular model previously described in our group [35].

The specific aims of this study can be summarized as follows:

- evaluate the mitochondrial organization in pancreatic CSCs through the analysis of mitochondrial abundance and proteins involved in mitochondrial dynamics;
- evaluate the mitochondrial function in pancreatic CSCs through the analysis of ROS production and of electron transport chain protein complexes expression and activity;
- identify possible molecular targets by functional analysis of specific proteins overexpressed in CSCs;
- assess the effect of inhibitors of mitochondrial respiration on pancreatic CSCs.

6. MATERIALS AND METHODS

6.1. Cell culture

The pancreatic ductal adenocarcinoma cell line Panc1, here called parental (P) cells, was grown in RPMI-1640 supplemented with 10% FBS and 50 µg/ml gentamicin sulfate (all from Gibco, Life Technologies, USA), here reported as differentiated-cell medium (DM) and were maintained in standard conditions for a few passages at 37°C in a 5% CO_2 atmosphere. CSCs were obtained as described previously [35]. Briefly, adherent cells were washed twice in 1X PBS, trypsinized, centrifuged, washed in 1X PBS, and then cultured in stem-specific medium (SsM), i.e., DMEM/F-12 without glucose (from Biowest, France) supplemented with 1 g/L glucose, B27, 1 µg/mL fungizone, 1% penicillin/streptomycin (all from Gibco/Life Technologies, USA), 5 µg/mL heparin (Sigma/Merck), 20 ng/mL fibroblast growth factor (FGF), and 20 ng/mL epidermal growth factor (EGF) (both from PeproTech, United Kingdom). The cells were cultured in non-treated cell culture flasks ideal for the growth of suspension cells and were maintained at 37°C with 5% CO_2 in the SsM until 8 weeks, refreshing twice a week with a new medium. Before each experiment, the cells were passed through a cell strainer (40 µm) to separate and maintain only the cell aggregates/spheres, which were trypsinized to obtain a single-cell suspension. The cell number and cell viability were determined by the trypan blue exclusion test.

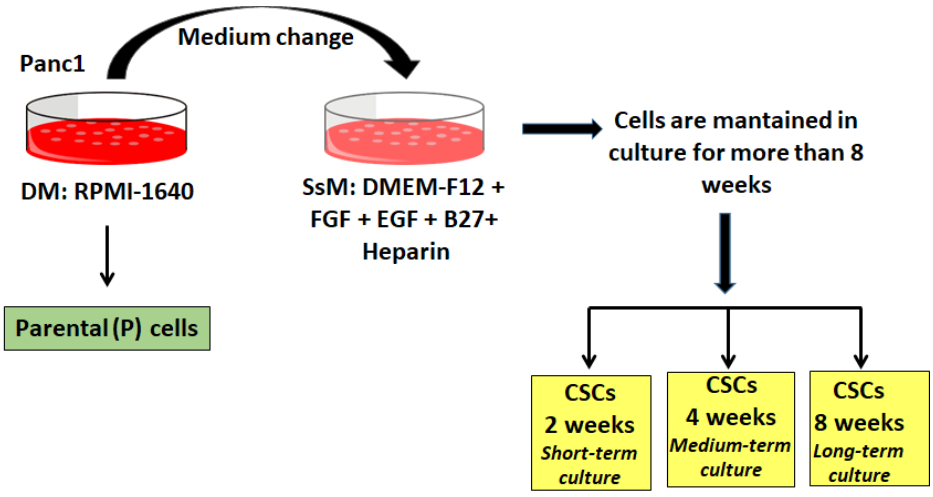

Figure 5. Cell culture of Panc1 parental cells and CSCs. Panc1 parental cells are grown in a differentiated-cell medium (DM), while CSCs are grown in a stem-specific medium (SsM) for 2-,4-, and 8 weeks.

6.2. RNA extraction

Total RNA was extracted from $1x10^6$ cells using TRIzol Reagent (Life Technologies) according to the manufacturer's instructions. Briefly, frozen pellets were resuspended in 400

μL of TRIzol and completely homogenized by pipetting the cell lysate up and down. The samples were incubated for 5 min on ice to permit the complete dissociation of the nucleoproteins, then 80 μL of chloroform was added and subsequently were incubated for 3 min on ice. After incubation, the samples were centrifuged at 12,000 g for 15 min at 4°C and then the aqueous phase containing the RNA was transferred to a new tube by angling the tube at 45°C. To precipitate the RNA, 200 μL of isopropanol was added to the aqueous phase and the RNA pellet was obtained by centrifugation at 12,000 g for 10 min at 4 ^{0}C. To wash the RNA, the pellet was resuspended in 400 μL of 75% ethanol and centrifuged at 7,500 g for 15 min at 4°C. After centrifugation, the resulting pellet was air dry for 20 min at room temperature and finally resuspended in 30 μL of RNase-free water. Purified RNA was quantified with a Nanodrop Spectrophotometer (Thermo Fisher Scientific).

6.3. Real-time PCR (qPCR)

RNA integrity was determined by electrophoresis on a denaturing agarose gel. Total RNA (1μg) was used to synthesize first-strand cDNA by RT-PCR. qPCR was performed in triplicate samples by SYBRGreen detection chemistry using GoTaq qPCR Master Mix (Promega, USA) on a QuantStudio™ 3 Real-Time PCR System (Thermo Fisher Scientific). The cycling conditions used were: 95°C for 10 min, 40 cycles at 95°C for 15 sec, 60°C for 1 min, 95°C for 15 sec, and 60°C for 15 sec. The results were analyzed according to the $2^{-\Delta\Delta Ct}$ method using the *SDHA* gene as endogenous control. The primers used in this study are listed in Table 1.

Table 1. List of human primers sequences used for real-time PCR

Gene	Primer pairs - Sequence (5'-3')	
	Forward	Reverse
NRF1	CCACGTTACAGGGAGGTGAG	TGTAGCTCCCTGCTGCATCT
NRF2	GCGACGGAAAGAGTATGAGC	GTTGGCAGATCCACTGGTTT
TFAM	GTGGTTTTCATCTGTCTTGGC	ACTCCGCCCTATAAGCATCTTG
PGC1α	TGACTGGCGTCATTCAGGAG	CCAGAGCAGCACACTCGAT
CDH1	GACACCAACGATAATCCTCCGA	GGCACCTGACCCTTGTACGT
ZEB1	GTTACCAGGGAGGAGCAGTGAAA	GACAGCAGTGTCTTGTTGTTGTAGAAA
SOX2	GGGAAATGGGAGGGGTGCAAAAGAGG	TTGCGTGAGTGTGGATGGGATTGGTG
NANOG	AGTCCCAAAGGCAAACAACCCACTTC	TGCTGGAGGCTGAGGTATTTCTGTCTC
OCT3/4	GACAGGGGGAGGGGAGGAGCTAGG	CTTCCCTCCAACCAGTTGCCCCAAAC
ND1*	GTCAACCTCGCTTCCCCACCCT	TCCTGCGAATAGGCTTCCGGCT
B2M*	CGACGGGAGGGTCGGGACAA	GCCCCGCGAAAGAGCGGAAG
DRP1	AAGAACCAACCACAGGCAAC	GTTCACGGCATGACCTTTTT
FIS1	CTTGCTGTGTCCAAGTCCAA	GCTGAAGGACGAATCTCAGG
MFN1	TTGGAGCGGAGACTTAGCAT	TTCGATCAAGTTCCGGATTC
MFN2	AGAGGCATCAGTGAGGTGCT	GCAGAACTTTGTCCCAGAGC
OPA1	GGCCAGCAAGATTAGCTACG	ACAATGTCAGGCACAATCCA
MnSOD	CGTGCTCCCACACATCAATC	TGAACGTCACCGAGGAGAAG
CuZnSOD	TCAGGAGACCATTCATCATT	CGCTTTCCTGTCTTTGTACTTTCTTC

POX	GGTAGTCCCCAACGCACA	GCTGTAGCATCCTGGTCATCT
GPX	CCAGTTTGGGCATCAGGAG	CGATGTCAATGGTCTGGAAG
IDH1	CAAGTGACGGAACCCAAAAG	ACCCTTAGACAGAGCCATTTG
CAT	CATCGCCACATGAATGGATA	CCAACTGGGATGAGAGGGTA
IF1	GTGGGGCCTTCGGAAAGAGA	ACAAGGACACGGTGGTCAG
SDHA	GGACCTGGTTGTCTTTGGTC	CCAGCGTTTGGTTTAATTGG

*Primer pairs designed to amplify genomic DNA (gDNA)

6.4. mtDNA Quantification

DNA was extracted by digestion with proteinase K-based protocol. Briefly, cells were resuspended in 700 µL lysis buffer (1 M Tris-HCl, 0.5 M EDTA, 10% SDS, and 5 M NaCl) supplemented with 10mg/ml of proteinase K (all from Sigma/Merck, USA). The samples were incubated at 55˚C for 2 hours and then centrifuged for 10 min at 14,000 rpm. DNA was precipitated with 700 µL isopropyl alcohol, centrifuged for 5 min at 14,000 rpm, washed with 70% v/v ethanol, centrifuged for 5 min at 14,000 rpm, resuspended in 100 µL TE buffer, and quantified with NanoDrop One (Thermo Fisher Scientific). Mitochondrial DNA was quantified by SYBRGreen detection chemistry on a QuantStudio™ 3 Real-Time PCR System (Thermo Fisher Scientific) according to the $2^{-\Delta\Delta Ct}$ method. The mitochondrial gene *MT-ND1* and the nuclear gene *B2M* were amplified from approximately 20 ng of total DNA (primers are listed in Table 1). *MT-ND1/B2M* ratio equals mtDNA copy number per cell, providing an indirect measure of the abundance of mitochondria per cell [125]. Mitochondrial DNA was also quantified by digital droplet PCR. For this procedure, DNA concentration was quantified using the Qubit 4 fluorometer (Invitrogen, Life Technologies) in combination with the Qubit dsDNA HS Assay Kit (Invitrogen, Life Technologies). The QX200 Droplet Digital PCR System (Bio-Rad) and a QX200 ddPCR EvaGreen Supermix (Bio-Rad) were used to determine the concentration in copies/µl of *ND1* gene in our samples. Briefly, 20 µL of reaction mix (supermix, 10 µM primer forward and reverse, 5U/µl restriction enzyme, water, and 0.002 ng of sample) and 70 µL of Qx200 droplet generator oil were transferred into a droplet generator cartridge. To perform the droplet generation, the cartridge was placed into a QX200 droplet generator. The partitioned samples were transferred into a 96-well plate and then placed into a SimpliAmp Thermal Cycler (Applied Biosystems) for the end-point PCR amplification. The cycling conditions used were: 1 cycle at 95˚C for 5 min, 40 cycles at 95˚C for 30 sec and 57˚C for 1 min, 1 cycle at 4˚C for 5 min, and 1 cycle at 95˚C for 5 min. Finally, the fluorescence of the samples was read using Droplet Reader. The absolute copy number was analysed using the QuantaSoft™ Software version 1.7 (Bio-Rad).

6.5.Protein Extraction and Immunoblotting

To prepare samples, frozen cell pellets were resuspended in lysis buffer, i.e., 1 mM Na_3VO_4, 1 mM NaF, 2 mM EDTA, 0.2 mM phenylmethylsulfonyl fluoride (PMSF), 150 mM NaCl, 100x complete protease inhibitor cocktail, and RIPA buffer pH 8.0 (150 mM NaCl, 50 mM Tris-HCl, 1% Igepal, 0.5% sodium deoxycholate, and 0.1% SDS). The lysate was centrifuged at 5,000 rpm for 10 min at 4°C and the supernatant was used for immunoblotting. Protein concentration was measured with Bradford Reagent (SERVA electrophoresis, Germany) using bovine serum album as a standard. Next, 30-40 µg protein suspended in SDS loading buffer was run on 12% SDS polyacrylamide gels and electrotransferred to PVDF membranes (Merck Millipore). Membranes were then incubated for 1 hour at room temperature with blocking solution, i.e. 5% non-fat dried milk in TBST pH 7.5 (100 mM Tris-HCl, 0.1% Tween-20, and 0.9% NaCl). Then membranes were incubated with the primary antibodies at appropriate dilution in blocking solution overnight at 4°C. Primary antibodies included: α-Tubulin (1:1,500, CP06, Oncogene), OXPHOS cocktail (1:1,000, ab110413, Abcam), anti-human IF1 (1:100, clone14/2) [126], HSP60 (1:2,000, Stressgene SPA-807), NDUFA9 (1:1,000, #459100, Invitrogen), ATP5A (1:100, #459240, Invitrogen), MTCO1 (1:1,000, #459600, Novex), SDHB (1:1,000, #459230, Novex), Core1 (1:1,000, #459140, Invitrogen), catalase (1:1000, C0979, Sigma Aldrich). Antibodies against LC3 (1:1,500, #2775), DRP1 (1:1,000, #8570), P-DRP1 (1:1,000, #4494), MFN1 (1:1,000, #14739), MFN2 (1:1,000, #11925) OPA1 (1:1,000, #80471), MFF (1:1,000, #84580), TOM20 (1:1,500, #42406), were obtain from Cell Signaling Technology (Danvers, USA). Blots were then incubated with secondary antibodies for 1 hour at room temperature and the LiteAblot® Plus substrate (EuroClone, Italy) was used for the development of immunoreactive bands. The immunocomplexes were visualized by chemiluminescence using the Chemidoc MP imaging system. Densitometric analysis was conducted using ImageJ software (NIH Image, USA).

6.6. Mitochondrial Staining

The mitochondrial structural network was stained using MitoTracker Green (Invitrogen) according to the manufacturer's instructions. Briefly, cells were grown in a chambered coverslip for cell live imaging (Ibidi, Germany) for 24 hours, then the medium was removed and the solution containing 50 nM MitoTracker Green was added. Cells were incubated for 30 min in the dark and in standard conditions. After incubation, the staining solution was removed, the cells were washed twice with 1X PBS, and a fresh pre-warmed medium was added. Images

were recorded with a confocal laser-scanning fluorescence microscope Leica SP5 (Leica Microsystem, Germany) at 63X magnification.

6.7. Spheroid formation assay

Panc1 parental cells were plated in non-adherent Nunclon Sphera 96-well plates (ThermoFisher Scientific) at a density of 300 viable cells per well and grown in CSC medium. The plate was centrifuged at 1,500 rpm for 10 min at room temperature to bring the cells together and then incubated at 37°C with 5% CO_2 for 8 days. Bright field cell images were acquired using an inverted microscope (Axio Vert. A1, Zeiss, Oberkochen, Germany). The spheroid area was measured using ImageJ software (NIH Image, USA).

6.8. siRNA Knockdown

Panc1 parental cells were plated in a 6-well plate at a density of 3 x 10^5 cells per well and grown in standard conditions for 24 hours. Then cells were transfected with 15 nM of siRNA against OPA1 (SI03019429) or IF1 (SI00908075) and non-specific negative control (#1027281) purchased from Qiagen (Germany), using Lipofectamine 3,000 transfection reagent (Invitrogen, USA) according to the manufacturer's instructions. Briefly, two tubes were prepared as follow: in the first, 3 µl of 15 nM siRNA were added to 125 µl of Opti-MEM (ThermoFisher Scientific); in the second one, 7 µl of Lipofectamine 3,000 were added to 125 µl of Opti-MEM. Both tubes were gently mixed and incubated for 20 min at room temperature, about 250 µl of the mixture was added to the cells. After 48 hours, the medium was removed, and cells were washed twice in 1X PBS, trypsinized, centrifuged, washed in 1X PBS, and then cultured in stem-specific medium (SsM) for 10 days to evaluate the expression of stem markers. The knockdown of OPA1 was confirmed using real-time PCR and immunoblotting.

6.9. Isolation of mitochondria

Mitochondria were isolated according to Nuevo-Tapioles et. al with minor modifications [127]. Cell pellets were homogenized in a glass-Teflon homogenizer with a hypotonic buffer (10 mM MOPS, 83 mM sucrose, pH 7,2) and then incubated on ice for 2 min. After incubation, the same volume of hypertonic buffer (30 mM MOPS, 250 mM sucrose, pH 7,2) was added and then centrifuged at 1,000 x *g* for 5 min at 4°C to eliminate the nucleus and unbroken cells. The supernatant was centrifuged at 1,2000 x *g* for 12 min at 4°C to separate the cytoplasmic fraction. After centrifugation, the pellet was resuspended in buffer A (1 mM EDTA, 10 mM Tris-HCL, 320 mM sucrose, pH 7,4), stored at 80°C, and used within 6 months.

6.10. Sample preparation for Blue Native Gel Electrophoresis (BNGE)

Cells pellets were resuspended in 200 µL of cold 1X PBS, 200 µL of 8 mg/ml digitonin, and incubated on ice for 10 min. After incubation, 1 mL of 1X PBS was added and the samples were centrifugated at 10,000 x *g* for 5 min at 4°C. After the supernatant was removed, the pellet was resuspended in 100 µL of buffer (1,5 M aminocaproic acid, 50 mM Bis-Tris/HCl pH 7), 10 µL of 10% digitonin (200 mg/ml of the one with 50% purity), incubated on ice for 5 min, and centrifuged at 18,000 x *g* for 30 min at 4°C. The supernatant was transferred into another tube and 10 µL of sample buffer (750 mM aminocaproic acid, 50 mM Bis-Tris/HCl, 0,5 mM EDTA, 5% Coomassie Brilliant Blue G-250, pH 7) was added. The samples were stored at -80°C until use. All reagents were purchased from Sigma-Aldrich (Germany).

6.11. Blue Native Gel Electrophoresis and 2D- BNGE

Blue native gel electrophoresis (BNGE) was performed according to Nijtmans et.al and Wittig et.al [128,129]. In brief, for one-dimension BNGE, 50 µg of cellular protein solubilized with digitonin, as described above, were loaded in Pre-cast NativePAGE 3%–12% Bis-Tris gels (# BN1001BOX, Invitrogen, USA). Electrophoresis was carried out at 120 V for 2 hours. To remove excess of blue G-250, cathode buffer B (cathode buffer A, 0.02% Coomassie Brilliant Blue G-250) was replaced by cathode buffer A (50mM Tricine, 15mM Bis-Tris/HCl, pH 7.0) after the blue running front migrated to the middle of the gel. Electrophoresis was maintained under the same conditions until the blue dye front reached the end of the gel. Electroblotting and immunodetection of protein complexes from one-dimensional BNGE were carried out as described above (section 2.4). Two-dimensional blue native gel (2D- BNGE) was performed cutting out a lane of the one-dimension gel with a razor blade. The strips were incubated with a dissociating solution (1% SDS, 1% 2-mercaptoethanol) for 1 hour at room temperature, then they were compressed between the glass plates, leaving the space to cast the separating and stacking gel (this one poured around the one-dimension trip). The second dimension was a 10% SDS-polyacrylamide gel. The samples were electrophoresed at 30 V for 20 min until they entered the stacking gel, after which the voltage was increased to 120 V for 1.5 h. Electroblotting and immunodetection of the protein complexes were performed as described above (section 6.5).

6.12. Mitochondrial Enzyme Activities

Mitochondrial enzyme activities were measured by spectrophotometric determination as previously described [130] with slight modifications. Complex II activity was measured at Abs_{600} using 100 µg of isolated mitochondria in buffer (5 mM $MgCl_2$, 25 mM potassium

phosphate buffer, 3 mM KCN and 2.5 mg/ml BSA) containing 30 μM DCPIP, 1 μM antimycin A, 1 μM rotenone, 10 mM succinate, and 6 mM phenazine methosulfate. The samples to measure complex IV and citrate synthase activities were prepared according to Bugiani et al [131] and Signorile et al [132]. Briefly, the cell pellet was homogenized in 700 μl of buffer A (20 mM MOPS, 0,25 M sucrose, pH 7.4) and 1 ml of 200 μg digitonin. The homogenate was centrifuged at 5,000 x *g* for 5 min at 4°C, the resultant pellet was resuspended in 1 ml of buffer B (20 mM MOPS, 0.25 M sucrose, 1 mM EDTA tetrasodium salt, pH 7.4), centrifuged at 10,000 x *g* for 5 min at 4°C. The supernatant was removed, and the pellet was stored at -80°C. Complex IV activity was measured in 10 mM phosphate buffer, pH 7,4, using 40 μg of protein, and following the oxidation of 10 μM cytochrome c at 550 nm. The citrate synthase activity was measured in a buffer solution (0.5 mM oxaloacetate, 0.1 M Tris-HCl, 0.2% Triton X-100, 0.5 mM acetyl-CoA, and 0.5 mM 5,5-dithio-bis-(2-nitrobenzoic acid)), the reaction was followed at 420 nm.

6.13. ROS production

The 2,7-Dichlorodihydroflurescein diacetate (DCFH-DA) fluorogenic dye (Sigma-Aldrich) was used to measure ROS production. This probe becomes highly fluorescent upon oxidation with hydroxyl, peroxyl, and other ROS. For this assay, cells were plated in 96-well plates (6 x 10^3 cells/well). After 24 hours, cells were incubated in PBS containing 10 μM DCFH-DA for 15 min at 37°C. The cells were washed twice with 1X PBS. The fluorescence (Ex_{485} and Em_{535nm}) was measured using a multimode microplate reader (GENios, Pro, Tecan, Milan, Italy).

6.14. Drug library screening

The effect of seven compounds (sulfameter, butoconazole, glyburide, lomerizine, cimetidine, crystal violet, and telaprevir) from an FDA-Approved Drug library (Selleckchem, Houston, USA) on cellular proliferation of Panc1 cells was determined by crystal violet assay. These compounds were reported in 2021 by Nuevo-Tapioles et.al [127] as inhibitors of mitochondrial respiration in colon cancer cells. For cell proliferation assay, 15,000 cells/well were seeded in a 96-well plate, and after 24 hours, cells were treated with each compound at 1, 10, and 50 μM. Forty-eight hours later, the medium was removed, cells were washed with 1X PBS twice, and incubated with crystal violet solution (0.75% Crystal violet, 0.25% NaCl, 50% ethanol, and 37% formaldehyde) for 5 min at room temperature. The plate was washed three times with Milli-Q water and air-dry overnight. The fixed cells were lysed with 100 μL of lysis buffer (1% SDS and 1X PBS) and incubated for 40 min at room temperature on a shaker. After incubation,

the absorbance (Abs_{595}) was measured using a multimode microplate reader (GENios, Pro, Tecan, Milan, Italy).

6.15. Cell viability assay

Cell viability was determined using the OZBlue Cell Viability kit following the manufacturer's instructions. This method is based on fluorimetric/colorimetric quantification of metabolic activity in living cells. Cells were seeded in 96 opaque-walled cell culture plates (clear bottom). After treatments, 10 µL of OZBlue reagent was added directly into the cell medium and then cells were incubated for 4 hours in the standard culture conditions. After incubation, the fluorescence (560 nm_{Ex}/590 nm_{Em}) was measured using a multimode microplate reader (GENios, Pro, Tecan, Milan, Italy).

6.16. Flow cytometry

For flow cytometry analysis, a suspension of cells in PBS was centrifuged at 1,200 rpm for 5 min at 4°C and the resulting pellet was resuspended in FACS solution (1% FBS, 0.1 % NaN_3, and 1X PBS). The cell suspension (at least 10,000 events) was analyzed using a flow cytometer FACS Calibur (Becton Dickson, USA). The procedures performed using flow cytometry are described below:

6.17. Cellular proliferation assay

Cellular proliferation was determined by the incorporation of a fluorescent stain into cytoplasm using CellTrace™ Far Red (Thermo Fisher Scientific) following the manufacturer's instructions. The stock concentration of 1 mM was made by the addition of 20 µL dimethyl sulfoxide (DMSO). A working concentration of 1 µM was made by the addition of 1 µl of stock solution in 1 ml of 1X PBS. Cells at 50% of confluence were incubated in the dark for 20 min at 37°C with 1 µM CellTrace Far Red. After incubation, the cells were washed twice with 1X PBS and prepared for flow cytometry analysis. The analysis of cellular proliferation was carried out at 24 and 48 hours after treatments.

6.18. Cell death assay

Cell death was determined by flow cytometry after staining with propidium iodide and annexin V (Annexin V-FITC apoptosis detection kit, eBioscience, USA). After trypsinization, cells were washed twice with 1X PBS and resuspended in 200 µL of 1X binding buffer. After adding 5 µL Annexin V, the cell suspension was incubated for 10 min at room temperature, and then cells were washed twice with 1X binding buffer. Finally, the cells were incubated with 10 µL propidium iodide before FACS analysis.

6.19. Statistical Analysis

Results are presented as mean ± standard error of the mean (SEM) of at least three different biological replicates. Statistical differences were determined by Student's t-student two-sided and one-way analysis of variance (ANOVA) for multiple comparisons. Data were analyzed using Excel Microsoft 365 and GraphPad Prism 7, and statistical significance was defined as $p < 0.05$.

7. RESULTS

7.1. Panc1 CSCs have increased mitochondrial mass

To study the mitochondrial arrangement and function of CSCs, we cultured Panc1 parental (P) cells in a stem-specific medium (SsM) at three different time points, short-term (2 weeks), medium-term (4 weeks), and long term (8 weeks), as previously described by our group [35]. Indeed, with this cellular model, we showed that gradually de-differentiated CSCs present metabolic plasticity that ends with the acquisition of a quiescent state. In order to understand the role of mitochondria in the metabolic adaptability of CSCs, we evaluated the protein expression of TOMM20 (Figure 6 A), a known mitochondrial marker, by western blotting: the densitometric analysis shows that the expression of this protein is significantly higher in CSCs relative to parental cells (Figure 6 A). In addition to this, we also evaluated the expression of another mitochondrial marker, i.e. HSP60, whose expression shows a similar pattern to that of TOMM20 (Figure 6 A). Furthermore, the quantification of mitochondrial DNA copy numbers (mtDNA) performed through digital droplet PCR (Figure 6 B) and qPCR (Figure 6 C) also evidences a significant increase of mtDNA in CSCs compared to parental cells, particularly in medium- and long-term culture CSCs (4 and 8 weeks). Since an increase of mitochondrial mass might be associated with a higher production of new mitochondria or with a reduction of mitochondria engulfment through mitophagy, we determined the expression of genes involved in mitochondrial biogenesis and of the autophagosomal marker LC3-II, respectively, in Panc1 CSCs. Figure 6 D shows that the mRNA expression levels of four genes regulating mitochondria biogenesis, such as NRF1, NRF2, TFAM, and PGC1α, are significantly higher in CSCs than in parental cells. Nevertheless, there are no significant differences between CSCs, suggesting that a sustained expression of these genes would be necessary to maintain the stemness at all three-time points. On the other side, the analysis of LC3-II protein expression does not show any marked difference between parental and CSCs, suggesting that basal autophagy is similar in both types of cells (Figure 6 E). These results indicate that Panc1 CSCs show more mitochondrial mass, likely attributable to increased mitochondrial biogenesis.

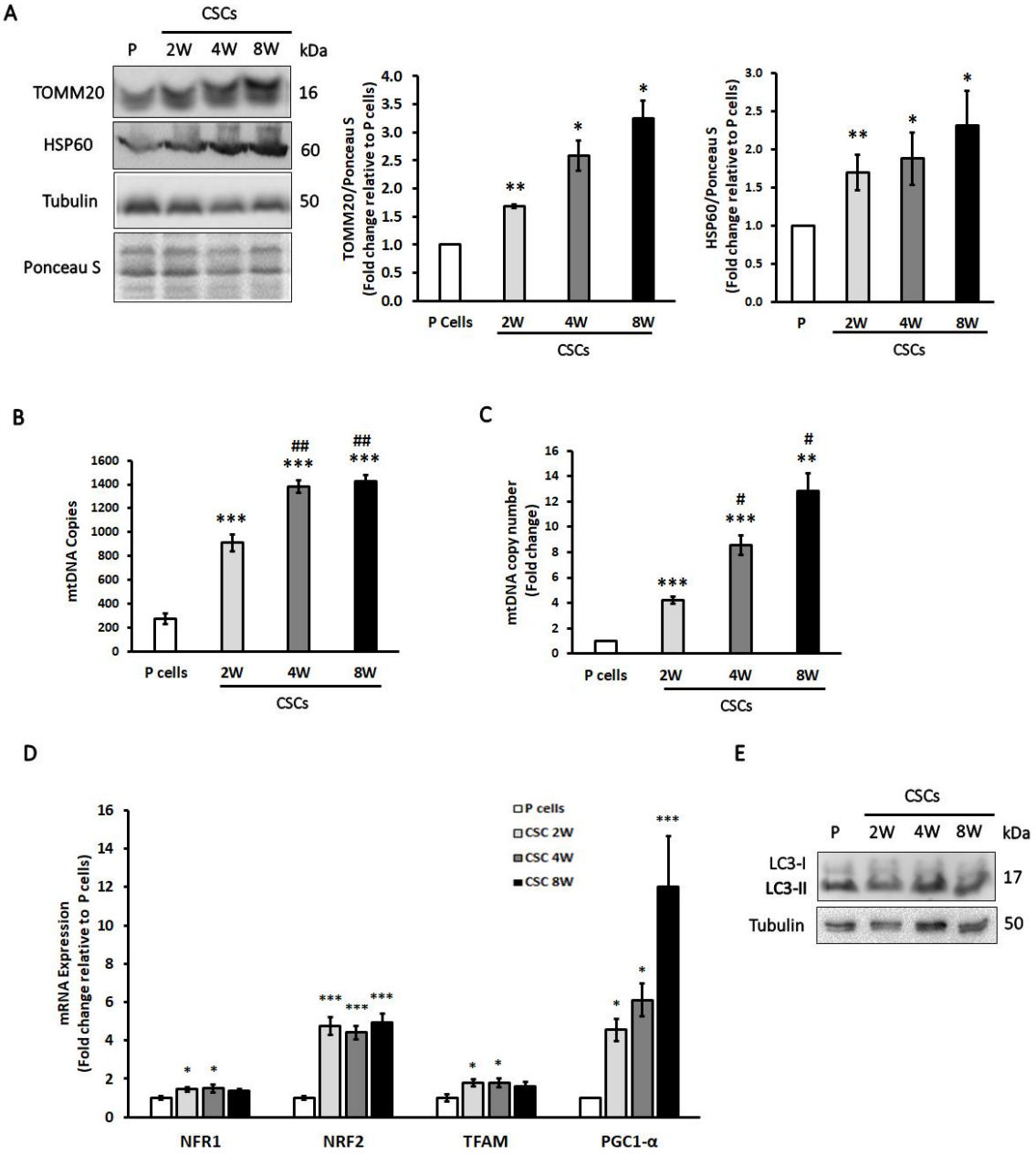

Figure 6. Panc1 cells cultured in the stem-specific medium for 2-, 4-, and 8-weeks exhibit an increase of mitochondrial mass. (A) Left panel, representative immunoblot of TOMM20 and HSP60 in Panc1 parental (P) cells and CSCs at 2 weeks (2W), 4 weeks (4W), and 8 weeks (8W) of culture; right panel, densitometry analysis of TOMM20 and HSP60. **(B)** Quantification of mtDNA copies by digital droplet PCR and **(C)** real-time PCR (qPCR). **(D)** mRNA expression levels of genes involved in mitochondrial biogenesis in P cells and CSCs. Levels are normalized to SDHA. The Values are reported as fold change relative to P cells. **(E)** Representative immunoblot of LC3-II. Histogram legends: white: P cells; light grey: CSCs 2 weeks (2W); dark grey: CSCs 4 weeks (4W); black: CSCs 8 weeks (8W). Bars indicate the mean ± SEM of the indicated samples. Statistical legends: Parental vs CSCs = * $p < 0.05$, ** $p < 0.01$, ***$p<0.001$; 2W CSCs vs CSCs= # $p < 0.05$, # # $p < 0.01$

7.2. Mitochondrial fusion is increased in Panc1 CSCs

To investigate the link between stemness acquisition and mitochondrial dynamics, we compared the mitochondrial morphology of CSCs with parental cells using the MitoTracker Green fluorescent probe. This probe is a green-fluorescent dye that localizes to mitochondria regardless of mitochondrial membrane potential. Figure 7 shows that mitochondria exhibit a more tubular and less fragmented shape in CSCs compared to parental cells. To confirm this observation at a molecular level, we evaluated the expression at mRNA and protein levels of the main mediators of mitochondrial fusion and fission, such as DRP1 and FIS1, which regulate fission, and OPA1, MFN1, and MFN2, which support fusion. The analysis of the expression at mRNA levels of these markers shows that there are no significant differences between CSCs and parental cells independently of the term culture (Figure 8). However, it is well known that mitochondrial dynamics proteins are strongly regulated at the posttranslational level, e.g. the phosphorylation of DRP1 on Ser616 enhances its function supporting mitochondrial fission. Thus, we quantified the protein expression levels of these fission and fusion markers by immunoblot, as shown in Figure 9 A. Our data show that CSCs exhibit significantly lower phosphorylation of DRP1 at Ser616 than parental cells and this decrease is substantial in CSCs at medium- and long-term cultures, i.e. 4- and 8-weeks (Figure 9 B). On the other side, the expression of OPA1 is significantly higher in CSCs in comparison to parental cells (Figure 9 A). Interestingly, the quantitative analysis of OPA1 by western-blot (Figure 9 C) reveals that CSCs present an imbalance in the isoforms of OPA1, predominating short isoforms. In addition, as shown in Figure 9 D, the transition from long (upper band) to short isoforms (lower band) takes place during the first days of culture in SsM, which suggests that the cleavage of OPA1 is an early event and might be important during the process of stemness acquisition. In addition to OPA1, the expression of MFN2 is increased in CSCs at 4 weeks of culture (Figure 9 A). Taken together, these data indicate that Panc1 CSCs show increased mitochondrial fusion; of note, the higher expression of short isoforms of OPA1 in CSCs than parental cells**.**

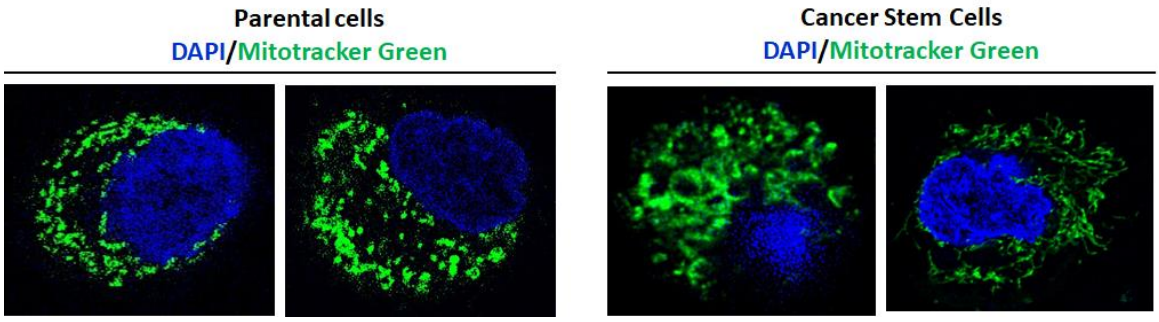

Figure 7. Panc1 CSCs show elongated mitochondria. Representative confocal images of mitochondria stained with Mitotracker green (green signal) and nucleus stained with DAPI (blue signal) in parental cells and cancer stem cells at 63X magnification.

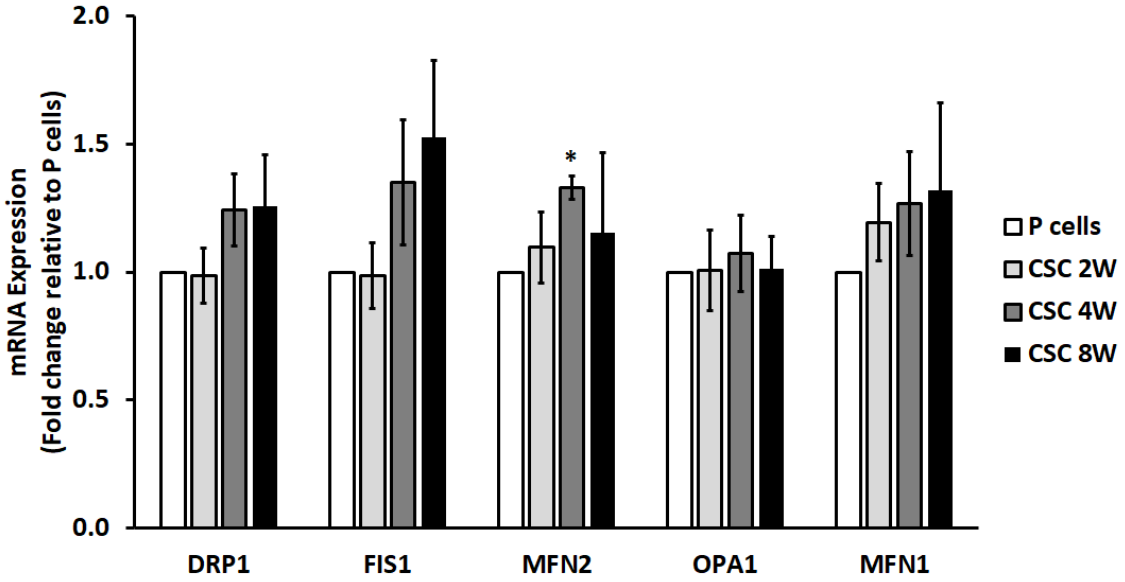

Figure 8. Expression of genes involved in mitochondrial dynamics in Panc1 cells cultured in the stem-specific medium for 2-,4-, and 8-weeks. Real-time PCR analysis of relative mRNA expression levels of genes involved in mitochondrial fusion (OPA1, MFN1, and MFN2) and mitochondrial fission (DRP1 and FIS1) in P cells and CSCs. Levels are normalized to SDHA. The Values are reported as fold change relative to P cells. Histogram legends: white: P cells; light grey: CSCs 2 weeks; dark grey: CSCs 4 weeks; black: CSCs 8 weeks. Bars indicate the mean ± SEM of the indicated samples. Statistical legends: Parental vs CSCs = * $p < 0.05$.

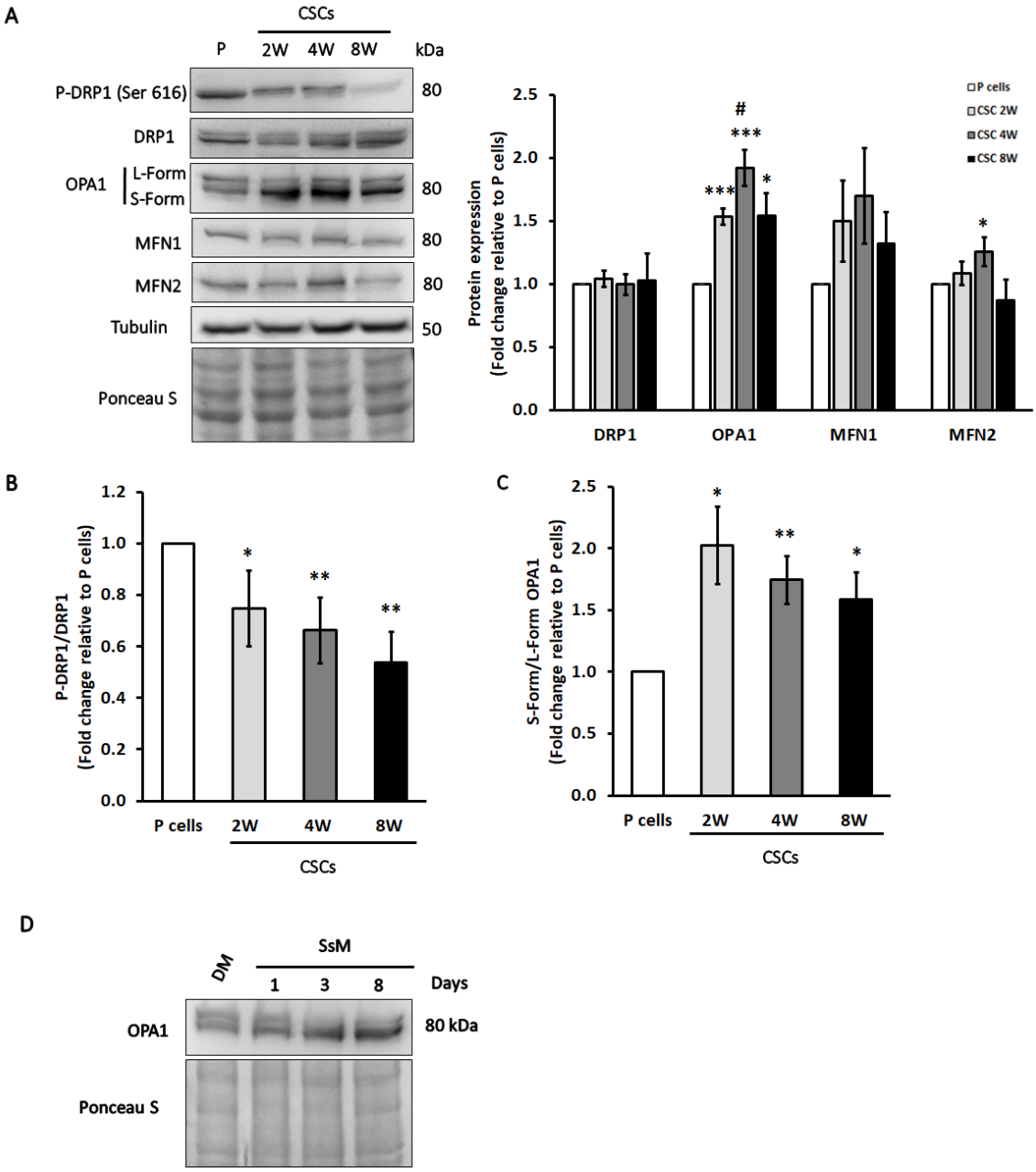

Figure 9. Mitochondrial fusion is enhanced in Panc11 CSCs. (A) Left panel, representative immunoblots of the expression of proteins regulating mitochondrial dynamics for parental cells and CSCs; right panel, densitometry analysis average of three different biological samples of the total amount of proteins. Ponceau Stain and tubulin are shown as loading controls. The ratio of the densitometry analysis of **(B)** phosphorylation of DRP1 (Ser616)/total DRP1 and **(C)** short/long OPA1 isoforms. **(D)** Representative immunoblot of the expression of OPA1 in Panc1 cells grown in differentiated-cell medium (DM) and stem-specific medium (SsM) for 1, 2, and 8 days. Ponceau stain is shown as the loading control. The values are reported as fold change relative to P cells. Histogram legends: white: P cells; light grey: CSCs 2 weeks (2W); dark grey: CSCs 4 weeks (4W); black: CSCs 8 weeks (8W). Bars indicate the mean ± SEM of the indicated samples. Statistical legends: Parental vs CSCs = * $p < 0.05$, ** $p < 0.01$, ***$p<0.001$; 2W CSCs vs CSCs= # $p < 0.05$

7.3. OPA1 modulates the tumorsphere formation

Considering the overexpression of OPA1 in CSCs, next we studied the role of this protein in tumorsphere formation in the Panc1 cell line by silencing OPA1 with siRNA. Real-time PCR and immunoblotting were used to analyze the efficiency of OPA1 silencing (Figure 10 A). Roughly, the reduction of OPA1 was 80% and 60% at mRNA and protein levels, respectively. To study the role of OPA1 in the determination of stemness, we analyzed the tumorsphere forming ability: we seeded transfected cells in SsM and measured sphere size after 8 days of incubation in standard conditions. Figure 10 B shows that sphere size is significantly reduced to more than 50% in siOPA cells compared with control cells. To further investigate the effect of OPA1 silencing on stemness, we assessed the expression of some key stem markers using real-time PCR (Figure 10 C). A significant decrease in the expression of *OCT3/4* was observed in siOPA cells compared with that in the control cells. Conversely, the expression of *CDH1*, which decreases during EMT, is significantly higher in siOPA1 cells relative to control cells. The expression of the other stem markers remained unaltered after OPA1 silencing. Interestingly, the levels of OPA1 mRNA are maintained successfully decreased in Panc1 CSCs after 10 days of incubation in SsM using the siRNA method (Figure 10 C). These results indicate that OPA1 modulates the tumorsphere formation, likely through a possible role in EMT.

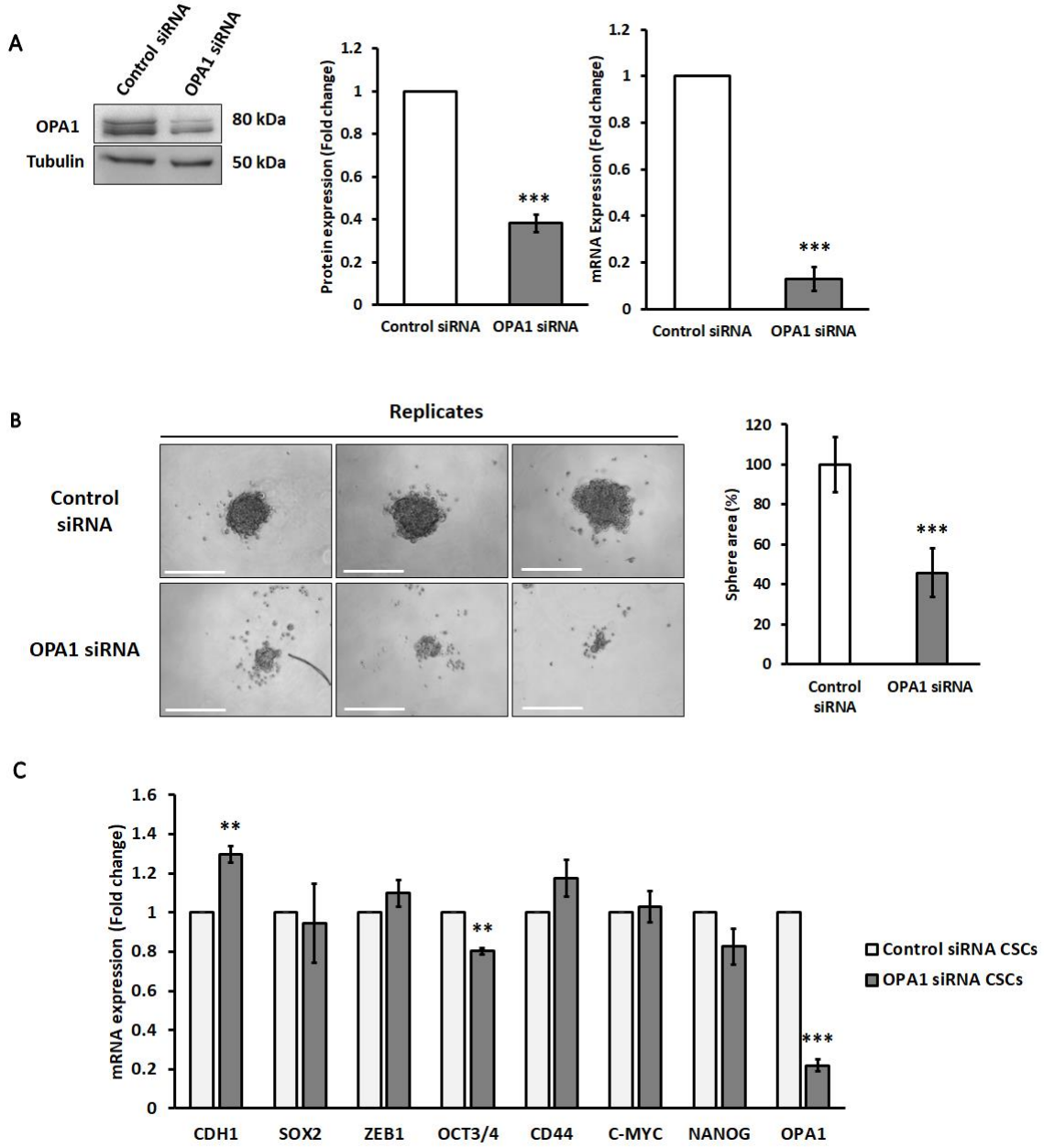

Figure 10. Knockdown of OPA1 reduces sphere formation in Panc1 cells. (A) Protein and mRNA expression levels of OPA1 after its silencing in Panc1 parental cells: the left panel depicts a representative immunoblot against OPA1 in Panc1 cells after 72 hours of transfection using siRNA OPA1. Whereas the right panel shows the mRNA expression levels of OPA1 in Panc1 cells after 48 hours of transfection using siRNA OPA1. **(B)** After 48 of transfection with siRNA OPA1, Panc1 cells were seeded in non-adherent Nunclon Sphera 96-well plates for 8 days. The left panel is bright field microscopy images of spheres in control and silenced cells and the right panel is the quantification of the sphere size. Scale bar 100 µm. **(c)** QPCR analysis of relative mRNA expression levels of key EMT/stemness genes in Panc1 cells transfected with siRNA OPA1 and grown in the stem-specific medium for 10 days. mRNA OPA1 expression was also quantified. Levels are normalized to *SDHA*. Histogram legends: light grey: control siRNA cells; dark grey: siRNA OPA1 cells. The Values are reported as fold change relative to control siRNA cells. Statistical legends: control siRNA cells vs siRNA OPA1 cells = * $p < 0.05$, ** $p < 0.01$, ***$p<0.001$

7.4. Panc1 CSCs show altered mitochondrial respiratory complex activity

The increase of mitochondrial mass in CSCs prompted us to investigate the mitochondrial function in these cells, particularly the expression of proteins involved in the electron transport chain that have recently been proposed as possible therapeutical targets in refractory cancers, such as PDAC [73,133]. The immunoblotting and the relative densitometric analysis of the subunits that constitute OXPHOS machinery show a significant increase of complex II (CII), III (CIII), and IV (CIV) at protein levels in CSCs relative to parental cells (Figure 11 A**).** However, as above described, CSCs show a higher amount of mitochondria, thus we normalized the expression of the complexes on the expression levels of TOMM20. Indeed, the densitometric quantification normalized on TOMM20 levels shows that, despite CSCs present a higher mitochondrial mass, the expression of the OXPHOS complexes is similar to that of the parental cells **(**Figure 11 B). On the other side, the expression of ATPase inhibitor factor (IF1), a physiological inhibitor of mitochondrial ATP synthase, is significantly increased in CSCs compared to parental cells, notably in CSCs at 8 weeks (Figure 11 C). In order to analyze whether OXPHOS complexes in CSCs have altered functionality, we investigated the activity of the respiratory complexes II and IV by spectrophotometric assays (Figure 11 D). A significantly decreased activity for both complexes is observed in CSCs at 2 weeks compared to parental and other CSCs. At the next step of de-differentiation, i.e. CSCs at 4 weeks, there is a marked increase in these activities, whereas CSCs at 8 weeks of culture show a trend of decrease of CIV in comparison to the previous time point. In addition to the analysis of CII and CIV, we also analyzed citrate synthase activity as an internal control and, in line with our previous published data [35], its activity is increased at 4 weeks of culture and decreased at 8 weeks. Taken together, these data confirm the previous observations regarding the metabolic plasticity of these cells during the epithelial-mesenchymal transition and the acquisition of stemness [35].

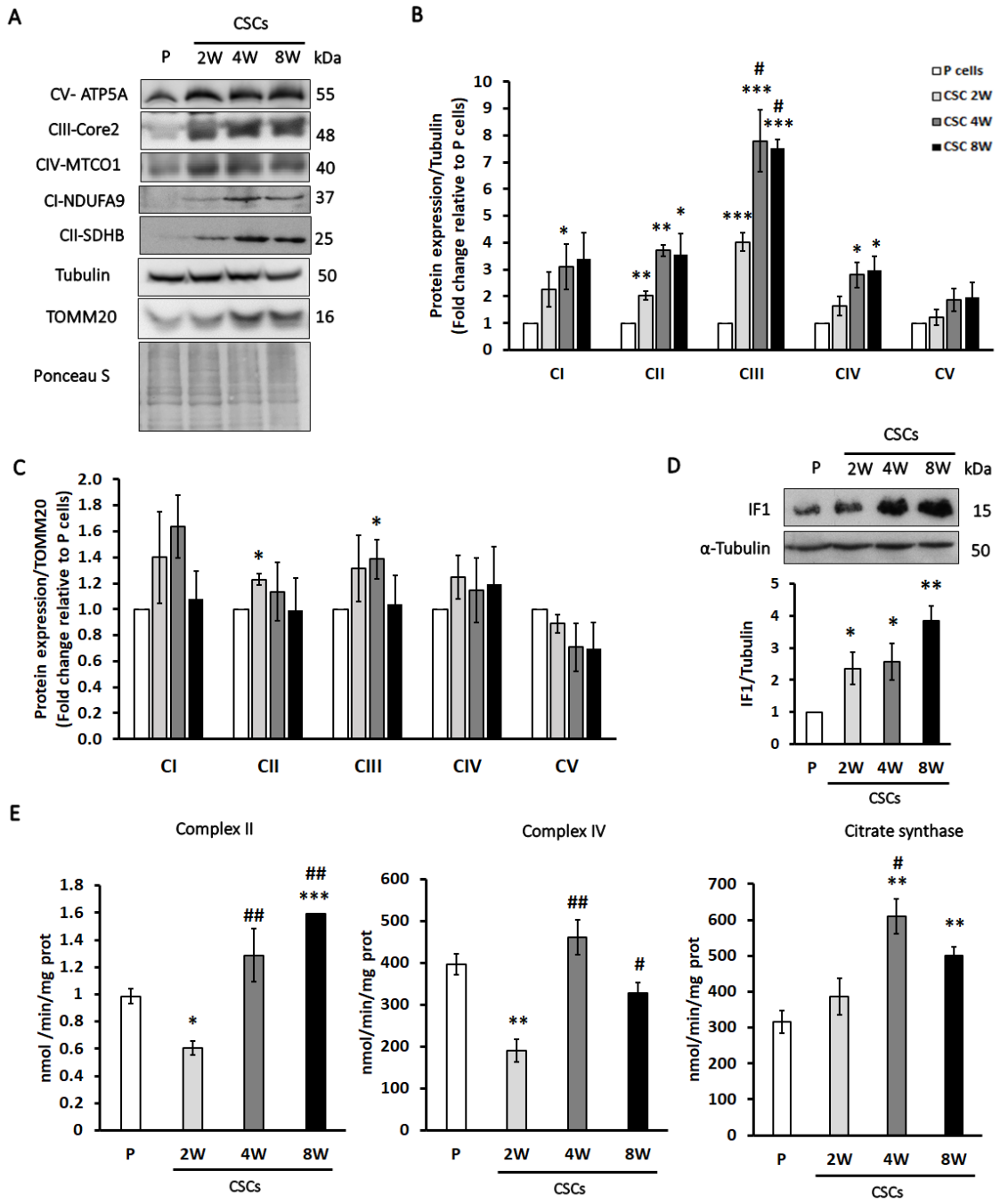

Figure 11. Panc1 CSCs show altered mitochondrial respiratory complex activity. (A) Representative immunoblots of three different biological samples of the expression of mitochondrial respiratory proteins from complex I (NDUFA9), complex II (SDHB), complex III (core2), complex IV (MTCO1), complex V (ATP5A). Ponceau Stain, tubulin, and TOMM20 are shown as loading controls. **(B)** Densitometric quantification of mitochondrial respiratory proteins normalized to tubulin. **(C)** Densitometric quantification of mitochondrial respiratory proteins normalized to TOMM20. **(D)** Representative immunoblot of ATPase inhibitory factor 1 (IF1) and densitometric quantification (histogram) of three different biological replicates of IF1 expression. Tubulin is shown as a loading control. **(E)** The histograms show the enzymatic activity of the complex II, complex IV, and citrate synthase of three different biological replicates by spectrophotometry. The values are reported as fold change relative to P cells. Histogram legends: white: P cells; light grey: CSCs 2

weeks; dark grey: CSCs 4 weeks; black: CSCs 8 weeks. Bars indicate the mean ± SEM of different experiments as indicated. Statistical legends: Parental vs CSCs = * $p < 0.05$, ** $p < 0.01$, ***$p<0.001$; 2W CSCs vs CSCs= # $p < 0.05$, # # $p < 0.01$

7.5. Panc1 CSCs have a reorganization of OXPHOS Complexes

Because changes in mitochondrial respiratory activity might also be linked to the assembly of OXPHOS complexes into structures called supercomplexes, we carried out a comparative analysis of supercomplex (SC) formation in mitochondria-enriched samples of parental cells and CSCs by blue native gel electrophoresis (BNGE). One-dimension (1D)-BNGE revealed that CIII and CIV are mainly found in their monomeric form, with the remainder spread between SC+CIII, and SC+CIV supercomplexes (Figure 12 A). The quantitative analysis of the blots shows that CSCs at 4 and 8 weeks exhibit a significantly decreased formation of supercomplexes containing CIII in comparison to the parental cells (Figure 12 A, lower part). Interestingly, between CSCs, the group of CSCs at 4 weeks of culture show the lowest abundance of CIV-containing supercomplexes. No significant differences were found in CI-containing supercomplexes, whereas CV and CII did not participate in mitochondrial supercomplex formation, as reported by other authors [66]. The levels of free complexes are higher in CSCs than in parental cells; this increase for CIII and CIV is marked in CSCs at medium- and long-time cultures (4 and 8 weeks, respectively) (Figure 12 A, lower part). Next, the supramolecular assemblies that are present during 1D-BNGE were dissociated into the individual complex subunits by 2D-BNGE and detected with an OXPHOS antibody cocktail. Typical results from each sample type are shown in Figure 12 B. Complex V is visible only in a monomeric state in parental cells, whereas CSCs show different oligomeric states of complex V that likely correspond to dimeric forms (see red rows). Taken together, the findings demonstrate that the abundance and composition of respiratory supercomplexes are substantially changed in CSCs compared to parental cells, suggesting a possible role of these structures to maintain the metabolic requirements during the program of dedifferentiation.

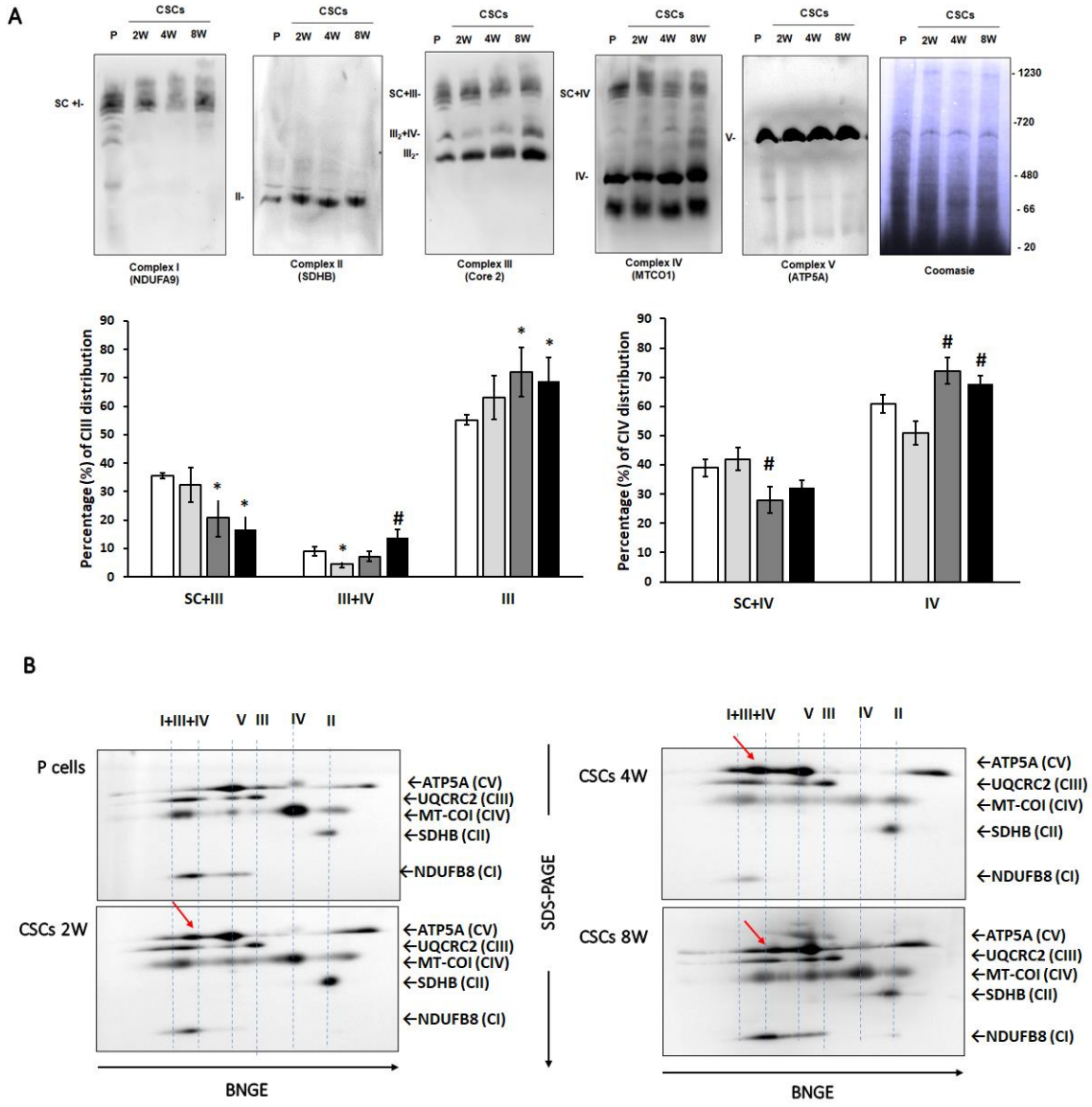

Figure 12. Panc1 CSCs show an increased amount of mitochondrial respiratory supercomplexes (SCs). (A) one-dimensional blue native gel (1D-BNGE) characterization of mitochondrial supercomplexes in Panc1 parental and CSCs. The upper panel depicts representative BN-immunoblots using antibodies against the indicated subunits of the OXPHOS complexes. The migration of SC+CI (NDUFA9); CII (SDHB); SC+CIII, $CIII_2$ + CIV, and CIII (Core 2); SC+CIV and CIV (MTCO1); CV (ATP5A) are indicated. Coomassie-stained gel is shown as the loading control. The lower panels show the histograms with the densitometric analysis of supercomplexes containing CIII and CIV. The values are reported as percentages. Histogram legends: white: P cells; light grey: CSCs 2 weeks (2W); dark grey: CSCs 4 weeks (4W); black: CSCs 8 weeks (8W). Bars indicate the mean ± SEM of different experiments as indicated. Statistical legends: Parental vs CSCs = * $p < 0.05$; 2W CSCs vs CSCs= # $p < 0.05$. **(B)** Samples of parental and CSCs were run on a 2D-BNGE and immunodetected with the indicated antibodies. Red arrows point the dimeric form of ATP synthase.

7.6. Pancreatic CSCs have increased reactive oxygen species production

The reorganization of OXPHOS complexes is also involved in the generation of reactive oxygen species that are important signaling molecules during the acquisition of stem-like phenotype. In fact, the major sites for ROS production in normal metabolism are the CI and CIII of the mitochondrial electron transport chain. Therefore, total ROS levels were measured in parental cells and CSCs using DCFH-DA fluorescent probe. The ROS levels are significantly higher in all CSCs compared to the parental cells (Figure 13 A). However, it is noteworthy that among CSCs, the ones at 8 weeks of culture show significant lower levels in comparison to CSCs at 2 weeks. This finding suggests that CSCs increase the ROS production during the early stages of dedifferentiation, but once they accomplish the quiescent state, ROS levels begin to decline. As an increase of ROS generation also implies the regulation of the different proteins to respond to oxidative stress, the expression of the genes involved in antioxidant response was evaluated by real-time PCR. As expected, the results in the Figure 13 B indicate that mRNA expression levels of mitochondrial antioxidant manganese superoxide dismutase (*MnSOD*), peroxidase (*POX*), and glutathione peroxidase (*GPX*) are significantly higher in CSCs than parental cells. In contrast, the mRNA levels of cytosolic copper-zinc superoxide dismutase (*CuZnSOD*) and catalase are significantly decreased in CSCs relative to parental cells. The decrease of catalase level was further confirmed at the protein level by immunoblotting (Figure 13 C). Altogether, these results demonstrate that CSCs have an overall increase of ROS production accompanied by overexpression of antioxidant genes, excepting catalase and CuZnSOD. Of note, the marked reduction of the catalase expression in CSCs suggests that maintaining the levels of H_2O_2 could be necessary to support the stemness at all three CSCs time-points.

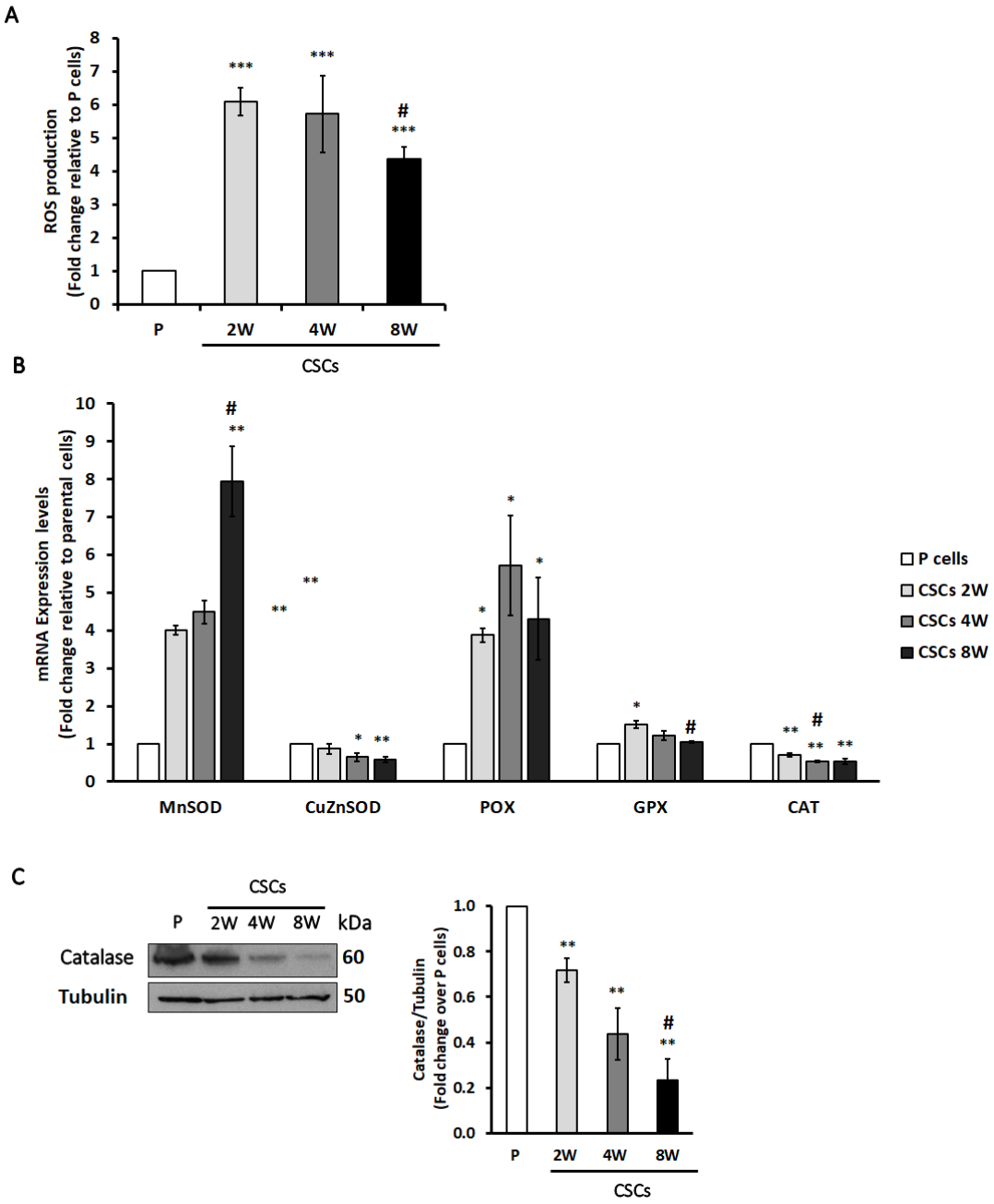

Figure 13. Panc1 CSCs have increased reactive oxygen species production. (A) Histograms show ROS production in parental (P) cells and CSCs measured by DCFH-DA assay. **(B)** Real-time PCR analysis of relative mRNA expression levels of genes involved in ROS response (*MnSOD, CuZnSOD, POX, GPX*, and *CAT*) in P cells and CSCs. Levels are normalized to *SDHA*. **(C)** Representative immunoblot of catalase and densitometric quantification (histogram) of three different biological replicates of catalase expression. Tubulin was used as the loading control. The values are reported as fold change relative to P cells. Histogram legends: white: P cells; light grey: CSCs 2 weeks; dark grey: CSCs 4 weeks; black: CSCs 8 weeks. Bars indicate the mean ± SEM of the indicated samples. Statistical legends: Parental vs CSCs = * $p < 0.05$, ** $p < 0.01$, ***$p<0.001$; 2W CSCs vs CSCs= # $p < 0.05$.

7.7. IF1 supports the stem features of PDAC CSCs

As previously shown in Figure 11 C, the levels of the ATPase inhibitor factor IF1 are significantly higher in CSCs compared to parental cells. However, the biological function of this protein in the acquisition of stemness in cancer cells is currently unknown. To evaluate the role of IF1 in pancreatic CSCs, we used the siRNA strategy to transiently silence this protein in the Panc1 cell line. The knockdown efficacy was assessed by real-time PCR and immunoblotting (Figure 14 A and B), showing that IF1 was reduced at mRNA level by 80%. Our first approach was to identify whether the viability of parental Panc1 cells was influenced by the silencing of this protein. As shown in Figure 14 C-E, IF1 knockdown does not cause any significant change in the viability, apoptosis, and cellular proliferation in parental Panc1 compared to control siRNA cells.

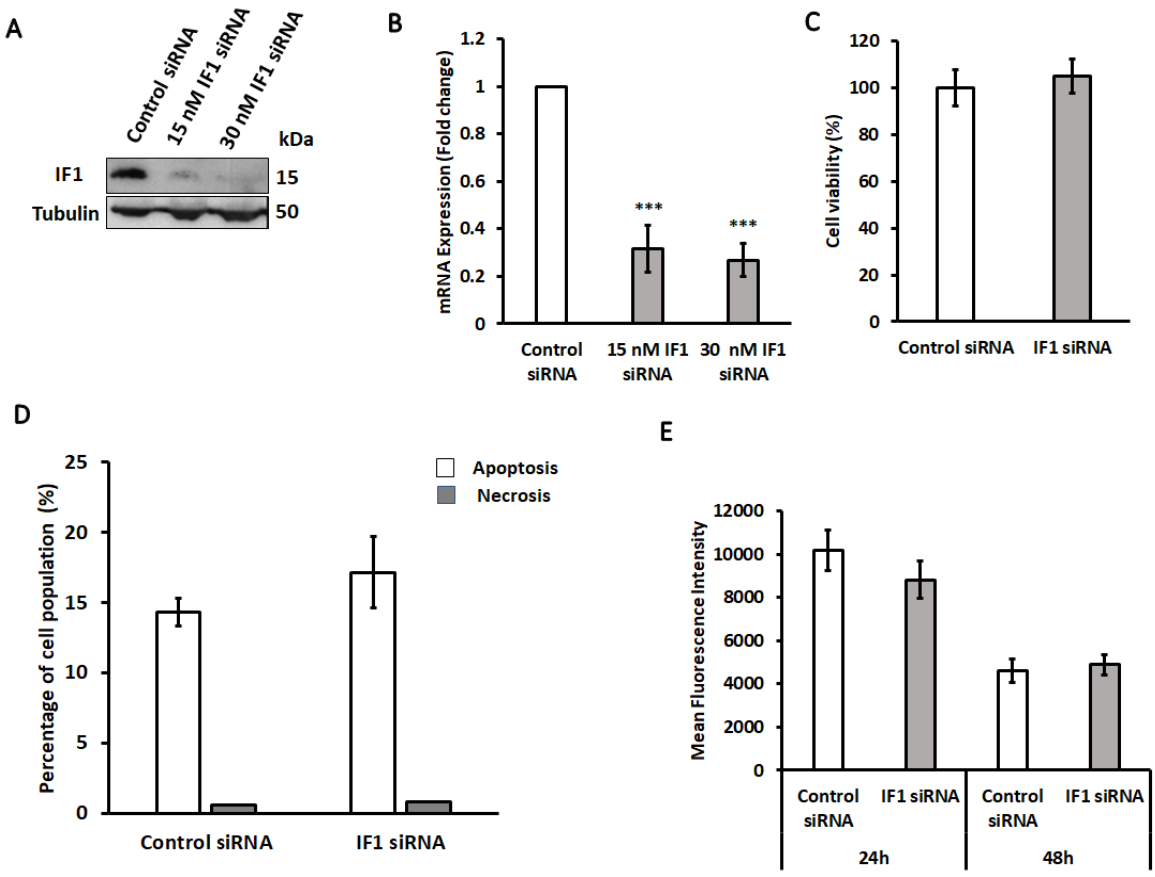

Figure 14. Knockdown IF1 does not affect the viability of Panc1 cells. The knockdown of IF1 was confirmed using immunoblotting and real-time PCR. **(A)** Representative immunoblot against IF1 in Panc1 cells after 72 hours of transfection using IF1 siRNA at two different concentrations. **(b)** mRNA expression levels of IF1 in Panc1 cells after 48 hours of transfection using IF1 siRNA at two different concentrations. **(C)** Cell viability in control cells and IF1 siRNA cells was assessed by crystal violet after 48 hours of transfection. **(D)** Cell death quantification by flow cytometry using annexing V staining after 48 hours of transfection. **(E)** Cellular proliferation in control cells and IF1 siRNA cells

was assessed by the incorporation of the CellTrace™ Far Red probe after 24h and 48h of transfection. Histograms show the results of three different biological replicates

Considering the overexpression of IF1 in CSCs, we further tested whether IF1 could affect the tumorsphere forming ability: we seeded transfected cells in SsM and measured the sphere size after 8 days of incubation in standard conditions. Interestingly, the IF1 protein remained silenced even after cells were grown in SsM for 10 days (Figure 15 A). As shown in Figure 15 B, the sphere area is significantly reduced by approximately 50% in siIF1 cells when compared to control cells. In order to find an explanation for this drastic reduction in tumorsphere formation, we assessed the expression of some key stem markers using real-time PCR (Figure 15 C). A significant decrease in the mRNA expression of *OCT3/4* and *SOX2* is observed in siIF1 cells compared to control cells, whereas the expression of *CDH1* is significantly higher in siIF1 cells than control cells. The expression of the other stem markers remained unaltered after IF1 silencing (Figure 15 C). These results indicate for the first time that IF1 knockdown affects the tumorsphere formation in pancreatic CSCs, likely through modulation of the EMT program and energy metabolism.

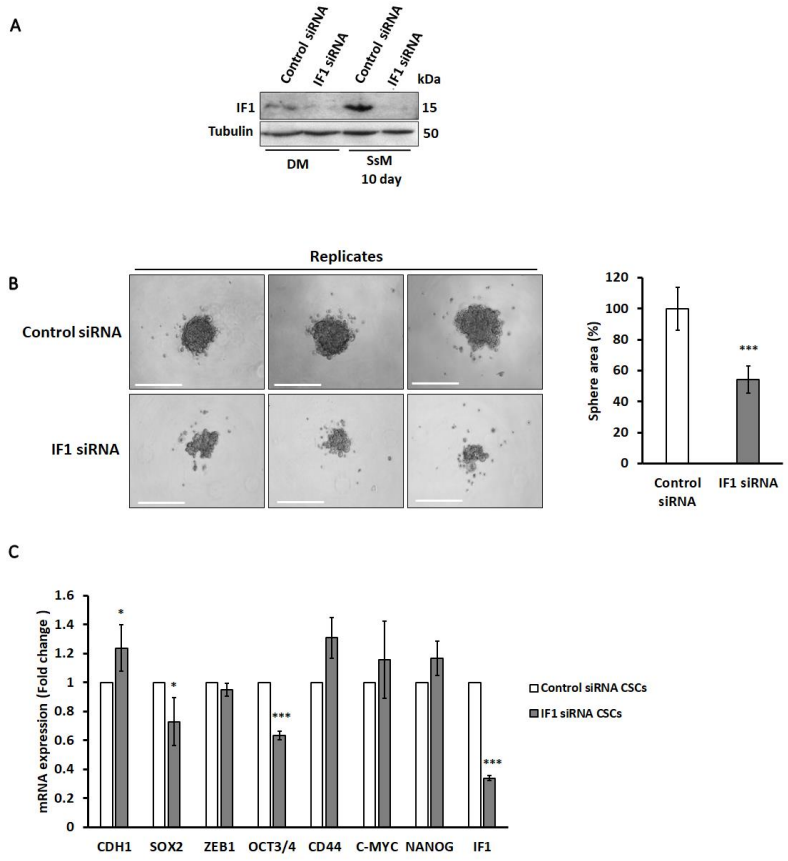

Figure 15. Knockdown of IF1 reduces sphere formation in Panc1 cells. (A) Protein expression levels of IF1 after its silencing in Panc1 parental cells after 48 of transfection in differentiated medium (DM)

and after 10 days in stem-specific medium (SsM) using IF1 siRNA. **(B)** After 48 hours of transfection with IF1 siRNA, Panc1 cells were seeded in non-adherent Nunclon Sphera 96-well plates for 8 days. The left panel is bright field microscopy images of spheres in control and silenced cells and the right panel is the quantification of the sphere size. Scale bar 100 μm. **(C)** qPCR analysis of relative mRNA expression levels of key EMT/stemness genes in Panc1 cells transfected with IF1 siRNA and grown in the stem-specific medium for 10 days. IF1 mRNA expression was also quantified. Levels are normalized to SDHA. Histogram legends: light grey: control siRNA cells; dark grey: IF1 siRNA cells. The Values are reported as fold change relative to control siRNA cells. Statistical legends: control siRNA cells vs IF1 siRNA cells = * $p < 0.05$, ** $p < 0.01$, ***$p<0.001$.

7.8. Lomerizine inhibits cellular proliferation and sphere formation in Panc1 cells

Based on our findings about the increase of mitochondrial mass in pancreatic cancer stem cells, we hypothesized that inhibition of mitochondrial respiration could be a therapeutic strategy to eliminate CSCs. Recently, Nuevo-Tapioles et al. reported a group of FDA-approved compounds as potent inhibitors of mitochondrial respiration in colon cancer cells [127]. As a first approach, we evaluated the effect of seven of these compounds (sulfameter, butoconazole, glyburide, lomerizine, cimetidine, crystal violet, and telaprevir) on cell viability of Panc1 cells. As shown in Figure 16, six of these compounds inhibit the cell viability of Panc1 cells after 48 hours of treatment. However, lomerizine, butoconazole, and crystal violet are the most effective in reducing the cell viability at low concentrations compared to cells treated with dimethyl sulfoxide (the vehicle). Butocanozole is an imidazole antifungal used against *Candida* spp. infections and it is only administered as a vaginal cream. Crystal violet is a triarylmethane dye used as a histological stain and it has antibacterial and antifungal properties; nevertheless, numerous studies discouraged the use of this compound for medical purposes because of its high carcinogenic potential [134]. Meanwhile, lomerizine is a calcium channel blocker widely used for the treatment of glaucoma and migraine. Hence, of these three compounds that affect cell viability and based on drug repurposing strategy, we focused on lomerizine for further in-depth study on pancreatic CSCs because it is already used in human therapy with acceptable known side effects.

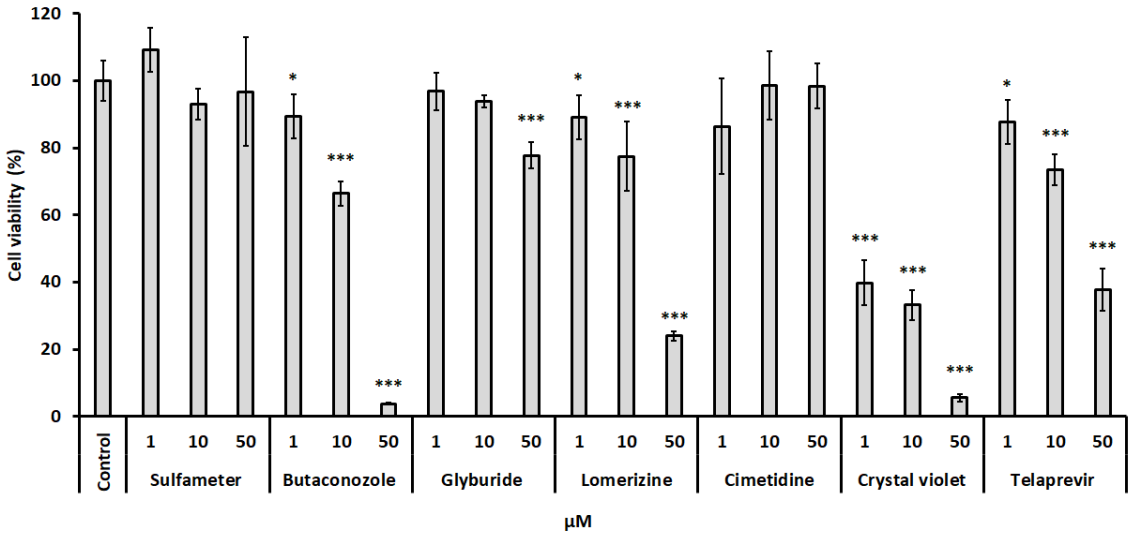

Figure 16. Effect of mitochondrial respiration inhibitors on the viability of Panc1 parental cells. Panc1 cells were treated with FDA-approved drugs at three different concentrations (1,10, and 50 μM) or the vehicle (dimethyl sulfoxide). The cell viability was determined by spectrophotometry using the crystal violet assay after 48 hours of treatment. The histogram shows the mean ± SEM of three different biological replicates. Statistical legends: control vs treated cells = * $p < 0.05$, ** $p < 0.01$, ***$p<0.001$.

Parental cells, CSCs at different time points, and fibroblasts were treated with increasing concentrations of lomerizine (at 5, 10, 15, 25, and 50 μM) for 48 hours and cell viability was assessed. Cell viability curves reveal an IC_{50} of ~13 and ~11 μM in parental and CSCs, respectively (Figure 17 A). The statistical analysis shows that CSCs are significantly more sensitive than parental cells ($p<0.05$), but no significant differences were found between CSCs cultured at different time points. Remarkably, only concentrations of lomerizine above 25 μM affected the cell viability of fibroblasts, in line with the observation that at the dose corresponding to cancer cell IC_{50} this drug does not show toxicity in normal cells (Figure 17 A). For cellular proliferation, Panc1 cells were seeded at 50% of confluence and treated with 15 μM lomerizine for 24 and 48 hours. The analysis of proliferation by flow cytometry shows that lomerizine significantly reduces the cellular proliferation of Panc1 cells compared to DMSO control (Figure 17 B). To study the effect of lomerizine on sphere formation, Panc1 cells were seeded to form a sphere and then treated with lomerizine at 5 and 10 μM. Next, the sphere area was measured after 8 days of incubation in standard conditions. Figure 17 C shows that sphere size is significantly reduced by 60% in cells treated with 5 μM lomerizine compared to cells treated with the vehicle (DMSO). Most interestingly, lomerizine at 10 μM completely abolishes the sphere formation. Taken together, the sum of these data indicates that lomerizine inhibits cellular proliferation and sphere formation in Panc1 cells.

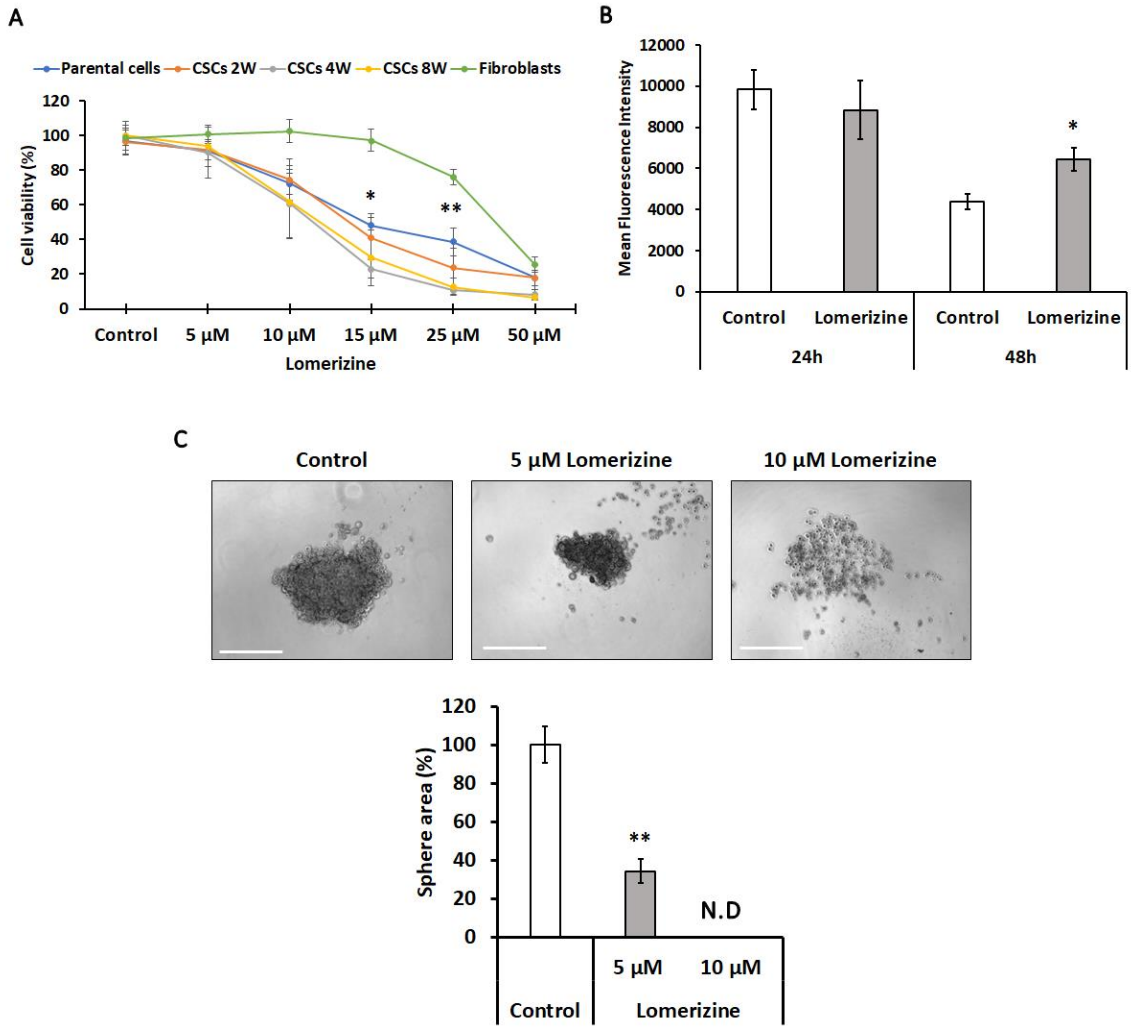

Figure 17. Lomerizine inhibits cellular proliferation and sphere formation in Panc1 cells. (A) Fibroblasts, Panc1 parental cells, and CSCs were treated with increasing concentrations of lomerizine for 48 hours and then cell viability was measured using the OZBlue kit. The line chart shows the mean ± SEM of three different biological replicates. Statistical legends: parental cells vs CSCs = * $p < 0.05$, ** $p < 0.01$. **(B)** Cellular proliferation was assessed in Panc1 parental cells by the incorporation of the CellTrace™ Far Red probe after 24 and 48 hours of treatment with 15 µM lomerizine. **(C)** Panc1 cells were seeded in non-adherent Nunclon Sphera 96-well plates and treated with 15 µM lomerizine for 8 days. The upper panel is bright field microscopy images of spheres in control and treated cells and the lower panel is the quantification of the sphere size. Scale bar 100 µm. The histograms show the mean ± SEM of three different biological replicates. Statistical legends: control (DMSO) vs treated cells = * $p < 0.05$, ** $p < 0.01$. N.D = not determined.

8. DISCUSSION

Cancer stem cells (CSCs) are considered primarily responsible for the aggressiveness of pancreatic ductal adenocarcinoma and relapse after chemotherapy [135]. Thus, the identification of the main features of these cells as possible therapeutical targets is crucial to eliminate the tumor by the root. Considering that CSCs have different grades of differentiation and metabolic profiles within the tumor, some authors have proposed the mitochondrion as a key player in metabolic plasticity and drug resistance profile [60,136]. With this idea in mind, numerous studies have been performed to elucidate the role of mitochondria in cancer metabolism; however, the precise mechanisms underlying the alterations of mitochondria in CSCs remain controversial [34,50,137]. One of the main issues is the method of isolation or obtainment of CSCs. Indeed, the isolation of CSCs from primary tumors based on the expression of stem markers represents a big challenge because these cells quickly return to their heterogeneity present in the tumor within a few days of culture and, more importantly, the use of specific surface markers would select only a subpopulation of CSCs that is not always representative of the whole tumor heterogeneity. This has led other authors to study the characteristics of CSCs in short-term culture; however, it has been shown that this stem cell model does not necessarily reflect the metabolic plasticity and quiescence-like state associated with CSCs phenotypes [34,35]. For these reasons, we decided to study the mitochondrial function in an *in vitro* model of CSCs derived from Panc1 cell line cultured in a stem-specific medium (SsM) at three different time points, short-term (2 weeks), medium-term (4 weeks), and long-term (8 weeks) [35]. In this model, CSCs at three-time points show a significantly high expression of stem and EMT markers, although long-term culture cells show the highest grade of stemness. During the process of de-differentiation, these cells switch from a glycolytic to an oxidative metabolism to finally reduce their metabolism to gain a quiescent state [35].

In the present work, we show that Panc1 CSCs, regardless of the culture term, increase mitochondrial mass and the expression of genes involved in mitochondrial biogenesis in comparison to parental cells. These findings are consistent with previous studies in which CSCs from different tumor types exhibited enhanced mitochondrial mass [138–140]. Increased mitochondrial biogenesis is commonly associated with a higher tumorigenic rate, anchorage-independent survival, and evasion of chemotherapy [140]. Given the differences in mitochondrial mass in CSCs, we focused our attention on the expression of proteins involved in mitochondrial dynamics, a process that regulates mitochondrial number, size, and distribution within the cytoplasm [62]. CSCs show an increase in mitochondria elongation with

respect to parental cells. In line with this, CSCs display a decreased phosphorylation of DRP1 on Ser616 and an increased expression of OPA1. The expression of any OPA1 isoform is crucial to preserve the supra-molecular organization of respiratory complexes, as well as to maintain the level of mtDNA content [97]. Interestingly, the electrophoretic profile of OPA1 revealed an increase in S-isoforms and a decrease in L-isoforms in CSCs compared to parental cells, and it is more evident in CSCs at 2 and 4 weeks. In the literature it has been reported that the S-isoforms support a more efficient energy preservation and regulate the metabolic shift from glycolysis to mitochondrial respiration in human fibroblasts [96,141]. Thus, the higher presence of short-OPA1 in CSCs in comparison to parental cells might support the previously described metabolic plasticity of these cells [35]. In addition, OPA1 knockdown reduces the tumorsphere size and affects the expression of *OCT3/4*, a key stem marker. Despite the effect of OPA1 silencing on stemness appears crucial, other authors have reported that CSCs exhibited highly fragmented mitochondria mediated by DRP1 activation [142,143]. These differences are possibly due to the fact that in these studies CSCs were grown in different medium conditions and for a short period of culture. In fact, our findings call into question the effectiveness of using DRP1 inhibitors as therapeutics agents to eliminate pancreatic CSCs, considering that during the process of stemness acquisition these cells could present an oxidative phenotype [34,35,50], which is favored by mitochondrial fusion [97]. On the contrary, our results lead us to propose the inhibition of OPA1 as a possible therapeutic target to reduce mitochondrial fusion in CSCs, and eventually disturbed their oxidative metabolism. Indeed, some authors have recently shown the crucial role of OPA1 in tumor cell metabolism [144] and angiogenesis [116].

Although it has been reported that several CSCs present metabolic plasticity, mainly relying on mitochondrial OXPHOS for energy production, the role of mitochondrial respiratory complexes and their assembly in this metabolic adaptation remains unexplored. Our study shows that the expression of the ETC complexes I-IV at protein levels does not change significantly in CSCs in comparison to parental cells, instead, the activity of complex II and IV is changed in CSCs. Interestingly, CSCs at 2 weeks show the lowest enzymatic activity of complex II and IV, supporting that short-term CSCs prefer a glycolytic metabolism, as has been reported by Ambrosini et al. [35]. Consistently, the increased activity of these two complexes in CSCs 4 weeks and their decrease at 8 weeks of culture, further corroborate our previous findings in which we showed that, at an intermediate dedifferentiation process, CSCs increase their oxidative capacity, whereas when cells acquire the highest stemness grade they

decrease the metabolic requests and enter in a quiescent state [35]. The analysis of the supercomplexes assembly evidences that these structures are markedly decreased in CSCs at 4 and 8 weeks relative to parental cells. Regarding CV, the 2D-BNGE reveals that CSCs present the formation of ATP synthase dimers whereas these structures are absent in parental cells. The formation of ATP synthase dimers is also favored by the expression of mitochondrial ATPase inhibitory factor 1 (IF1) [145]. It has been shown that the oligomycin-sensitive respiration, which provides a measure of the ATP synthetic activity of the enzyme, is significantly reduced when the cells overexpress IF1 [126]. To our surprise, the expression of IF1 was significatively increased in CSCs relative to parental cells, particularly in CSCs at 8 weeks. The overexpression of this factor in CSCs at 8 weeks could partly explain the low ATP-linked respiration reported in these cells by Ambrosini et al [35]. Although the role of IF1 has been widely studied in the metabolism of differentiated cancer cells [146], interestingly there are no studies exploring the function of IF1 in pancreatic CSCs. Remarkably in our study, IF1 knockdown reduces the tumorsphere area and affects the expression of *OCT3/4*, a key stem marker, whereas it increases the expression of *CDH1*, a key gene involved in the EMT program. In agreement with our results, other authors have reported that IF1 knockdown in hepatic cell lines decreased the colony formation and migratory capacity, suggesting a possible role of this protein in EMT [147]. These results lead us to hypothesize that IF1 could be a link between reprogramming of energy metabolism and stemness acquisition; however, further studies are needed to understand if this protein has any potential as a new therapeutic target for the treatment of pancreatic cancer.

Under physiological conditions, the mitochondrial electron transport chain is the primary source of ROS, which promote cell proliferation and cell survival. However, excess of ROS can cause cell damage and induce apoptosis [148]. Therefore, it is fundamental for the cells to balance ROS production through regulating antioxidant systems. Regarding CSCs, it is expected that like normal cells, low levels of ROS could contribute to their self-renewal capacity and resistance to conventional chemotherapy [148]. In fact, CSCs in some breast and gastrointestinal tumors have lower ROS levels than differentiated cancer cells, but it is not clear if these lower ROS are because of less ROS generation or increased ROS scavenging systems [79,148]. In contrast with this assumption, our results show that ROS levels are significantly increased in pancreatic CSCs compared to parental cells. Importantly, CSCs at 8 weeks exhibited the lowest ROS levels between CSCs, suggesting that in our system ROS might act as a motive force during the first stages of dedifferentiation (2- and 4 weeks) and once CSCs

accomplish the quiescent state (8 weeks) the ROS levels begin to decline. A quiescent state has been always associated with lower ROS levels in both normal stem cells and CSCs [149]. Other studies have observed that enhanced production of ROS is fundamental during anchorage-independent growth, an important property of CSCs. But at the same time, this increase in ROS levels triggers different metabolic and antioxidant responses in order to reduce mitochondrial damage [80]. No surprisingly, our results reveal that mRNA expression levels of different antioxidant genes such as MnSOD, POX, IDH1, and GPX are increased in CSCs. On the other side, the expression of catalase, the enzyme that metabolizes H_2O_2, is significantly decreased in CSCs compared to parental cells. Thus, we hypothesized that hydrogen peroxide levels could play an important role during the process of dedifferentiation and stemness acquisition. However, further studies should be performed to understand if a decreased expression of catalase renders the CSCs more sensitive to oxidative stress.

As mentioned above, our findings of increased mitochondrial mass in pancreatic cancer stem cells led us to think that mitochondrial metabolism could provide a promising specific target to eliminate CSCs. Currently, drug repurposing offers a valuable approach to accelerate the development of anticancer therapies and reduce the cost burden of cancer treatments. With this idea in mind, we screened seven compounds from an FDA-approved library that trigger inhibition of mitochondrial respiration in different cancer cell lines [127]. We found that three of these compounds e.g., lomerizine, butoconazole, and crystal violet exhibit potent anticancer activity against pancreatic cancer cells. Lomerizine is a calcium channel blocker widely used for migraine headaches, glaucoma, and nerve injury; however, there have been no studies to investigate the effect of lomerizine in pancreatic cancer. Based on drug repurposing and relative safety for humans, we focused on lomerizine for further in-depth study on Panc1 parental and CSCs. We show that lomerizine suppresses cell growth in both parental and CSCs, being significantly more toxic in CSCs compared to parental cells. Remarkably, the cytotoxic effects of lomerizine on fibroblasts are only evident at high concentrations, emphasizing its low toxicity in normal cells. Similar results were reported in colorectal cancer cells, where lomerizine inhibited cell proliferation through the PI3K/AKT/mTOR signaling pathway [150]. Furthermore, our data demonstrate that lomerizine significantly inhibits the sphere formation of Panc1 CSCs. However, it remains to be established whether the exact mechanism by which lomerizine inhibits CSC formation is related to the mitochondrial function or calcium homeostasis. Recently, Heejin Lee et al, reported that calcium channel inhibitors significantly decreased the expression of stem markers in ovarian CSCs. Furthermore, a synergistic effect

of these inhibitors with cisplatin was demonstrated in inhibiting the viability and proliferation of CSC [151]. Altogether, these results point out that lomerizine is a promising compound to be repurposed as a potential antitumor drug alone or in combined therapy.

9. CONCLUSION

Pancreatic ductal adenocarcinoma is a highly lethal neoplasia and the currently used therapeutic approaches are not effective in a wide range of patients. Currently, the evidence points out that cancer stem cells are key players during tumor development, metastasis, chemoresistance, and tumor relapse. Thus, there is a need to deeply study the biological features of pancreatic CSCs in order to identify new possible therapeutic targets and ultimately improve the patient survival. Due to the importance in the regulation of cellular functions, especially metabolic energy, mitochondria may represent important targets to be hit. Despite the increasing interest in this aspect, the role of mitochondria in pancreatic CSCs remains controversial. In this thesis, we study for the first-time mitochondrial physiology in a long-term *in vitro* model of pancreatic CSCs. Our results show that during progressive de-differentiation, CSCs undergo an increased mitochondrial mass, higher ROS generation, and regulation of mitochondrial SCs assembly. We also found that two important proteins, OPA1 and IF1, are overexpressed in CSCs and can modulate the tumorsphere formation. Inhibition of these proteins could be exploited as promising therapeutic targets to specifically eliminate CSCs. Furthermore, we identified that lomerizine, which is a calcium channel blocker, exhibits potent anticancer activity, particularly against pancreatic cancer stem cells. Our findings suggest that lomerizine could be a promising compound to be repurposed as an effective strategy to improve chemotherapy in PDAC patients. As a final comment, more studies are needed to characterize the role of mitochondrial in PDAC considering that it may be a key target for the generation of new promising therapies and that the exploitation of these therapeutic approaches should necessarily avoid secondary effects on normal tissues.

10. FUNDING

The project leading to this application has received funding from the European Union's Horizon 2020 research and innovation programme under the Marie Skłodowska-Curie grant agreement No 754345, under Region of Veneto Decree nr. 193 of 13/09/2016 and under Università degli Studi di Verona.

REGIONE DEL VENETO

UNIVERSITÀ di VERONA

11. ACKNOWLEDGMENTS

First of all, I would like to express my sincere gratitude to my research supervisors Professor Ilaria Dando and Professor Marta Palmieri. Their patient guidance, unconditional support, and useful suggestions were fundamental for the development of the project. Thanks for believing in me and encouraging me to pursue my ideas. This great opportunity in their laboratory certainly made me grow both scientifically and personally.

Thanks to my laboratory mates for their constant company during this journey. To Elisa for her help and "mentoring" when the days were not so good. To Giulia for her patience and clear explanations. To Andrea for his unconditional friendship inside and outside of the lab.

I would also like to thank Emanuela Bottani for her advice and scientific support. I have been extremely lucky to have a person who responded to all my questions about mitochondria.

I would also like to thank Professor Jose Manuel Cuezva for opening me the doors of his lab in Madrid. This opportunity was a great experience and help me to understand the mitochondrial world.

Appreciation is extended to the members of Massimo's group: Massimo, Raffaella, Nidula, Francesca, and Giovanna. Our interesting talks during lunch will be unforgettable.

I would also like to all staff of the biochemistry section: technicians, PhD students, Professors, and Postdocs. In particular, I would like to thank Giovanni for his sincere friendship and his useful advice from my first day in the lab.

In closing, I would like to extend my special thanks to the INVITE project and University staff. Without its financial support and immediate help for different administrative issues, this work would not have been achievable.

12. REFERENCES

1. Sung, H.; Ferlay, J.; Siegel, R.L.; Laversanne, M.; Soerjomataram, I.; Jemal, A.; Bray, F. Global Cancer Statistics 2020: GLOBOCAN Estimates of Incidence and Mortality Worldwide for 36 Cancers in 185 Countries. *CA: A Cancer Journal for Clinicians* **2021**, *71*, doi:10.3322/caac.21660.

2. Ushio, J.; Kanno, A.; Ikeda, E.; Ando, K.; Nagai, H.; Miwata, T.; Kawasaki, Y.; Tada, Y.; Yokoyama, K.; Numao, N.; et al. Pancreatic Ductal Adenocarcinoma: Epidemiology and Risk Factors. *Diagnostics* **2021**, *11*, doi:10.3390/diagnostics11030562.

3. Nevala-Plagemann, C.; Hidalgo, M.; Garrido-Laguna, I. From State-of-the-Art Treatments to Novel Therapies for Advanced-Stage Pancreatic Cancer. *Nature Reviews Clinical Oncology* 2020, *17*.

4. Mizrahi, J.D.; Surana, R.; Valle, J.W.; Shroff, R.T. Pancreatic Cancer. *The Lancet* 2020, *395*.

5. Manuel, H. Pancreatic Cancer. *New England Journal of Medicine* **2010**, *362*, 1605, doi:10.1056/NEJMra0901557.

6. Wu, C.; Yang, P.; Liu, B.; Tang, Y. Is There a Cdkn2a-Centric Network in Pancreatic Ductal Adenocarcinoma? *OncoTargets and Therapy* 2020, *13*.

7. Mantovani, F.; Collavin, L.; del Sal, G. Mutant P53 as a Guardian of the Cancer Cell. *Cell Death and Differentiation* 2019, *26*.

8. Ahmed, S.; Schwartz, C.; Dewan, M.; Xu, R. The Promising Role of TGF- β/SMAD4 in Pancreatic Cancer: The Future Targeted Therapy. *Journal of Cancer Treatment and Diagnosis* **2019**, *3*, doi:10.29245/2578-2967/2019/2.1141.

9. Kerk, S.A.; Papagiannakopoulos, T.; Shah, Y.M.; Lyssiotis, C.A. Metabolic Networks in Mutant KRAS-Driven Tumours: Tissue Specificities and the Microenvironment. *Nature Reviews Cancer* 2021, *21*.

10. Hanahan, D.; Weinberg, R.A. Hallmarks of Cancer: The next Generation. *Cell* 2011, *144*.

11. Pascale, R.M.; Calvisi, D.F.; Simile, M.M.; Feo, C.F.; Feo, F. The Warburg Effect 97 Years after Its Discovery. *Cancers* 2020, *12*.

12. Liberti, M. v.; Locasale, J.W. The Warburg Effect: How Does It Benefit Cancer Cells? *Trends in Biochemical Sciences* 2016, *41*.

13. Rodríguez-Enríquez, S.; Hernández-Esquivel, L.; Marín-Hernández, A.; el Hafidi, M.; Gallardo-Pérez, J.C.; Hernández-Reséndiz, I.; Rodríguez-Zavala, J.S.; Pacheco-Velázquez, S.C.; Moreno-Sánchez, R. Mitochondrial Free Fatty Acid β-Oxidation Supports Oxidative Phosphorylation and Proliferation in Cancer Cells. *International Journal of Biochemistry and Cell Biology* **2015**, *65*, doi:10.1016/j.biocel.2015.06.010.

14. Salem, A.F.; Whitaker-Menezes, D.; Howell, A.; Sotgia, F.; Lisanti, M.P. Mitochondrial Biogenesis in Epithelial Cancer Cells Promotes Breast Cancer Tumor Growth and Confers Autophagy Resistance. *Cell Cycle* **2012**, *11*, doi:10.4161/cc.22376.

15. Ralph, S.J.; Rodríguez-Enríquez, S.; Neuzil, J.; Moreno-Sánchez, R. Bioenergetic Pathways in Tumor Mitochondria as Targets for Cancer Therapy and the Importance of the ROS-Induced Apoptotic Trigger. *Molecular Aspects of Medicine* 2010, *31*.

16. Yuneva, M.O.; Fan, T.W.M.; Allen, T.D.; Higashi, R.M.; Ferraris, D. v.; Tsukamoto, T.; Matés, J.M.; Alonso, F.J.; Wang, C.; Seo, Y.; et al. The Metabolic Profile of Tumors Depends on Both the Responsible Genetic Lesion and Tissue Type. *Cell Metabolism* **2012**, *15*, doi:10.1016/j.cmet.2011.12.015.

17. Lau, A.N.; Li, Z.; Danai, L. v.; Westermark, A.M.; Darnell, A.M.; Ferreira, R.; Gocheva, V.; Sivanand, S.; Lien, E.C.; Sapp, K.M.; et al. Dissecting Cell-Type-Specific Metabolism in Pancreatic Ductal Adenocarcinoma. *eLife* **2020**, *9*, doi:10.7554/eLife.56782.

18. Chaika, N. v.; Yu, F.; Purohit, V.; Mehla, K.; Lazenby, A.J.; DiMaio, D.; Anderson, J.M.; Yeh, J.J.; Johnson, K.R.; Hollingsworth, M.A.; et al. Differential Expression of Metabolic Genes in Tumor and Stromal Components of Primary and Metastatic Loci in Pancreatic Adenocarcinoma. *PLoS ONE* **2012**, *7*, doi:10.1371/journal.pone.0032996.

19. Humpton, T.J.; Alagesan, B.; Denicola, G.M.; Lu, D.; Yordanov, G.N.; Leonhardt, C.S.; Yao, M.A.; Alagesan, P.; Zaatari, M.N.; Park, Y.; et al. Oncogenic KRAS Induces NIX-Mediated Mitophagy to Promote Pancreatic Cancer. *Cancer Discovery* **2019**, *9*, doi:10.1158/2159-8290.CD-18-1409.

20. Wang, P.; Song, M.; Zeng, Z.L.; Zhu, C.F.; Lu, W.H.; Yang, J.; Ma, M.Z.; Huang, A.M.; Hu, Y.; Huang, P. Identification of NDUFAF1 in Mediating K-Ras Induced Mitochondrial Dysfunction by a Proteomic Screening Approach. *Oncotarget* **2015**, *6*, doi:10.18632/oncotarget.2968.

21. Meng, N.; Glorieux, C.; Zhang, Y.; Liang, L.; Zeng, P.; Lu, W.; Huang, P. Oncogenic K-Ras Induces Mitochondrial OPA3 Expression to Promote Energy Metabolism in Pancreatic Cancer Cells. *Cancers* **2020**, *12*, doi:10.3390/cancers12010065.

22. Qin, C.; Yang, G.; Yang, J.; Ren, B.; Wang, H.; Chen, G.; Zhao, F.; You, L.; Wang, W.; Zhao, Y. Metabolism of Pancreatic Cancer: Paving the Way to Better Anticancer Strategies. *Molecular Cancer* **2020**, *19*, 1–19, doi:10.1186/s12943-020-01169-7.

23. Karasinska, J.M.; Topham, J.T.; Kalloger, S.E.; Jang, G.H.; Denroche, R.E.; Culibrk, L.; Williamson, L.M.; Wong, H.L.; Lee, M.K.C.; O'Kane, G.M.; et al. Altered Gene Expression along the Glycolysis–Cholesterol Synthesis Axis Is Associated with Outcome in Pancreatic Cancer. *Clinical Cancer Research* **2020**, *26*, doi:10.1158/1078-0432.CCR-19-1543.

24. Pereira, M.A.; Chio, I.I.C. Metastasis in Pancreatic Ductal Adenocarcinoma: Current Standing and Methodologies. *Genes* 2020, *11*.

25. Wang, Z.; Li, Y.; Ahmad, A.; Banerjee, S.; Azmi, A.S.; Kong, D.; Sarkar, F.H. Pancreatic Cancer: Understanding and Overcoming Chemoresistance. *Nature Reviews Gastroenterology and Hepatology* 2011, *8*.

26. Páez, D.; Labonte, M.J.; Bohanes, P.; Zhang, W.; Benhanim, L.; Ning, Y.; Wakatsuki, T.; Loupakis, F.; Lenz, H.J. Cancer Dormancy: A Model of Early Dissemination and Late Cancer Recurrence. *Clinical Cancer Research* 2012, *18*.

27. Sergeant, G.; Vankelecom, H.; Gremeaux, L.; Topal, B. Role of Cancer Stem Cells in Pancreatic Ductal Adenocarcinoma. *Nature Reviews Clinical Oncology* 2009, *6*.

28. Stoica, A.F.; Chang, C.H.; Pauklin, S. Molecular Therapeutics of Pancreatic Ductal Adenocarcinoma: Targeted Pathways and the Role of Cancer Stem Cells. *Trends in Pharmacological Sciences* 2020, *41*.

29. García-Heredia, J.M.; Carnero, A. Role of Mitochondria in Cancer Stem Cell Resistance. *Cells* **2020**, *9*, 1–28, doi:10.3390/cells9071693.

30. Valle, S.; Martin-Hijano, L.; Alcalá, S.; Alonso-Nocelo, M.; Sainz, B. The Ever-Evolving Concept of the Cancer Stem Cell in Pancreatic Cancer. *Cancers* **2018**, *10*, doi:10.3390/cancers10020033.

31. Abel, E. v.; Simeone, D.M. Biology and Clinical Applications of Pancreatic Cancer Stem Cells. *Gastroenterology* **2013**, *144*, doi:10.1053/j.gastro.2013.01.072.

32. Miranda-Lorenzo, I.; Dorado, J.; Lonardo, E.; Alcala, S.; Serrano, A.G.; Clausell-Tormos, J.; Cioffi, M.; Megias, D.; Zagorac, S.; Balic, A.; et al. Intracellular Autofluorescence: A Biomarker for Epithelial Cancer Stem Cells. *Nature Methods* **2014**, *11*, doi:10.1038/nmeth.3112.

33. Pozza, E.D.; Dando, I.; Biondani, G.; Brandi, J.; Costanzo, C.; Zoratti, E.; Fassan, M.; Boschi, F.; Melisi, D.; Cecconi, D.; et al. Pancreatic Ductal Adenocarcinoma Cell Lines Display a Plastic Ability to Bi-Directionally Convert into Cancer Stem Cells. *International Journal of Oncology* **2015**, *46*, 1099–1108, doi:10.3892/ijo.2014.2796.

34. Valle, S.; Alcalá, S.; Martin-Hijano, L.; Cabezas-Sáinz, P.; Navarro, D.; Muñoz, E.R.; Yuste, L.; Tiwary, K.; Walter, K.; Ruiz-Cañas, L.; et al. Exploiting Oxidative Phosphorylation to Promote the Stem and Immunoevasive Properties of Pancreatic Cancer Stem Cells. *Nature Communications* **2020**, *11*, doi:10.1038/s41467-020-18954-z.

35. Ambrosini, G.; Dalla Pozza, E.; Fanelli, G.; di Carlo, C.; Vettori, A.; Cannino, G.; Cavallini, C.; Carmona-Carmona, C.A.; Brandi, J.; Rinalducci, S.; et al. Progressively De-Differentiated Pancreatic Cancer Cells Shift from Glycolysis to Oxidative Metabolism and Gain a Quiescent Stem State. *Cells* **2020**, *9*, doi:10.3390/cells9071572.

36. Shah, A.N.; Summy, J.M.; Zhang, J.; Park, S.I.; Parikh, N.U.; Gallick, G.E. Development and Characterization of Gemcitabine-Resistant Pancreatic Tumor Cells. *Annals of Surgical Oncology* **2007**, *14*, doi:10.1245/s10434-007-9583-5.

37. Lee, C.J.; Dosch, J.; Simeone, D.M. Pancreatic Cancer Stem Cells. *Journal of Clinical Oncology* 2008, *26*, 2806–2812.

38. Makena, M.R.; Gatla, H.; Verlekar, D.; Sukhavasi, S.; Pandey, M.K.; Pramanik, K.C. Wnt/β-Catenin Signaling: The Culprit in Pancreatic Carcinogenesis and Therapeutic Resistance. *International Journal of Molecular Sciences* 2019, *20*.

39. Ercan, G.; Karlitepe, A.; Ozpolat, B. Pancreatic Cancer Stem Cells and Therapeutic Approaches. *Anticancer Research* 2017, *37*.

40. Wang, Q.-E. DNA Damage Responses in Cancer Stem Cells: Implications for Cancer Therapeutic Strategies. *World Journal of Biological Chemistry* **2015**, *6*, doi:10.4331/wjbc.v6.i3.57.

41. Mathews, L.A.; Cabarcas, S.M.; Hurt, E.M.; Zhang, X.; Jaffee, E.M.; Farrar, W.L. Increased Expression of DNA Repair Genes in Invasive Human Pancreatic Cancer Cells. *Pancreas* **2011**, *40*, doi:10.1097/MPA.0b013e31821ae25b.

42. Perusina Lanfranca, M.; Thompson, J.K.; Bednar, F.; Halbrook, C.; Lyssiotis, C.; Levi, B.; Frankel, T.L. Metabolism and Epigenetics of Pancreatic Cancer Stem Cells. *Seminars in Cancer Biology* 2019, *57*.

43. Heeschen, C.; Sancho, P. More Challenges Ahead—Metabolic Heterogeneity of Pancreatic Cancer Stem Cells. *Molecular and Cellular Oncology* **2016**, *3*, doi:10.1080/23723556.2015.1105353.

44. Rhim, A.D.; Mirek, E.T.; Aiello, N.M.; Maitra, A.; Bailey, J.M.; McAllister, F.; Reichert, M.; Beatty, G.L.; Rustgi, A.K.; Vonderheide, R.H.; et al. EMT and Dissemination Precede Pancreatic Tumor Formation. *Cell* **2012**, *148*, doi:10.1016/j.cell.2011.11.025.

45. Yasuda, T.; Ishimoto, T.; Baba, H. Conflicting Metabolic Alterations in Cancer Stem Cells and Regulation by the Stromal Niche. *Regenerative Therapy* **2021**, *17*, doi:10.1016/j.reth.2021.01.005.

46. Zhou, Y.; Zhou, Y.; Shingu, T.; Feng, L.; Chen, Z.; Ogasawara, M.; Keating, M.J.; Kondo, S.; Huang, P. Metabolic Alterations in Highly Tumorigenic Glioblastoma Cells: Preference for Hypoxia and High Dependency on Glycolysis. *Journal of Biological Chemistry* **2011**, *286*, doi:10.1074/jbc.M111.260935.

47. Shen, Y.-A.; Wang, C.-Y.; Hsieh, Y.-T.; Chen, Y.-J.; Wei, Y.-H. Metabolic Reprogramming Orchestrates Cancer Stem Cell Properties in Nasopharyngeal Carcinoma. *Cell Cycle* **2015**, *14*, doi:10.4161/15384101.2014.974419.

48. Ciavardelli, D.; Rossi, C.; Barcaroli, D.; Volpe, S.; Consalvo, A.; Zucchelli, M.; de Cola, A.; Scavo, E.; Carollo, R.; D'Agostino, D.; et al. Breast Cancer Stem Cells Rely on Fermentative Glycolysis and Are Sensitive to 2-Deoxyglucose Treatment. *Cell Death and Disease* **2014**, *5*, doi:10.1038/cddis.2014.285.

49. Loureiro, R.; Mesquita, K.A.; Magalhães-Novais, S.; Oliveira, P.J.; Vega-Naredo, I. Mitochondrial Biology in Cancer Stem Cells. *Seminars in Cancer Biology* 2017, *47*.

50. Sancho, P.; Burgos-Ramos, E.; Tavera, A.; Bou Kheir, T.; Jagust, P.; Schoenhals, M.; Barneda, D.; Sellers, K.; Campos-Olivas, R.; Graña, O.; et al. MYC/PGC-1α Balance Determines the Metabolic Phenotype and Plasticity of Pancreatic Cancer Stem Cells. *Cell Metabolism* **2015**, *22*, 590–605, doi:10.1016/j.cmet.2015.08.015.

51. Gao, C.; Shen, Y.; Jin, F.; Miao, Y.; Qiu, X. Cancer Stem Cells in Small Cell Lung Cancer Cell Line H446: Higher Dependency on Oxidative Phosphorylation and Mitochondrial Substrate-Level Phosphorylation than Non-Stem Cancer Cells. *PLoS ONE* **2016**, *11*, doi:10.1371/journal.pone.0154576.

52. Pastò, A.; Bellio, C.; Pilotto, G.; Ciminale, V.; Silic-Benussi, M.; Guzzo, G.; Rasola, A.; Frasson, C.; Nardo, G.; Zulato, E.; et al. Cancer Stem Cells from Epithelial Ovarian Cancer Patients Privilege Oxidative Phosphorylation, and Resist Glucose Deprivation. *Oncotarget* **2014**, *5*, doi:10.18632/oncotarget.2010.

53. Sousa, C.M.; Biancur, D.E.; Wang, X.; Halbrook, C.J.; Sherman, M.H.; Zhang, L.; Kremer, D.; Hwang, R.F.; Witkiewicz, A.K.; Ying, H.; et al. Pancreatic Stellate Cells Support Tumour Metabolism through Autophagic Alanine Secretion. *Nature* **2016**, *536*, doi:10.1038/nature19084.

54. Sansone, P.; Savini, C.; Kurelac, I.; Chang, Q.; Amato, L.B.; Strillacci, A.; Stepanova, A.; Iommarini, L.; Mastroleo, C.; Daly, L.; et al. Packaging and Transfer of Mitochondrial DNA via Exosomes Regulate Escape from Dormancy in Hormonal Therapy-Resistant Breast Cancer. *Proceedings of the National Academy of Sciences of the United States of America* **2017**, *114*, doi:10.1073/pnas.1704862114.

55. Viale, A.; Pettazzoni, P.; Lyssiotis, C.A.; Ying, H.; Sánchez, N.; Marchesini, M.; Carugo, A.; Green, T.; Seth, S.; Giuliani, V.; et al. Oncogene Ablation-Resistant Pancreatic Cancer Cells Depend on Mitochondrial Function. *Nature* **2014**, *514*, doi:10.1038/nature13611.

56. Lonardo, E.; Cioffi, M.; Sancho, P.; Sanchez-Ripoll, Y.; Trabulo, S.M.; Dorado, J.; Balic, A.; Hidalgo, M.; Heeschen, C. Metformin Targets the Metabolic Achilles Heel of Human Pancreatic Cancer Stem Cells. *PLoS ONE* **2013**, *8*, doi:10.1371/journal.pone.0076518.

57. Nimmakayala, R.K.; Leon, F.; Rachagani, S.; Rauth, S.; Nallasamy, P.; Marimuthu, S.; Shailendra, G.K.; Chhonker, Y.S.; Chugh, S.; Chirravuri, R.; et al. Metabolic Programming of Distinct Cancer Stem Cells Promotes Metastasis of Pancreatic Ductal Adenocarcinoma. *Oncogene* **2021**, *40*, doi:10.1038/s41388-020-01518-2.

58. Blanco, A.; Blanco, Gustavo. *Medical Biochemistry*; Academic Press, 2017; ISBN 9780128035504.

59. Giacomello, M.; Pyakurel, A.; Glytsou, C.; Scorrano, L. The Cell Biology of Mitochondrial Membrane Dynamics. *Nature Reviews Molecular Cell Biology* **2020**, *21*, 204–224, doi:10.1038/s41580-020-0210-7.

60. Fu, Y.; Ricciardiello, F.; Yang, G.; Qiu, J.; Huang, H.; Xiao, J.; Cao, Z.; Zhao, F.; Liu, Y.; Luo, W.; et al. The Role of Mitochondria in the Chemoresistance of Pancreatic Cancer Cells. *Cells* **2021**, *10*, 1–31, doi:10.3390/cells10030497.

61. Guerra, F.; Arbini, A.A.; Moro, L. Mitochondria and Cancer Chemoresistance. *Biochimica et Biophysica Acta - Bioenergetics* **2017**, *1858*, 686–699, doi:10.1016/j.bbabio.2017.01.012.

62. Maycotte, P.; Marín-Hernández, A.; Goyri-Aguirre, M.; Anaya-Ruiz, M.; Reyes-Leyva, J.; Cortés-Hernández, P. Mitochondrial Dynamics and Cancer. *Tumor Biology* **2017**, *39*, doi:10.1177/1010428317698391.

63. Ashton, T.M.; Gillies McKenna, W.; Kunz-Schughart, L.A.; Higgins, G.S. Oxidative Phosphorylation as an Emerging Target in Cancer Therapy. *Clinical Cancer Research* 2018, *24*.

64. Milenkovic, D.; Blaza, J.N.; Larsson, N.G.; Hirst, J. The Enigma of the Respiratory Chain Supercomplex. *Cell Metabolism* 2017, *25*.

65. Vartak, R.; Porras, C.A.M.; Bai, Y. Respiratory Supercomplexes: Structure, Function and Assembly. *Protein and Cell* 2013, *4*.

66. Schägger, H.; Pfeiffer, K. Supercomplexes in the Respiratory Chains of Yeast and Mammalian Mitochondria. *EMBO Journal* **2000**, *19*, doi:10.1093/emboj/19.8.1777.

67. Boumans, H.; Grivell, L.A.; Berden, J.A. The Respiratory Chain in Yeast Behaves as a Single Functional Unit. *Journal of Biological Chemistry* **1998**, *273*, doi:10.1074/jbc.273.9.4872.

68. Jang, S.; Javadov, S. Current Challenges in Elucidating Respiratory Supercomplexes in Mitochondria: Methodological Obstacles. *Frontiers in Physiology* 2018, *9*.

69. Raimondi, V.; Ciccarese, F.; Ciminale, V. Oncogenic Pathways and the Electron Transport Chain: A DangeROS Liaison. *British Journal of Cancer* 2020, *122*.

70. Marco-Brualla, J.; Al-Wasaby, S.; Soler, R.; Romanos, E.; Conde, B.; Justo-Méndez, R.; Enríquez, J.A.; Fernández-Silva, P.; Martínez-Lostao, L.; Villalba, M.; et al. Mutations in the ND2 Subunit of Mitochondrial Complex I Are Sufficient to Confer Increased Tumorigenic and Metastatic Potential to Cancer Cells. *Cancers* **2019**, *11*, doi:10.3390/cancers11071027.

71. Curtarello, M.; Zulato, E.; Nardo, G.; Valtorta, S.; Guzzo, G.; Rossi, E.; Esposito, G.; Msaki, A.; Pastò, A.; Rasola, A.; et al. VEGF-Targeted Therapy Stably Modulates the Glycolytic Phenotype of Tumor Cells. *Cancer Research* **2015**, *75*, doi:10.1158/0008-5472.CAN-13-2037.

72. Ikeda, K.; Horie-Inoue, K.; Suzuki, T.; Hobo, R.; Nakasato, N.; Takeda, S.; Inoue, S. Mitochondrial Supercomplex Assembly Promotes Breast and Endometrial Tumorigenesis by Metabolic Alterations and Enhanced Hypoxia Tolerance. *Nature Communications* **2019**, *10*, doi:10.1038/s41467-019-12124-6.

73. Masoud, R.; Reyes-Castellanos, G.; Lac, S.; Garcia, J.; Dou, S.; Shintu, L.; Abdel Hadi, N.; Gicquel, T.; el Kaoutari, A.; Diémé, B.; et al. Targeting Mitochondrial Complex I Overcomes Chemoresistance in High OXPHOS Pancreatic Cancer. *Cell Reports Medicine* **2020**, *1*, doi:10.1016/j.xcrm.2020.100143.

74. Bleier, L.; Wittig, I.; Heide, H.; Steger, M.; Brandt, U.; Dröse, S. Generator-Specific Targets of Mitochondrial Reactive Oxygen Species. *Free Radical Biology and Medicine* **2015**, *78*, doi:10.1016/j.freeradbiomed.2014.10.511.

75. Tuy, K.; Rickenbacker, L.; Hjelmeland, A.B. Reactive Oxygen Species Produced by Altered Tumor Metabolism Impacts Cancer Stem Cell Maintenance. *Redox Biology* **2021**, *44*, doi:10.1016/j.redox.2021.101953.

76. Storz, P. KRas, ROS and the Initiation of Pancreatic Cancer. *Small GTPases* 2017, *8*.

77. al Saati, T.; Clerc, P.; Hanoun, N.; Peuget, S.; Lulka, H.; Gigoux, V.; Capilla, F.; Béluchon, B.; Couvelard, A.; Selves, J.; et al. Oxidative Stress Induced by Inactivation of TP53INP1 Cooperates with KrasG12D to Initiate and Promote Pancreatic Carcinogenesis in the Murine Pancreas. *American Journal of Pathology* **2013**, *182*, doi:10.1016/j.ajpath.2013.02.034.

78. Diehn, M.; Cho, R.W.; Lobo, N.A.; Kalisky, T.; Dorie, M.J.; Kulp, A.N.; Qian, D.; Lam, J.S.; Ailles, L.E.; Wong, M.; et al. Association of Reactive Oxygen Species Levels and Radioresistance in Cancer Stem Cells. *Nature* **2009**, *458*, doi:10.1038/nature07733.

79. Jiang, J.; Wang, K.; Chen, Y.; Chen, H.; Nice, E.C.; Huang, C. Redox Regulation in Tumor Cell Epithelial–Mesenchymal Transition: Molecular Basis and Therapeutic Strategy. *Signal Transduction and Targeted Therapy* 2017, *2*.

80. Jiang, L.; Shestov, A.A.; Swain, P.; Yang, C.; Parker, S.J.; Wang, Q.A.; Terada, L.S.; Adams, N.D.; McCabe, M.T.; Pietrak, B.; et al. Reductive Carboxylation Supports Redox Homeostasis during Anchorage-Independent Growth. *Nature* **2016**, *532*, doi:10.1038/nature17393.

81. Zhang, Z.; Duan, Q.; Zhao, H.; Liu, T.; Wu, H.; Shen, Q.; Wang, C.; Yin, T. Gemcitabine Treatment Promotes Pancreatic Cancer Stemness through the Nox/ROS/NF-KB/STAT3 Signaling Cascade. *Cancer Letters* **2016**, *382*, doi:10.1016/j.canlet.2016.08.023.

82. Jagust, P.; Alcalá, S.; Jr, B.S.; Heeschen, C.; Sancho, P. Glutathione Metabolism Is Essential for Self-Renewal and Chemoresistance of Pancreatic Cancer Stem Cells. *World Journal of Stem Cells* **2020**, *12*, doi:10.4252/wjsc.v12.i11.1410.

83. Schrepfer, E.; Scorrano, L. Mitofusins, from Mitochondria to Metabolism. *Molecular Cell* 2016, *61*.

84. Gomes, L.C.; Benedetto, G. di; Scorrano, L. During Autophagy Mitochondria Elongate, Are Spared from Degradation and Sustain Cell Viability. *Nature Cell Biology* **2011**, *13*, doi:10.1038/ncb2220.

85. Yang, D.; Ying, J.; Wang, X.; Zhao, T.; Yoon, S.; Fang, Y.; Zheng, Q.; Liu, X.; Yu, W.; Hua, F. Mitochondrial Dynamics: A Key Role in Neurodegeneration and a Potential Target for Neurodegenerative Disease. *Frontiers in Neuroscience* 2021, *15*.

86. Chen, H.; Detmer, S.A.; Ewald, A.J.; Griffin, E.E.; Fraser, S.E.; Chan, D.C. Mitofusins Mfn1 and Mfn2 Coordinately Regulate Mitochondrial Fusion and Are Essential for Embryonic Development. *Journal of Cell Biology* **2003**, *160*, doi:10.1083/jcb.200211046.

87. Liesa, M.; Bord-d'Água, B.; Medina-Gómez, G.; Lelliott, C.J.; Paz, J.C.; Rojo, M.; Palacín, M.; Vidal-Puig, A.; Zorzano, A. Mitochondrial Fusion Is Increased by the Nuclear Coactivator PGC-1β. *PLoS ONE* **2008**, *3*, doi:10.1371/journal.pone.0003613.

88. Sebastián, D.; Hernández-Alvarez, M.I.; Segalés, J.; Sorianello, E.; Muñoz, J.P.; Sala, D.; Waget, A.; Liesa, M.; Paz, J.C.; Gopalacharyulu, P.; et al. Mitofusin 2 (Mfn2) Links Mitochondrial and Endoplasmic Reticulum Function with Insulin Signaling and Is Essential for Normal Glucose Homeostasis. *Proceedings of the National Academy of Sciences of the United States of America* **2012**, *109*, doi:10.1073/pnas.1108220109.

89. Segalés, J.; Paz, J.C.; Hernández-Alvarez, M.I.; Sala, D.; Muñoz, J.P.; Noguera, E.; Pich, S.; Palacín, M.; Enríquez, J.A.; Zorzano, A. A Form of Mitofusin 2 (Mfn2) Lacking the Transmembrane Domains and the COOH-Terminal End Stimulates Metabolism in Muscle and Liver Cells. *American Journal of Physiology - Endocrinology and Metabolism* **2013**, *305*, doi:10.1152/ajpendo.00546.2012.

90. Xue, R.; Yang, J.; Jia, L.; Zhu, X.; Wu, J.; Zhu, Y.; Meng, Q. Mitofusin2, as a Protective Target in the Liver, Controls the Balance of Apoptosis and Autophagy in Acute-on-Chronic Liver Failure. *Frontiers in Pharmacology* **2019**, *10*, doi:10.3389/fphar.2019.00601.

91. Kawalec, M.; Boratyńska-Jasińska, A.; Beresewicz, M.; Dymkowska, D.; Zabłocki, K.; Zabłocka, B. Mitofusin 2 Deficiency Affects Energy Metabolism and Mitochondrial Biogenesis in MEF Cells. *PLoS ONE* **2015**, *10*, doi:10.1371/journal.pone.0134162.

92. Cipolat, S.; de Brito, O.M.; Dal Zilio, B.; Scorrano, L. OPA1 Requires Mitofusin 1 to Promote Mitochondrial Fusion. *Proceedings of the National Academy of Sciences of the United States of America* **2004**, *101*, doi:10.1073/pnas.0407043101.

93. MacVicar, T.; Langer, T. OPA1 Processing in Cell Death and Disease - the Long and Short of It. *Journal of Cell Science* 2016, *129*.

94. Ishihara, N.; Fujita, Y.; Oka, T.; Mihara, K. Regulation of Mitochondrial Morphology through Proteolytic Cleavage of OPA1. *EMBO Journal* **2006**, *25*, doi:10.1038/sj.emboj.7601184.

95. Anand, R.; Wai, T.; Baker, M.J.; Kladt, N.; Schauss, A.C.; Rugarli, E.; Langer, T. The I-AAA Protease YME1L and OMA1 Cleave OPA1 to Balance Mitochondrial Fusion and Fission. *Journal of Cell Biology* **2014**, *204*, doi:10.1083/jcb.201308006.

96. Lee, H.; Smith, S.B.; Yoon, Y. The Short Variant of the Mitochondrial Dynamin OPA1 Maintains Mitochondrial Energetics and Cristae Structure. *Journal of Biological Chemistry* **2017**, *292*, doi:10.1074/jbc.M116.762567.

97. del Dotto, V.; Fogazza, M.; Carelli, V.; Rugolo, M.; Zanna, C. Eight Human OPA1 Isoforms, Long and Short: What Are They For? *Biochimica et Biophysica Acta - Bioenergetics* **2018**, *1859*, 263–269, doi:10.1016/j.bbabio.2018.01.005.

98. del Dotto, V.; Mishra, P.; Vidoni, S.; Fogazza, M.; Maresca, A.; Caporali, L.; McCaffery, J.M.; Cappelletti, M.; Baruffini, E.; Lenaers, G.; et al. OPA1 Isoforms in the Hierarchical

Organization of Mitochondrial Functions. *Cell Reports* **2017**, *19*, 2557–2571, doi:10.1016/j.celrep.2017.05.073.

99. Friedman, J.R.; Lackner, L.L.; West, M.; DiBenedetto, J.R.; Nunnari, J.; Voeltz, G.K. ER Tubules Mark Sites of Mitochondrial Division. *Science* **2011**, *334*, doi:10.1126/science.1207385.

100. Kashatus, J.A.; Nascimento, A.; Myers, L.J.; Sher, A.; Byrne, F.L.; Hoehn, K.L.; Counter, C.M.; Kashatus, D.F. Erk2 Phosphorylation of Drp1 Promotes Mitochondrial Fission and MAPK-Driven Tumor Growth. *Molecular Cell* **2015**, *57*, 537–551, doi:10.1016/j.molcel.2015.01.002.

101. Chang, C.R.; Blackstone, C. Cyclic AMP-Dependent Protein Kinase Phosphorylation of Drp1 Regulates Its GTPase Activity and Mitochondrial Morphology. *Journal of Biological Chemistry* **2007**, *282*, doi:10.1074/jbc.C700083200.

102. Otera, H.; Wang, C.; Cleland, M.M.; Setoguchi, K.; Yokota, S.; Youle, R.J.; Mihara, K. Mff Is an Essential Factor for Mitochondrial Recruitment of Drp1 during Mitochondrial Fission in Mammalian Cells. *Journal of Cell Biology* **2010**, *191*, doi:10.1083/jcb.201007152.

103. Shen, Q.; Yamano, K.; Head, B.P.; Kawajiri, S.; Cheung, J.T.M.; Wang, C.; Cho, J.H.; Hattori, N.; Youle, R.J.; van der Bliek, A.M. Mutations in Fis1 Disrupt Orderly Disposal of Defective Mitochondria. *Molecular Biology of the Cell* **2014**, *25*, doi:10.1091/mbc.E13-09-0525.

104. Losó n, O.C.; Song, Z.; Chen, H.; Chan, D.C. Fis1, Mff, MiD49, and MiD51 Mediate Drp1 Recruitment in Mitochondrial Fission. *Molecular Biology of the Cell* **2013**, *24*, doi:10.1091/mbc.E12-10-0721.

105. Palmer, C.S.; Elgass, K.D.; Parton, R.G.; Osellame, L.D.; Stojanovski, D.; Ryan, M.T. Adaptor Proteins MiD49 and MiD51 Can Act Independently of Mff and Fis1 in Drp1 Recruitment and Are Specific for Mitochondrial Fission. *Journal of Biological Chemistry* **2013**, *288*, doi:10.1074/jbc.M113.479873.

106. Serasinghe, M.N.; Wieder, S.Y.; Renault, T.T.; Elkholi, R.; Asciolla, J.J.; Yao, J.L.; Jabado, O.; Hoehn, K.; Kageyama, Y.; Sesaki, H.; et al. Mitochondrial Division Is Requisite to RAS-Induced Transformation and Targeted by Oncogenic MAPK Pathway Inhibitors. *Molecular Cell* **2015**, *57*, doi:10.1016/j.molcel.2015.01.003.

107. Yu, M.; Nguyen, N.D.; Huang, Y.; Lin, D.; Fujimoto, T.N.; Molkentine, J.M.; Deorukhkar, A.; Kang, Y.; Anthony San Lucas, F.; Fernandes, C.J.; et al. Mitochondrial Fusion Exploits a Therapeutic Vulnerability of Pancreatic Cancer. *JCI Insight* **2019**, *4*, 1–16, doi:10.1172/jci.insight.126915.

108. Lin, Z.; Lin, X.; Chen, J.; Huang, G.; Chen, T.; Zheng, L. Mitofusin-2 Is a Novel Anti-Angiogenic Factor in Pancreatic Cancer. *Journal of Gastrointestinal Oncology* **2021**, *12*, doi:10.21037/jgo-21-176.

109. Xue, R.; Meng, Q.; Lu, D.; Liu, X.; Wang, Y.; Hao, J. Mitofusin2 Induces Cell Autophagy of Pancreatic Cancer through Inhibiting the PI3K/Akt/MTOR Signaling Pathway. *Oxidative Medicine and Cellular Longevity* **2018**, *2018*, doi:10.1155/2018/2798070.

110. Wai, T.; Langer, T. Mitochondrial Dynamics and Metabolic Regulation. *Trends in Endocrinology and Metabolism* 2016, *27*.

111. Zhang, Z.; Wakabayashi, N.; Wakabayashi, J.; Tamura, Y.; Song, W.J.; Sereda, S.; Clerc, P.; Polster, B.M.; Aja, S.M.; Pletnikov, M. v.; et al. The Dynamin-Related GTPase Opa1 Is

Required for Glucose-Stimulated ATP Production in Pancreatic Beta Cells. *Molecular Biology of the Cell* **2011**, *22*, doi:10.1091/mbc.E10-12-0933.

112. Li, J.; Huang, Q.; Long, X.; Guo, X.; Sun, X.; Jin, X.; Li, Z.; Ren, T.; Yuan, P.; Huang, X.; et al. Mitochondrial Elongation-Mediated Glucose Metabolism Reprogramming Is Essential for Tumour Cell Survival during Energy Stress. *Oncogene* **2017**, *36*, 4901–4912, doi:10.1038/onc.2017.98.

113. Herkenne, S.; Scorrano, L. OPA1, a New Mitochondrial Target in Cancer Therapy. *Aging* **2020**, *12*, doi:10.18632/aging.104207.

114. Wee, Y.; Liu, Y.; Lu, J.; Li, X.; Zhao, M. Identification of Novel Prognosis-Related Genes Associated with Cancer Using Integrative Network Analysis. *Scientific Reports* **2018**, *8*, doi:10.1038/s41598-018-21691-5.

115. Hu, L.P.; Zhou, K.X.; Huo, Y.M.; Liu, D.J.; Li, Q.; Yang, M.W.; Huang, P.Q.; Xu, C.J.; Tian, G.A.; Yao, L.L.; et al. Single-Cell RNA Sequencing Reveals That Targeting HSP90 Suppresses PDAC Progression by Restraining Mitochondrial Bioenergetics. *Oncogenesis* **2021**, *10*, doi:10.1038/s41389-021-00311-4.

116. Herkenne, S.; Ek, O.; Zamberlan, M.; Pellattiero, A.; Chergova, M.; Chivite, I.; Novotná, E.; Rigoni, G.; Fonseca, T.B.; Samardzic, D.; et al. Developmental and Tumor Angiogenesis Requires the Mitochondria-Shaping Protein Opa1. *Cell Metabolism* **2020**, *31*, 987-1003.e8, doi:10.1016/j.cmet.2020.04.007.

117. Rademaker, G.; Hennequière, V.; Brohée, L.; Nokin, M.J.; Lovinfosse, P.; Durieux, F.; Gofflot, S.; Bellier, J.; Costanza, B.; Herfs, M.; et al. Myoferlin Controls Mitochondrial Structure and Activity in Pancreatic Ductal Adenocarcinoma, and Affects Tumor Aggressiveness. *Oncogene* **2018**, *37*, 4398–4412, doi:10.1038/s41388-018-0287-z.

118. Nagdas, S.; Kashatus, J.A.; Nascimento, A.; Hussain, S.S.; Trainor, R.E.; Pollock, S.R.; Adair, S.J.; Michaels, A.D.; Sesaki, H.; Stelow, E.B.; et al. Drp1 Promotes KRas-Driven Metabolic Changes to Drive Pancreatic Tumor Growth. *Cell Reports* **2019**, *28*, 1845-1859.e5, doi:10.1016/j.celrep.2019.07.031.

119. Rademaker, G.; Costanza, B.; Anania, S.; Agirman, F.; Maloujahmoum, N.; di Valentin, E.; Goval, J.J.; Bellahcène, A.; Castronovo, V.; Peulen, O. Myoferlin Contributes to the Metastatic Phenotype of Pancreatic Cancer Cells by Enhancing Their Migratory Capacity through the Control of Oxidative Phosphorylation. *Cancers* **2019**, *11*, doi:10.3390/cancers11060853.

120. Liang, J.; Yang, Y.; Bai, L.; Li, F.; Li, E. DRP1 Upregulation Promotes Pancreatic Cancer Growth and Metastasis through Increased Aerobic Glycolysis. *Journal of Gastroenterology and Hepatology (Australia)* **2020**, *35*, 885–895, doi:10.1111/jgh.14912.

121. Shibue, T.; Weinberg, R.A. EMT, CSCs, and Drug Resistance: The Mechanistic Link and Clinical Implications. *Nature Reviews Clinical Oncology* 2017, *14*.

122. Chen, H.; Chan, D.C. Mitochondrial Dynamics in Regulating the Unique Phenotypes of Cancer and Stem Cells. *Cell Metabolism* **2017**, *26*, 39–48, doi:10.1016/j.cmet.2017.05.016.

123. Katajisto, P.; Döhla, J.; Chaffer, C.L.; Pentinmikko, N.; Marjanovic, N.; Iqbal, S.; Zoncu, R.; Chen, W.; Weinberg, R.A.; Sabatini, D.M. Asymmetric Apportioning of Aged Mitochondria between Daughter Cells Is Required for Stemness. *Science* **2015**, *348*, doi:10.1126/science.1260384.

124. Courtois, S.; de Luxán-Delgado, B.; Penin-Peyta, L.; Royo-García, A.; Parejo-Alonso, B.; Jagust, P.; Alcalá, S.; Rubiolo, J.A.; Sánchez, L.; Sainz, B.; et al. Inhibition of Mitochondrial Dynamics Preferentially Targets Pancreatic Cancer Cells with Enhanced Tumorigenic and Invasive Potential. *Cancers* **2021**, *13*, 1–21, doi:10.3390/cancers13040698.

125. Inak, G.; Rybak-Wolf, A.; Lisowski, P.; Pentimalli, T.M.; Jüttner, R.; Glažar, P.; Uppal, K.; Bottani, E.; Brunetti, D.; Secker, C.; et al. Defective Metabolic Programming Impairs Early Neuronal Morphogenesis in Neural Cultures and an Organoid Model of Leigh Syndrome. *Nature Communications* **2021**, *12*, doi:10.1038/s41467-021-22117-z.

126. Sánchez-Cenizo, L.; Formentini, L.; Aldea, M.; Ortega, Á.D.; García-Huerta, P.; Sánchez-Aragó, M.; Cuezva, J.M. Up-Regulation of the ATPase Inhibitory Factor 1 (IF1) of the Mitochondrial H+-ATP Synthase in Human Tumors Mediates the Metabolic Shift of Cancer Cells to a Warburg Phenotype. *Journal of Biological Chemistry* **2010**, *285*, doi:10.1074/jbc.M110.146480.

127. Nuevo-Tapioles, C.; Santacatterina, F.; Stamatakis, K.; Núñez de Arenas, C.; Gómez de Cedrón, M.; Formentini, L.; Cuezva, J.M. Coordinate β-Adrenergic Inhibition of Mitochondrial Activity and Angiogenesis Arrest Tumor Growth. *Nature Communications* **2020**, *11*, doi:10.1038/s41467-020-17384-1.

128. Nijtmans, L.G.J.; Henderson, N.S.; Holt, I.J. Blue Native Electrophoresis to Study Mitochondrial and Other Protein Complexes. *Methods* **2002**, *26*, doi:10.1016/S1046-2023(02)00038-5.

129. Wittig, I.; Braun, H.P.; Schägger, H. Blue Native PAGE. *Nature Protocols* **2006**, *1*, doi:10.1038/nprot.2006.62.

130. Kirby, D.M.; Thorburn, D.R.; Turnbull, D.M.; Taylor, R.W. Biochemical Assays of Respiratory Chain Complex Activity. *Methods in Cell Biology* 2007, *80*.

131. Bugiani, M.; Invernizzi, F.; Alberio, S.; Briem, E.; Lamantea, E.; Carrara, F.; Moroni, I.; Farina, L.; Spada, M.; Donati, M.A.; et al. Clinical and Molecular Findings in Children with Complex I Deficiency. In Proceedings of the Biochimica et Biophysica Acta - Bioenergetics; 2004; Vol. 1659.

132. Signorile, A.; de Rasmo, D.; Cormio, A.; Musicco, C.; Rossi, R.; Fortarezza, F.; Palese, L.L.; Loizzi, V.; Resta, L.; Scillitani, G.; et al. Human Ovarian Cancer Tissue Exhibits Increase of Mitochondrial Biogenesis and Cristae Remodeling. *Cancers* **2019**, *11*, doi:10.3390/cancers11091350.

133. Hollinshead, K.E.R.; Parker, S.J.; Eapen, V. v.; Encarnacion-Rosado, J.; Sohn, A.; Oncu, T.; Cammer, M.; Mancias, J.D.; Kimmelman, A.C. Respiratory Supercomplexes Promote Mitochondrial Efficiency and Growth in Severely Hypoxic Pancreatic Cancer. *Cell Reports* **2020**, *33*, 108231, doi:10.1016/j.celrep.2020.108231.

134. Mani, S.; Bharagava, R.N. Exposure to Crystal Violet, Its Toxic, Genotoxic and Carcinogenic Effects on Environment and Its Degradation and Detoxification for Environmental Safety. In *Reviews of Environmental Contamination and Toxicology*; 2016; Vol. 237.

135. Askan, G.; Sahin, I.H.; Chou, J.F.; Yavas, A.; Capanu, M.; Iacobuzio-Donahue, C.A.; Basturk, O.; O'Reilly, E.M. Pancreatic Cancer Stem Cells May Define Tumor Stroma Characteristics and Recurrence Patterns in Pancreatic Ductal Adenocarcinoma. *BMC Cancer* **2021**, *21*, doi:10.1186/s12885-021-08123-w.

136. Shin, M.K.; Cheong, J.H. Mitochondria-Centric Bioenergetic Characteristics in Cancer Stem-like Cells. *Archives of Pharmacal Research* **2019**, *42*, 113–127, doi:10.1007/s12272-019-01127-y.

137. Dai, W.; Wang, G.; Chwa, J.; Oh, M.E.; Abeywardana, T.; Yang, Y.; Wang, Q.A.; Jiang, L. Mitochondrial Division Inhibitor (Mdivi-1) Decreases Oxidative Metabolism in Cancer. *British Journal of Cancer* **2020**, *122*, doi:10.1038/s41416-020-0778-x.

138. Zhao, J.; Zhang, J.; Yu, M.; Xie, Y.; Huang, Y.; Wolff, D.W.; Abel, P.W.; Tu, Y. Mitochondrial Dynamics Regulates Migration and Invasion of Breast Cancer Cells. *Oncogene* **2013**, *32*, doi:10.1038/onc.2012.494.

139. Seo, S.K.; Kim, J.H.; Choi, H.N.; Choe, T.B.; Hong, S. il; Yi, J.Y.; Hwang, S.G.; Lee, H.G.; Lee, Y.H.; Park, I.C. Knockdown of TWIST1 Enhances Arsenic Trioxide- and Ionizing Radiation-Induced Cell Death in Lung Cancer Cells by Promoting Mitochondrial Dysfunction. *Biochemical and Biophysical Research Communications* **2014**, *449*, 490–495, doi:10.1016/j.bbrc.2014.05.030.

140. de Luca, A.; Fiorillo, M.; Peiris-Pagès, M.; Ozsvari, B.; Smith, D.L.; Sanchez-Alvarez, R.; Martinez-Outschoorn, U.E.; Cappello, A.R.; Pezzi, V.; Lisanti, M.P.; et al. Mitochondrial Biogenesis Is Required for the Anchorage-Independent Survival and Propagation of Stem-like Cancer Cells. *Oncotarget* **2015**, *6*, 14777–14795, doi:10.18632/oncotarget.4401.

141. Son, J.M.; Sarsour, E.H.; Kakkerla Balaraju, A.; Fussell, J.; Kalen, A.L.; Wagner, B.A.; Buettner, G.R.; Goswami, P.C. Mitofusin 1 and Optic Atrophy 1 Shift Metabolism to Mitochondrial Respiration during Aging. *Aging Cell* **2017**, *16*, 1136–1145, doi:10.1111/acel.12649.

142. Rehman, J.; Zhang, H.J.; Toth, P.T.; Zhang, Y.; Marsboom, G.; Hong, Z.; Salgia, R.; Husain, A.N.; Wietholt, C.; Archer, S.L. Inhibition of Mitochondrial Fission Prevents Cell Cycle Progression in Lung Cancer. *The FASEB Journal* **2012**, *26*, 2175–2186, doi:10.1096/fj.11-196543.

143. Xie, Q.; Wu, Q.; Horbinski, C.M.; Flavahan, W.A.; Yang, K.; Zhou, W.; Dombrowski, S.M.; Huang, Z.; Fang, X.; Shi, Y.; et al. Mitochondrial Control by DRP1 in Brain Tumor Initiating Cells. *Nature Neuroscience* **2015**, *18*, 501–510, doi:10.1038/nn.3960.

144. Li, M.; Wang, L.; Wang, Y.; Zhang, S.; Zhou, G.; Lieshout, R.; Ma, B.; Liu, J.; Qu, C.; Verstegen, M.M.A.; et al. Mitochondrial Fusion Via OPA1 and MFN1 Supports Liver Tumor Cell Metabolism and Growth. *Cells* **2020**, *9*, 1–16, doi:10.3390/cells9010121.

145. García, J.J.; Morales-Ríos, E.; Cortés-Hernández, P.; Rodríguez-Zavala, J.S. The Inhibitor Protein (IF1) Promotes Dimerization of the Mitochondrial F1F0-ATP Synthase. *Biochemistry* **2006**, *45*, doi:10.1021/bi060339j.

146. Sánchez-Aragó, M.; Formentini, L.; Martínez-Reyes, I.; García-Bermudez, J.; Santacatterina, F.; Sánchez-Cenizo, L.; Willers, I.M.; Aldea, M.; Nájera, L.; Juarránz, Á.; et al. Expression, Regulation and Clinical Relevance of the ATPase Inhibitory Factor 1 in Human Cancers. *Oncogenesis* **2013**, *2*, doi:10.1038/oncsis.2013.9.

147. Kong, J.; Yao, C.; Ding, X.; Dong, S.; Wu, S.; Sun, W.; Zheng, L. ATPase Inhibitory Factor 1 Promotes Hepatocellular Carcinoma Progression After Insufficient Radiofrequency Ablation, and Attenuates Cell Sensitivity to Sorafenib Therapy. *Frontiers in Oncology* **2020**, *10*, doi:10.3389/fonc.2020.01080.

148. Ding, S.; Li, C.; Cheng, N.; Cui, X.; Xu, X.; Zhou, G. Redox Regulation in Cancer Stem Cells. *Oxidative Medicine and Cellular Longevity* 2015, *2015*.

149. Lyublinskaya, O.G.; Borisov, Y.G.; Pugovkina, N.A.; Smirnova, I.S.; Obidina, J. v.; Ivanova, J.S.; Zenin, V. v.; Shatrova, A.N.; Borodkina, A. v.; Aksenov, N.D.; et al. Reactive Oxygen Species Are Required for Human Mesenchymal Stem Cells to Initiate Proliferation after the Quiescence Exit. *Oxidative Medicine and Cellular Longevity* **2015**, *2015*, doi:10.1155/2015/502105.

150. Tan, X.; He, Y.; Huang, Y.; Zheng, C.; Li, J.; Liu, Q.; He, M.; Li, B.; Xu, W. Lomerizine 2HCl Inhibits Cell Proliferation and Induces Protective Autophagy in Colorectal Cancer via the PI3K/Akt/MTOR Signaling Pathway. *MedComm* **2021**, *2*, doi:10.1002/mco2.83.

151. Lee, H.; Kim, J.W.; Kim, D.K.; Choi, D.K.; Lee, S.; Yu, J.H.; Kwon, O. bin; Lee, J.; Lee, D.S.; Kim, J.H.; et al. Calcium Channels as Novel Therapeutic Targets for Ovarian Cancer Stem Cells. *International Journal of Molecular Sciences* **2020**, *21*, doi:10.3390/ijms21072327.